UNIVERSITÀ DEGLI STUDI DI MILANO

Ph.D. Course in Molecular and Cellular Biology

XXXV Ciclo

Bioscience Department

Role of the *ALOG* gene family in the inflorescence development of *Oryza sativa* and *Arabidopsis thaliana*

BIO/18 - BIO/01

Veronica Maria Beretta

Ph.D. Thesis

Scientific supervisor: Prof. Martin Kater

Tutor: Prof. Veronica Gregis

Academic year: 2021-2022

INDEX

RIASSUNTO

La popolazione mondiale è in continua crescita. Questo determina la necessità di trovare nuove soluzioni per rendere la produzione agricola più efficiente. Uno dei fattori che influisce sulla produttività delle piante coltivate è l'architettura dell'infiorescenza: ad esempio, un'infiorescenza molto ramificata potrebbe permettere ad una pianta di produrre un maggior numero di semi.

Per studiare come viene regolato lo sviluppo dell'infiorescenza, vengono utilizzate *Arabidopsis thaliana,* una pianta modello per le dicotiledoni e *Oryza sativa,* pianta modello per le monocotiledoni. In entrambe le specie, lo sviluppo dell'infiorescenza è controllato da un complesso network genico che controlla l'attività dei meristemi riproduttivi.

Molti fattori coinvolti in questo network sono stati già caratterizzati, ma di molti altri non si conosce ancora il ruolo. Per individuarne di nuovi, i meristemi riproduttivi di Arabidopsis e riso sono stati dissezionati tramite laser e sottoposti ad un'analisi del trascrittoma. L'analisi dei geni differenzialmente espressi nei diversi meristemi riproduttivi ha evidenziato come alcuni membri della famiglia genica degli *ALOG* (*Arabidopsis LIGHT-DEPENDENT SHORT HYPOCOTYL 1* and *Oryza G1*) presentino un pattern di espressione simile fra loro. Questo fatto suggerisce il coinvolgimento di alcuni membri della famiglia *ALOG* nello sviluppo dell'architettura dell'infiorescenza. I geni individuati sono *OsG1L1, OsG1L2* e *TAW1/OsG1L5*; e *AtLSH1, AtLSH3* e *AtLSH4*.

È interessante notare come *TAW1* sia già stato caratterizzato come un fondamentale regolatore dell'architettura dell'infiorescenza di riso, permettendoci di ipotizzare come anche altri membri della famiglia *ALOG* siano coinvolti nello sviluppo dell'architettura dell'infiorescenza.

Durante il mio dottorato la mia attività di ricerca è stata volta a chiarire quale ruolo ricoprono i geni della famiglia *ALOG* durante lo sviluppo dell'infiorescenza sia in Arabidopsis che in riso.

Come prima cosa, abbiamo generato singoli e multipli mutanti per i geni di interesse utilizzando la tecnologia CRISPR-Cas9 e ci siamo focalizzati sull'analisi della loro infiorescenza.

L'analisi fenotipica e molecolare dei mutanti ottenuti ci ha permesso di stabilire che il knock-out di questi geni determina difetti nell'architettura dell'infiorescenza che sono ricollegabili al processo di acquisizione e mantenimento dell'identità dei meristemi riproduttivi.

ABSTRACT

Human population growth makes it of primary importance to find new ways to sustainably increase agricultural crop production to meet the increasing food demand. In this context, inflorescence architecture is one of the key agronomical traits which determines grain yield; thus, it has been a major target for crop domestication and improvement. For example, in rice an increased number of branches allows the panicle to bear more seeds, leading to a higher yield.

To study the molecular genetic processes that lead to inflorescence architecture establishment, we used two model plant species: *Oryza sativa*, model plant for monocotyledons, and *Arabidopsis thaliana*, model plant for dicotyledons. In both Arabidopsis and rice, inflorescence architecture development depends on a complex gene regulatory network that controls the identity and activity of the reproductive meristems.

A substantial number of genes involved in the pathways that lead to inflorescence architecture development have been identified, however, this complex developmental process is still far from understood. To identify new players involved in panicle development, reproductive meristems of Arabidopsis and rice were isolated by laser microdissection at different stages of development and used for RNA-seq analysis. The analysis of differentially expressed genes between the various stages of meristem development showed that several members of the *ALOG* (*Arabidopsis LIGHT-DEPENDENT SHORT HYPOCOTYL 1* and *Oryza G1*) gene family showed the same expression pattern in meristematic tissues, suggesting a possible role in the determination of inflorescence architecture. These genes are *OsG1L1*, *OsG1L2* and *TAW1/OsG1L5* of rice; and *AtLSH1*, *AtLSH3* and *AtLSH4* of Arabidopsis.

One member of the rice *ALOG* gene family, *TAW1/OsG1L5*, was already shown to be a fundamental regulator of inflorescence development in rice (Yoshida et al., 2013), further suggesting an important role for the *ALOG* gene family in reproductive development.

My Ph.D. research project was focused on elucidating the role of the *ALOG* genes in inflorescence development in both Arabidopsis and rice.

We generated single and multiple mutants in both species using CRISPR-Cas9. The molecular and morphological analysis of the mutants revealed that the knock-out of these genes determined defects in plant inflorescence architecture linked to the process of identity acquisition of the reproductive meristems.

AIMS OF THE PROJECT

Inflorescence architecture is one of the main traits that influences crop production. The establishment of inflorescence architecture is determined by the activity of different meristems and by the timing of the transition between indeterminate and determinate stages of reproductive meristems.

Gaining more knowledge of the genetic pathways that control these processes is a crucial step to contribute to improve crop plants. In this context, a laser-microdissection followed by an RNA-seq was performed using *Arabidopsis thaliana* and *Oryza sativa* reproductive meristems, to obtain transcriptomes specific for the different reproductive meristem types. From the analysis of the differentially expressed genes in the meristematic tissues in both the species, we observed that members of the *ALOG* gene family were good candidates to play an important role in inflorescence development. Indeed, *AtLSH1*, *AtLSH3* and *AtLSH4* in *Arabidopsis thaliana* and *OsG1L1*, *OsG1L2* and *OsG1L5/TAW1* in *Oryza sativa* resulted to be differentially expressed in the reproductive meristems tissues analysed with a similar expression profile. This co-expression profile could indicate a similar function of these genes in inflorescence development of both Arabidopsis and rice.

It was already known that *AtLSH3* and *AtLSH4* are involved in meristem maintenance and in organogenesis (Bencivenga et al., 2016; Cho & Zambryski, 2011a; S. Takeda et al., 2011), whereas *TAW1* has been proposed to be one of the master regulators of rice panicle architecture development (Yoshida et al., 2013). For these reasons, a better characterization of the genetics pathways in which the *ALOG* genes are involved could help to better understand how the inflorescence develops in both Arabidopsis and rice, and the possible conserved function of these genes in monocot and dicot species.

To address this goal, single and multiple mutant lines for *OsG1L1*, *OsG1L2* and *OsG1L5/TAW1;* as well as for *AtLSH1*, *AtLSH3* and *AtLSH4* were generated, and inflorescences of these mutants were analysed in detail.

In rice, we wanted to test the hypothesis that, given the same expression profile shared by *OsG1L1*, *OsG1L2* and *OsG1L5/TAW1*, that they would be all involved in the regulation of the transition of the reproductive meristems from an indeterminate to a determinate stage.

The mutant lines *osg1l1* and *osg1l2* showed defects in panicle development, that resulted to be smaller and less branched than the wild type. In-situ hybridization with *FRIZZY PANICLE* (*FZP*), a molecular marker of the determinate state of reproductive meristems, was performed on the developing panicles of the two mutants. The developing panicles of *osg1l1* and *osg1l2* were also analysed through scanning electron microscopy (SEM). The results that we obtained indicate that *OsG1L1* and *OsG1L2*

are like *TAW1* involved in the regulation of the transition of the reproductive meristems from an indeterminate to a determinate stage.

A transcriptome analysis was performed on developing panicles of *osg1l2*, the mutant that showed the most drastic phenotype, to determine the possible targets of this transcription factor. This analysis suggested that *OsG1L2* could interact with other known inflorescence architecture regulators and the datasets were used for the construction of a gene regulatory network (GRN) proposing interactions among genes potentially involved in controlling inflorescence development in rice. The analysis of the obtained GRN allowed us to individuate new players involved in the pathway of rice panicle development, like *HOX14*.

In Arabidopsis, the three ALOG genes showed to be fully redundant and only in the triple mutant *lsh1 lsh3 lsh4* plants showed an inflorescence phenotype. The triple mutant developed bracts that subtended the flowers, the development of these organs are normally in wild type Arabidopsis suppressed. This phenotype suggests that *AtLSH1*, *AtLSH3* and *AtLSH4* are involved in the correct development of the reproductive meristems. To try to elucidate the pathways in which these three genes are involved, we first analysed the phenotype by means of SEM. We then tested the possible interaction among *AtLSH1*, *AtLSH3* and *AtLSH4* and other known factors involved in the pathway of bract suppression by means of Yeast-two-hybrid.

Thanks to an ampDAP-seq performed by our collaborators from the group of Francois Parcy (Laboratoire Physiologie Cellulaire et Végétale, Grenoble, France), which allowed the identification of a binding motif for the ALOG proteins; and of a transcriptomic analysis performed on inflorescence meristem tissues of the triple mutant *lsh1 lsh3 lsh4,* we were able to identify interesting putative targets of *LSH1*, *LSH3* and *LSH4*. The expression of these candidates was then checked by means of in-situ hybridization in the triple mutant *lsh1 lsh3 lsh4* background.

Collectively, the results that I obtained indicate a role for the *ALOG* gene family in the maintenance of reproductive meristems and in inflorescence development.

INTRODUCTION

1. Inflorescence architecture development

Inflorescence architecture is one of the key agronomical traits that determines grain yield. For this reason, it has been a major target for crop domestication and improvement. Indeed, an inflorescence which can produce more branches, and consequently more grains, will lead to an increase in crop yield.

In plants, the overall structure of the inflorescence is determined by the activity of meristems, groups of pluripotent cells that contribute to plant growth and to the development of its organs. Reproductive meristems are defined as indeterminate until they develop floral meristems on their flank. Once this transition to floral meristem occurs, the meristem becomes determinate, meaning that the development of floral organs exhausts the meristematic activity. For this reason, the transition from determinate to indeterminate meristems determines how complex the developing inflorescence will be (Hake, 2008).

During evolution, flowering plants developed different types of inflorescences that can be grouped into three different architectural groups: panicles, racemes, and cymes. It is also possible to distinguish the different inflorescence types between determinate, where the inflorescence meristem ends in a terminal flower; or indeterminate if it continues to produce structures, including branches and flowers [**Figure 1**; (Prusinkiewicz et al., 2007; Han et al., 2014)].

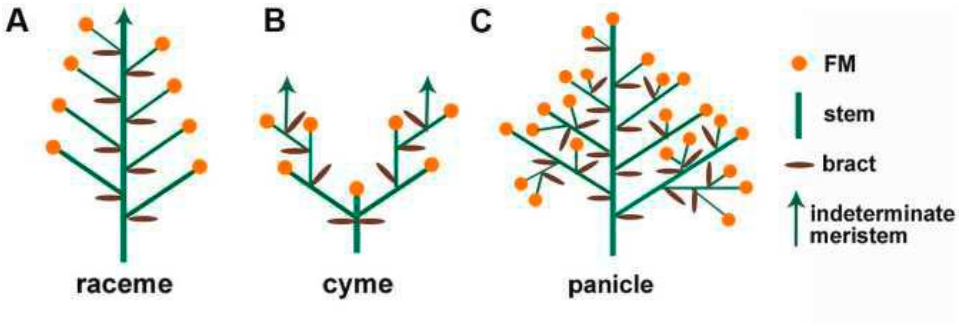

Figure 1. Schematic representations of the three main types of inflorescence architecture in plants. A, raceme; B, cyme; C, panicle. (Adapted from Han et al., 2014).

To better understand how inflorescence architecture is established, we use the model plants *Oryza sativa* (a monocotyledon) and *Arabidopsis thaliana* (a dicotyledon).

1.1 Inflorescence development in *Oryza sativa*

Oryza sativa, commonly known as rice, develops a determinate inflorescence called panicle (Bommert et al., 2005; Han et al., 2014). The overall structure of the panicle is determined by the activity of different meristems and by the timing of transition between an indeterminate to a determinate stage of the meristem.

During the vegetative phase the Shoot Apical Meristem (SAM) develops the vegetative tissues of the aerial part of the plant, such as the leaves. After the floral transition, the SAM becomes Inflorescence Meristem (IM), in rice also called Rachis Meristem (RM). The IM can develop Primary Branch Meristems (pBMs) that will in turn produce Axillary meristems (AMs) which could differentiate into indeterminate Secondary Branch Meristems (sBMs), or determinate Spikelet Meristems (SMs). In the same way, SBMs elongate and produce SMs. The BMs are programmed to differentiate in SMs only after they have produced a defined number of lateral branches; when this happens the pool of meristematic cells is consumed hampering the formation of more branches. In rice, the SM develops three floral meristems (FMs), of which one will differentiate into one fertile floret, whereas the other two will develop into empty glumes (sterile lemmas), exhausting the pool of meristematic cells (**Figure 2**; Caselli et al., 2020; Tanaka et al., 2013; Bommert et al., 2005; Han et al., 2014).

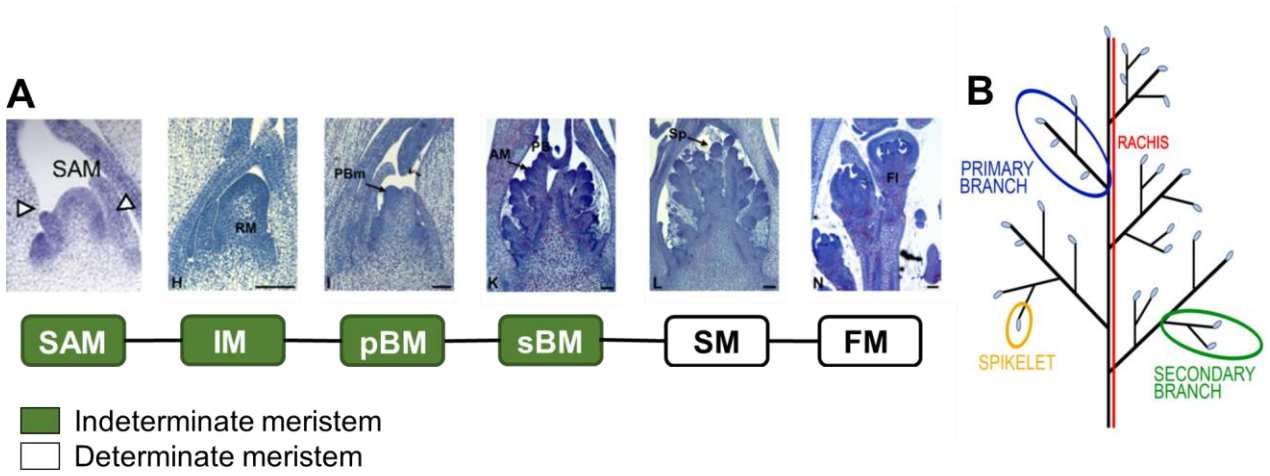

Figure 2. A, representation of the development of the inflorescence meristem in rice. B, overall structure of rice panicle. (SAM, Shoot Apical Meristem; IM, Inflorescence Meristem; pBM, Primary Branch Meristem; sBM, Secondary Branch Meristem; SM, Spikelet Meristem; FM, Flower Meristem. Meristem sections in A are adapted from Yoshida et al., 2013; Ta et al., 2017).

A complex gene network determines the establishment of inflorescence architecture. In rice, inflorescence architecture is determined by the activity of the different reproductive meristems already mentioned, and by the timing of the transition to the different meristem stages. Indeed, Rice plants in which early transitions to SM identity occur will develop less complex panicles with fewer

grains in contrast to plants in which the transition is delayed. Different factors promote an indeterminate or a determinate growth of the panicle.

Some of the genes involved, like *MONOCULM1* (*MOC1*), are regulators of axillary meristem formation (Li et al., 2003). *MOC1*, which is an ortholog of Arabidopsis *LATERAL SUPPRESSOR* (*LAS*), is expressed in axillary meristems. The *moc1* mutant develops one strong culm and loses its tillering capability, while the inflorescence produces less branches resulting in a lower grain yield (X. Li et al., 2003; Liang et al., 2014). *MOC1* can also regulate the expression of *Oryza sativa HOMEOBOX 1* (*OSH1*) and of *TEOSINTE BRANCHED1/FINE CULM 1* (*TB1/FC1*, that henceforth will be referred to as *FC1*), two genes that play a fundamental role in the maintenance/initiation of IM/BMs and in the regulation of AMs growth, respectively (X. Li et al., 2003). The *osh1* mutant produces a smaller inflorescence bearing fewer spikelets with respect to wild type plants, and *OsFC1* is already reported to be a negative regulator of tillering and inflorescence development (Cui et al., 2020; T. Takeda et al., 2003; Tsuda et al., 2011).

LAX PANICLE 1 (*LAX1*), which encodes for a basic helix-loop-helix protein, is necessary for the initiation and maintenance of branches, and for spikelet formation. Indeed, in the *lax1* mutant, initiation and/or maintenance of rachis-branches, plus lateral and terminal spikelet formation was severely impaired (M. Komatsu et al., 2001). Furthermore, it was published that *LAX1* works in an overlapping pathway with *SMALL PANICLE* (*SPA*) to promote axillary meristem initiation; even mild *lax* mutant alleles combined with *spa* mutations present dramatic defects in axillary meristem formation throughout plant development (K. Komatsu et al., 2003).

FZP encodes for a protein containing an *APETALA2/ETHYLENE RESPONSE FACTOR* (*AP2/ERF*) and it's expressed at the boundaries of rudimentary glumes during differentiation. This transcription factor is fundamental for the specification of spikelet meristems. Indeed, instead of producing florets, the *fzp1* mutant reiterates sequential rounds of branching (M. Komatsu et al., 2003). *Fzp2* shows a similar phenotype; the *lax1 fzp2* double mutant is unable to form spikelets and doesn't develop SBs but forms new meristems in the axis of lateral bracts, growing primary branches in a zigzag shape (M. Komatsu et al., 2001).

APO1 (*ABERRANT PANICLE ORGANIZATION 1*) and *APO2* have overlapping functions and encode for F-box proteins that repress FM transition. *APO1* is an ortholog of Arabidopsis *UNUSUAL FLORAL ORGANS* (UFO), while *APO2* is the ortholog of Arabidopsis *LEAFY* (*LFY*); *APO1* and *APO2* have opposite role in inflorescence development, respect to their Arabidopsis counterparts. Indeed, *UFO* and *LFY* promote floral identity, whereas *APO1* and *APO2* repress the transition to

determinate spikelet meristem. If mutated, *apo1* and *apo2* plants produce small inflorescences with reduced branching showing a reduction in IM size (Ikeda-Kawakatsu et al., 2009, 2012).

OsMADS34/PAP2 belongs to the *SEPALLATA* (*SEP*) subfamily of the *MADS*-box gene family and was already identified as a positive regulator of spikelet meristem identity. The *osmads34/pap2* mutant produces panicles with more branches because of the inability of the meristem to reach the determinate stage of SM (Gao et al., 2010; Kobayashi et al., 2012). The overexpression of *RICE CENTRORADIALIS 1* (*RCN1*) and of *RCN2* leads to the development of a more branched panicle with more internodes (C. Liu et al., 2013; Nakagawa et al., 2002) while knocking-down all the four *RNC* genes present in rice results in shorter panicles with fewer secondary branches (C. Liu et al., 2013). These observations indicate a role for the *RCN* genes in the suppression of the phase transition of the meristem from the indeterminate BM stage to the determinate SM identity. It was also recently published that *RCN4* is regulated by *OsMADS34*, where the double mutant *osmads34 rcn4* develops panicles that present less secondary branches and less spikelets than the wild type (Zhu et al., 2022).

Another important player in inflorescence architecture development is *TAWAWA1* (*TAW1*)/*G1-LIKE 5* (*G1L5*), a member of the *Arabidopsis LSH1 and Oryza G1* (*ALOG*) gene family. *TAW1* acts as a promotor of the BM identity and suppressor of the SM specification, by the activation of genes involved in the repression of floral transition (Yoshida et al., 2013). The dominant *taw1-D* gain-of-function mutant shows a delay in spikelet specification which results in increased branching and higher grain numbers (Yoshida et al., 2013; Yuan et al., 2021).

It is also worth to mention the role that phytohormones like auxin and cytokinin have in inflorescence development. Indeed, auxin maxima and dynamic re-localization of this hormone were seen at the initiation sites of inflorescence and spikelet primordia including BMs and female and male organ primordia (McSteen, 2009). For example, rice *ABERRANT SPIKELET AND PANICLE 1* (*ASP1*) a homolog of *TOPLESS* (*TPL*), which is a transcriptional corepressor in Arabidopsis, plays a role in auxin-related inflorescence development. In the *asp1* mutant, fewer inflorescence branches and flowers were observed, like in auxin-related pleiotropic defects. Though the exact function of *ASP1* in auxin signalling has not been clearly demonstrated a putative link between *ASP1* function and auxin response has been proposed (Yoshida et al., 2012).

Accumulation of cytokinins in reproductive meristems is also associated with the meristems function and regulation of inflorescence architecture. Mutations in Type-A Response Regulator genes, like *RR21*, *RR22* and *RR23* determine an impairment in inflorescence development. Indeed, panicles of the *rr21/22/23* mutants were smaller and had reduced branching compared with the wild type

(Worthen et al., 2019), indicating defects in the maintenance of an indeterminate stage of the reproductive meristems.

1.2 Inflorescence development in *Arabidopsis thaliana*

Arabidopsis thaliana, a model plant for dicotyledons, produces an indeterminate inflorescence called raceme (**Figure 3 B**). As mentioned before, the Shoot Apical Meristem (SAM) contains a pool of stem cells that can produce the aerial part of the plant. During the vegetative phase the SAM produces leaves. Then it undergoes the so-called floral transition, and it is reprogrammed to become the Inflorescence Meristem (IM). The Inflorescence Meristem generates the determinate Flower Meristems (FM) on its flanks in a spiral phyllotaxis. Each FM produces a single flower of which the pistil that contains the ovules will after fertilization develop a fruit, called silique, containing the seeds (Alvarez-Buylla et al., 2010).

The Arabidopsis inflorescence can be divided in phytomers, where a phytomer consists of a leaf, an internode, a node, and an axillary meristem (Chandler, 2012; Figure 3 C). For example, in Arabidopsis, the first few inflorescence nodes after the floral transition present phytomers that consist of an internode, a node, and a cauline leaf subtending a paraclade axillary meristem in its axil, that will give rise to secondary shoots (**Figure 3 C**, 2nd phytomer). Then, the later developing IM phytomers consist of a cryptic bract, a node, which gives rise to a FM in its axil, and an internode, the inflorescence stem. While in Arabidopsis the bract remains cryptic, in other flowering plants bracts of different colors and shapes are often produced with the function to attract pollinators or to protect the flower from abiotic stresses like intense solar radiation (H. Huang et al., 2022; Song et al., 2013). Indeed, in Arabidopsis, the FM constitutes an AM whose rapid proliferation represses outgrowth of the subtending leaf or bract, which doesn't develop (Long & Barton, 2000; **Figure 3 C**, 3rd phytomer).

The transition from the IM to the FM is regulated by three major players: *LEAFY* (*LFY*), *APETALA1* (*AP1*) and *TERMINATING FLOWER1* (*TFL1*). While *TFL1* is expressed in the IM, to allow the meristem to maintain its indeterminate stage, *LFY* and *AP1* are entitled to establish the FM identity.

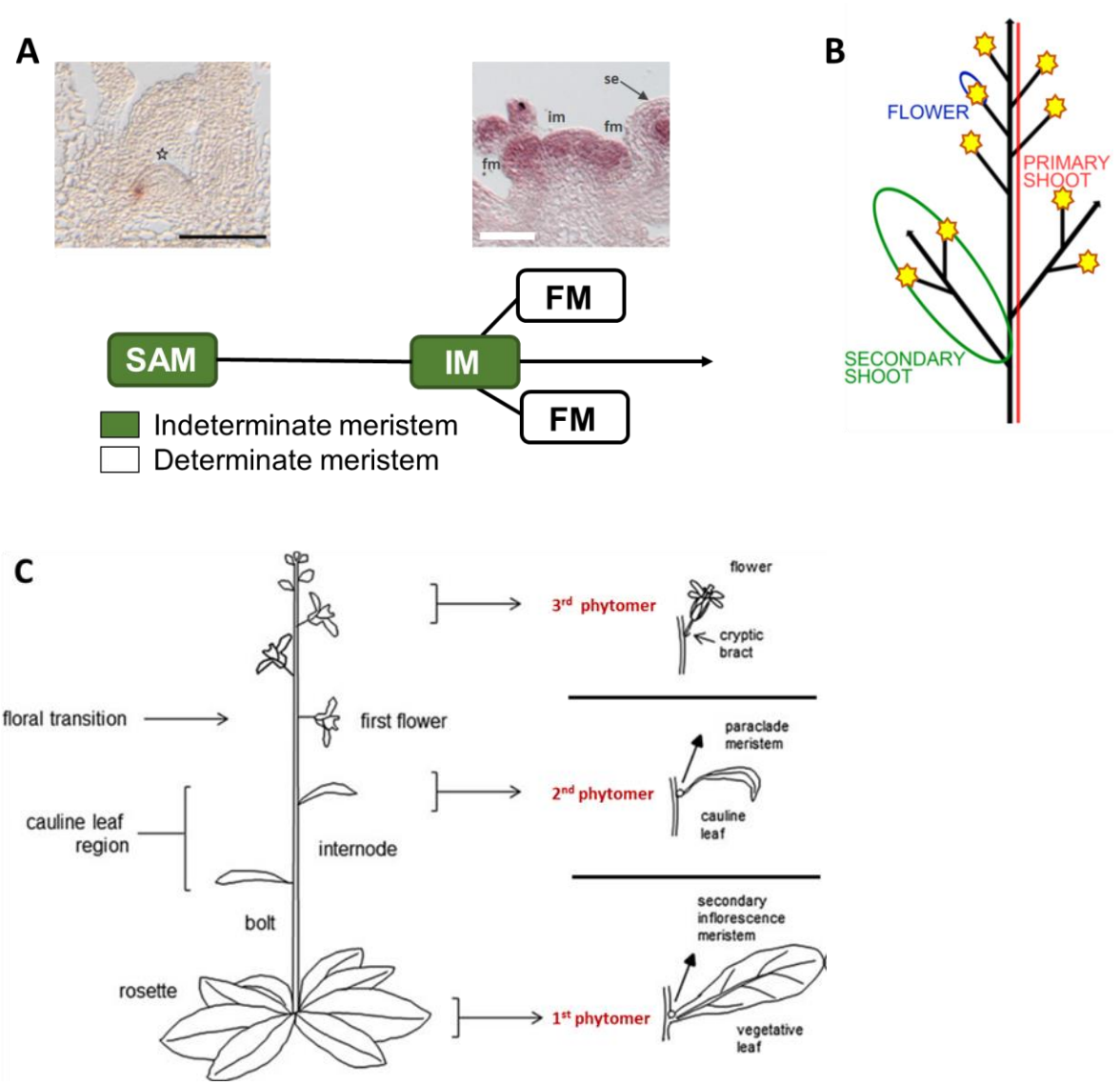

Figure 3. A, development of the meristems in *Arabidopsis thaliana*. B, overall structure of Arabidopsis inflorescence. C, structure of Arabidopsis inflorescence divided in phytomers. Each phytomer consists of an internode, a node, a leaf and an axillary meristem. (SAM, Shoot Apical Meristem; IM, Inflorescence Meristem; FM, Flower Meristem. Meristem sections in A are adapted from Mantegazza et al., 2014; Musialak-Lange et al., 2021; figure in C is adapted from Chandler, 2012).

The switch from the vegetative to the inflorescence meristem is triggered by endogenous and exogenous inputs which are integrated by the so called 'flowering time integration genes' (Boss, 2004).

FLOWERING LOCUS T (*FT*), the so called florigen, moves from the leaves to the shoot apical meristem where, acting together with its partner *FD*, triggers the activation of the transcription factor *SUPPRESSOR OF OVEREXPRESSION OF CONSTANS1* (*SOC1*). *SOC1* and the *FT/FD* complex play a major role in the determination of the inflorescence meristem identity, as they are able to induce

the expression of the floral meristem identity genes *LFY* and *AP1* in the cells that will give rise to the FM (Abe, 2009; Kaufmann et al., 2010; Wils & Kaufmann, 2017). *SHORT VEGETATIVE PHASE* (*SVP*) encodes for a MADS domain transcription factor that acts as a repressor of the floral transition and works in the thermo-sensory pathway. *SVP* represses *FT* expression via direct binding to the *FT* promoter. Mutations in *SVP* determines an early flowering phenotype (Hartmann et al., 2000).

LFY is expressed in young FMs at early stages of development (Weigel et al., 1992a; Yamaguchi, 2021), and it is both necessary and sufficient for the FM differentiation (Blázquez et al., 1997). Indeed, the *lfy* mutant develops structures with shoot characteristics instead of flowers, with a less pronounced phenotype in proximity of the apical part of the plant, because of the independent activation of other genes, like *AP1* (Huala & Sussex, 1992; Schultz & Haughn, 1991). On the other hand, if *LFY* is constitutively expressed, there is an earlier determination of all shoots into flowers, indicating that an overexpression of *LFY* upregulates *AP1*, that in turn activates the transcription of several genes implied in flower development (Benková et al., 2003).

AP1 is a *MADS*-box gene that, in conjunction with *LFY*, maintains flower identity. Its expression is distributed evenly in the young floral meristem but later becomes confined to sepals and petals. The *AP1* expression pattern follows *LFY* but is slightly delayed. The loss of function mutant *ap1* forms ectopic flowers in a "branched inflorescence" fashion. Rarely sepals are formed, and petals are homeotically transformed into sepal-like organs, from which axils new *ap1* mutant flowers can develop displaying the same phenotype (Mandel & Yanofsky, 1995). Constitutive expression of *AP1* under the *CaMV 35S* promoter causes early flowering shoots (Mandel & Yanofsky, 1995).
CAULIFLOWER (*CAL*) is partially redundant with *AP1*. The *cal* mutant has a wild type phenotype while, in combination with *AP1* mutation in the *ap1 cal* double mutant the inflorescence meristem is incapable to acquire flower meristem identity. This results in a proliferation of inflorescence meristems that resemble a cauliflower like curd (Mandel & Yanofsky, 1995; Bowman et al., 1993). The acquisition of FM identity is also controlled by *SVP* and *AGAMOUS LIKE24* (*AGL24*). Indeed, the inflorescences of the *agl24 svp* double mutant, when combined with the strong *apetala 1-10* (*ap1-10*) mutant, are unable to acquire FM identity. This leads to the development of a cauliflower-like curd inflorescence, which resembles the *ap1 cal* double mutant phenotype. This indicates that, like *AP1* and *CAL*, also *AGL24* and *SVP* are FM identity genes. Furthermore, *SVP* and *AGL24* are important for the specification of the floral primordium, by the repression of the floral organ identity genes. Once the FM is established, genes involved in floral organ differentiation start to be expressed and, together with *AP1*, they repress *AGL24* and *SVP* expression (Gregis et al., 2006, 2008, 2009).

Floral organs are organized in four concentric whorls that are, from the outside to the center of the flower: sepals, petals, stamens (male reproductive organs) and carpels (female reproductive organs). The development of the floral organs is orchestrated by three different classes of homeotic transcription factors, the A, B and C classes. This transcription factors act in different combination in each of the four whorls: genes belonging to the class A specify sepal identity, A and B genes act together for the specification of petals, the B and C genes together specify for stamens identity and class C determines the identity of carpels. *AP1* and *AP2* belong to the class A, *AP3* and *PISTILLATA* (*PI*) belong to class B and *AGAMOUS* (*AG*) belongs to class C. There is also a class E, composed by *SEPALLATA1*, *SEPALLATA2*, *SEPALLATA3* and *SEPALLATA4*, which are necessary for the specification of all floral organs (Dennis & Peacock, 2019; V. Irish, 2017).

The areas that separate the meristem from the growing primordia are called boundary regions. Many aspects of plant architecture are dependent on the boundaries (Ejaz et al., 2021; Žádníková & Simon, 2014). For example, in the context of architecture development they determine the production of the Axillary Meristems (AM), fruit dehiscence, and organ abscission.
In the boundaries, a unique set of transcription factors is expressed. These transcription factors play an important role in repressing cell proliferation, a prerequisite for the development of separate organs. Indeed, loss-of-function mutants for these transcription factors often present organ fusion, but also defects in organ development and altered phyllotactic patterning.
After the floral transition, at the IM level, the indeterminate stage is maintained by *SHOOT MERISTEMLESS* (*STM*), a class I *KNOTTED1-like* (*KNOX*) homeodomain protein; and two *BELL* homeodomain proteins encoded by *PENNYWISE* (*PNY*), also known as *REPLUMLESS* (*RPL*); and *POUND-FOOLISH* (*PNF*) (Endrizzi et al., 1996; Smith et al., 2004; Roth et al., 2018).

The *NAM-ATAF-CUC* (*NAC*)-type *CUP-SHAPED COTYLEDON* (*CUC1,2,3*) genes control the specification of organ boundaries, by repressing growth in these areas. The double mutant *cuc1 cuc2* displays organ fusions (Aida et al., 1997), while the *cuc3* mutant shows defects in axillary shoot formation (Hibara et al., 2006). Among the direct targets of *CUC1* there are the two *ALOG* (*Arabidopsis LSH1* and *Oryza G1*) family members *ORGAN BOUNDARY1/LIGHT-DEPENDENT SHORT HYPOCOTYL3* (*OBO1/LSH3*) and *OBO4/LSH4*, which are thought to repress differentiation of boundary cells (Cho & Zambryski, 2011b; S. Takeda et al., 2011).

Among *STM* and *CUC* genes exists a reciprocal regulation, where *CUC1* and *CUC2*, expressed in the organ boundaries, activate *STM* expression (Aida et al., 1999; Takada et al., 2001). *STM* in turn

confines the expression of *CUC* genes to the boundary domains likely through the direct regulation of *CUC1* and indirect regulation of *CUC2* and *CUC3* (Spinelli et al., 2011).

An important role for the correct positioning and development of plant organs is also played by the lateral organ boundary genes *BLADE-ON-PETIOLE1/2* (*BOP1/2*), which encode for BTB/POZ domain proteins that, acting together with the AP2/EREBP gene *PUCHI*, promote the development of the determinate FM through the promotion of *LFY* expression and the activation of *AP1* (Chahtane et al., 2018; Karim et al., 2009; M. Xu et al., 2010). *PNY* and *PNF* allow the correct localization of *BOP1*, *BOP2* and consequently of their downstream targets *KNOTTED-LIKE FROM ARABIDOPSIS THALIANA6* (*KNAT6*) and *ARABIDOPSIS THALIANA HOMEOBOX GENE1* (*ATH1*) (Ejaz et al., 2021; J. Liu et al., 2022). In the *pny pnf* double mutant there is an impairment in stem cells maintenance, in inflorescence elongation and flowering (Kanrar et al., 2006; Lal et al., 2011). These defects are due to the misexpression of *BOP1*, *BOP2*, *KNAT6* and *ATH1* which prevent the accumulation of the floral meristem identity genes like *LFY* and *AP1*, which are required for flower production (Khan et al., 2015).

As already mentioned, wild type Arabidopsis flowers are not subtended by bracts, which instead remain cryptic, meaning that there is no outgrowth of these organs. The correct development of the FM and of the boundary areas represses bract growth. Different mutants for genes involved in FM and boundary specification are reported to develop bracts. For example, the loss of floral identity in axillary meristems due to mutations in flower meristem identity genes, such as *lfy* and *ap1*, results in the outgrowth of bracts (Irish & Sussex, 1990; Schultz & Haughn, 1991; Weigel et al., 1992b). This indicates that *LFY* and *AP1* have a role in prevent the abaxial part of the FM to proliferate. Loss of function of the transcription factor *JAGGED* (*JAG*) combined with *lfy* or *ap1* suppresses bract outgrowth. Since ectopic *JAG* expression rescues bracts development, it is possible to hypothesize that expression of *AP1* and *LFY* in axillary meristems causes bract suppression repressing *JAG* in the subtending leaf primordium (Dinneny et al., 2004; Ohno et al., 2004).

Also the *bop1 bop2* double mutant is able to produce occasionally small bracts. This phenotype is enhanced in the *bop1 bop2 lfy* triple mutant, where all the flowers are subtended by bracts. This indicates a synergistic action of these three genes in the specification of FM identity and bract suppression (Norberg et al., 2005). Another player in this pathway is *PUCHI*; *puchi-1* plants indeed can develop rudimentary bracts subtending the flowers (Bellande et al., 2022). This phenotype is further enhanced in the triple mutant *puchi bop1 bop2*, where the flowers are subtended by well-developed bracts. This suggests that *BOP1*, *BOP2* and *PUCHI* are essential for the activation of the

expression of *LFY* and *AP1* and for the specification of the identity of the FM and to prevent bract formation (Karim et al., 2009). The correct balance among all these players allows the different areas of the inflorescence meristems to maintain their identity.

2. The *ALOG* gene family

As already described, the establishment of the inflorescence architecture of plants depends on the timing of the transition between determinate and indeterminate stages of the meristems and on the ability of the different meristems to maintain their identity.

A complex gene regulatory network regulates these processes. Although many genes taking part in these pathways have been characterized, many are still unknown. Previous work performed by our laboratory was focused on the identification of new players involved in inflorescence architecture development. Indeed, Mantegazza et al. (2014) and Harrop et al. (2016) performed a laser-microdissection followed by an RNA-seq on the different reproductive meristem tissues in Arabidopsis and rice respectively. The analysis of the differentially expressed genes in the different meristem types showed that members of the *ALOG* gene family are candidates to play a role in inflorescence development in both *Oryza sativa* and *Arabidopsis thaliana*.

The *ALOG* gene family takes its name from the *Arabidopsis LIGHT-DEPENDENT SHORT HYPOCOTYL 1* and *Oryza G1*, which were the first two members of this family characterized in *Arabidopsis thaliana* and *Oryza sativa* respectively. Ten *ALOG* genes are present in Arabidopsis and 14 in rice (N. Li et al., 2019). These genes encode for putative transcription factors which contain a DNA binding domain (also called *ALOG* domain) and a putative Nuclear Localization Signal (NLS). The *ALOG* domain is highly conserved among land plants and evolutionary studies propose that it is derived from DIRS1-like LTR retrotransposons, found in several eukaryotes (N. Li et al., 2019). Even if the *ALOGs* are widely diffused in plants, only few members of this family have already been characterized.

LIGHT-DEPENDENT SHORT HYPOCOTYLS 1 (*LSH1*) was the first *ALOG* gene to be characterized in Arabidopsis. The overexpression of *LSH1* determines a sensibilization of the plants to continuous red, far red and blue light. As a result, the transgenic plants develop a shorter hypocotyl than the wild type. Furthermore, the analysis of transgenic plants carrying the β-glucuronidase (GUS) gene under the control of the *LSH1* promoter; and a protein fusion between LSH1 and GFP showed that *LSH1* presents nuclear localization and that it is expressed in hypocotyls, shoot apices and root primordia (Zhao et al., 2004).

Other two *ALOG* genes that have been characterized in Arabidopsis are *LSH3* and *LSH4* (Bencivenga et al., 2016; Cho & Zambryski, 2011a; S. Takeda et al., 2011). These two genes are phylogenetically closely related and are reported to be expressed in the boundary cells of the shoot organs, where they are positively regulated by *CUC1* to suppress organ differentiation in the boundary region (Takeda et al., 2011). The overexpression of *LSH4* causes the plant to produce small, wrinkled leaves and, during the reproductive phase, flowers with extra organs. A similar but milder phenotype is reported for the overexpression of *LSH3*. When both *LSH3* and *LSH4* are ectopically expressed, they induce over proliferation of the shoot meristems and the formation of ectopic organs (Cho & Zambryski, 2011a; S. Takeda et al., 2011).

LSH4 was also reported to be repressed by *RPL*. RPL can control the directional division of the cells in the Rib Zone (RZ) of the meristem by repressing *LSH4* expression and confine it in the boundary region (Bencivenga et al., 2016).

The first *ALOG* gene to be studied in rice was *LONG STERILE LEMMA G1* (*G1*), which is involved in the repression of lemma identity to specify the sterile lemma in the context of spikelet development. *G1* is expressed in sterile lemma primordia throughout its development. In WT spikelets the sterile lemma is much smaller than the lemma and is attached to the base of the lemma. In contrast, in the *g1* mutant the sterile lemma enlarges and acquires lemma identity (Yoshida et al., 2009).

Another member of the *ALOG* gene family that has been studied is *TRIANGULAR HULL1* (*TH1*), is involved in the regulation of spikelet formation. The *th1* mutant presents lemmas and paleas that are narrower than the wild type (Peng et al., 2017; Sato et al., 2014; Wang et al., 2019).

The latest *ALOG* gene that was characterized in rice is *TAWAWA 1/G1-LIKE 5* (*TAW1/G1L5*), a regulator of panicle branching with an effect on grain yield (Yoshida et al., 2013; Yuan et al., 2021).

The role of *TAW1* during the reproductive development of rice is to negatively regulate the transition from the indeterminate stage of BMs to a determinate stage of SM. The overexpression of *TAW1* causes a delay in the timing of this transition, resulting in a more branched panicle. On the other hand, a reduction in the activity of *TAW1* determines a precocious specification of the BMs in SMs, that finally results in a less branched panicle (Yoshida et al., 2013; Yuan et al., 2021).

Members of the *ALOG* gene family were also characterized in other plant species, such as *Solanum lycopersicum*. *TERMINATING FLOWER* (*TMF*), an ortholog of *TAW1* in tomato, results to be expressed in the shoot apex, where it regulates inflorescence development by repressing the floral meristem identity genes like *FALSIFLORA* (*FA*) and *MACROCALYX* (*MC*) (the tomato orthologs of

Arabidopsis *LFY* and *AP1*). Indeed, in *tmf* mutant plants the FM identity genes show a precocious activation that leads to the development of a single flower instead of a sympodial inflorescence. On the other hand, the overexpression of *TMF* leads to ectopic leaves formation, reversion to vegetative meristem identity and more branches, indicating a delay in the specification of FMs (MacAlister et al., 2012).

It was also reported that TMF can interact with two orthologs of the Arabidopsis BLADE ON PETIOLE 1 (BOP1), BOP2, SlBOP1 and SlBOP2; but also with SlBOP3. In Arabidopsis BOP factors are already known to have a role in growth and development, in leaf complexity and organ abscission (Hepworth et al., 2005; McKim et al., 2008; Norberg et al., 2005). *TMF* can interact with the three tomato SlBOPs, recruiting them to the nucleus and suggesting the formation of a transcriptional complex. This hypothesis is sustained by the fact that mutations in *SlBOPs* cause pleiotropic defects, that are more severe in double and triple mutants; notably the inflorescences simplify into single flowers, resembling *tmf* mutants (Izhaki et al., 2018; C. Xu et al., 2016).

In *Lotus japonicus* a member of the *ALOG* gene family, *LjALOG1*, was identified as one of the promoters of the nodulation process in roots (Lei et al., 2019).

All these studies suggest the importance of the *ALOG* gene family in developmental processes in different plant species, making it an important gene family to study. We tried to determine the role of some members of the *ALOG* gene family in the context of reproductive development of rice and Arabidopsis. Since little is known about their protein structure and their ability to bind DNA as transcription factors, we collaborated with the group of Francois Parcy, at the Laboratoire Physiologie Cellulaire et Végétale, in Grenoble (France), which performed experiments to elucidate the biochemical structure of ALOG proteins and their ability to bind DNA (unpublished data).

2.1 *ALOG* genes in *Oryza sativa*

As already mentioned, from the analysis of the transcriptome data obtained from a previous work in our laboratory (Harrop et al., 2016), three members of the *ALOG* gene family, *G1-LIKE 1* (*G1L1*), *G1-LIKE 2* (*G1L2*) and *TAWAWA 1/G1-LIKE 5* (*TAW1/G1L5*) were found to be differentially expressed with a similar pattern in the different reproductive meristem types of rice (**Figure 4**). Except for *G1* (mildly expressed during spikelet development), *G1L4* and *G1L6* (both mildly expressed in the early stages of inflorescence development), the expression of the other members of the *ALOG* gene family was undetectable during rice reproductive meristem development.

Furthermore, the expression pattern of *G1L1* and *G1L2* was found to be similar to that of the already characterized *TAW1*, one of the fundamental regulators of panicle development, involved in the

transition of the reproductive meristems from an indeterminate to a determinate stage (Yoshida et al., 2013). This can indicate that the three factors might have a similar function during the inflorescence development of *Oryza sativa*.

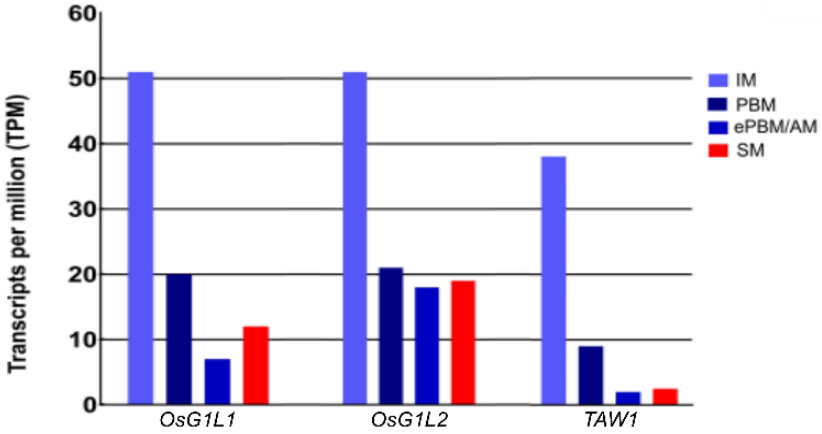

Figure 4. The *ALOG* family genes *OsG1L1*, *OsG1L2* and *TAW1* are highly expressed in reproductive meristems. *OsG1L1* and *OsG1L2* expression in four reproductive meristem types analysed by RNA-seq (Harrop et al. 2016). Read counts are presented in transcripts per million [Inflorescence Meristem (IM), Primary Branch Meristem (PBM), elongated PBM with Axillary Meristem (ePBM/AM), Spikelet Meristem (SM), Flower Meristem (FM)].

2.2 *ALOG* genes in *Arabidopsis thaliana*

The *ALOG* gene family members may also have an important role during reproductive development in *Arabidopsis thaliana*. Indeed, *LSH1*, *LSH3* and *LSH4*, three members of the *ALOG* gene family, were found to be differentially expressed in the IM, FMs, and Stage-3 (ST3) flower tissues RNA seq datasets obtained by our group through laser microdissection (Mantegazza et al., 2014). The expression of the other members of the *ALOG* gene family in the reproductive meristems of Arabidopsis was almost undetectable.

LSH3 and *LSH4* showed a similar pattern, characterized by a higher expression in the IM tissues, respectively 30 and 20 transcripts per million (TPM); progressively lower in the FM tissues (8 and 1 TPM) and to the ST3 tissues (almost undetected for *LSH3* and 1 TPM for *LSH4*). *LSH1* shares this same pattern, but with more than double of the transcript levels in the IM phase. Since *LSH2* is the gene phylogenetically closer to *LSH1*, its expression levels were also checked; but its expression resulted almost undetectable in the reproductive meristem tissues (**Figure 5**).

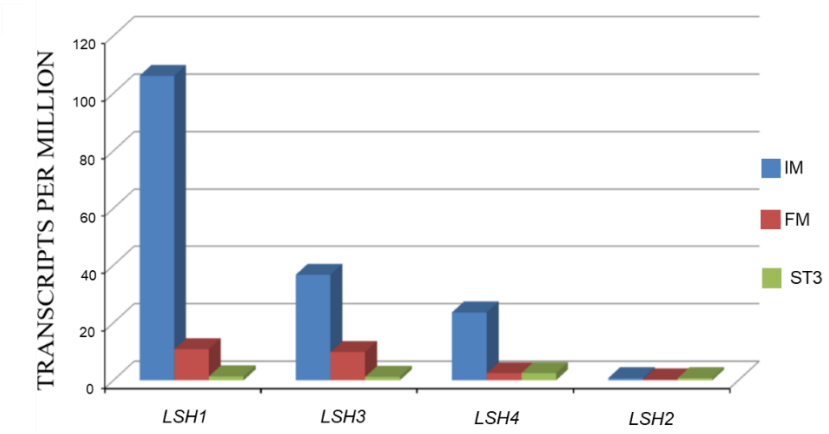

Figure 5. Expression of *LSH1*, *LSH3*, *LSH4* and *LSH2* in the three reproductive tissues analyzed by RNA-seq (Mantegazza et al., 2014). Read counts are presented in transcripts per million. [Inflorescence Meristem (IM), Flower Meristem (FM), Flower primordia at stage 3 (ST3)].

LSH3 and *LSH4* were already published to be involved in the specification of the organ boundaries and in reproductive meristem development. Indeed, the overexpression of *LSH3* and *LSH4* causes the formation of ectopic organs and the over proliferation of meristematic tissues (Cho & Zambryski, 2011a; S. Takeda et al., 2011). Since *LSH1* shares with *LSH3* and *LSH4* a similar expression pattern in the reproductive meristems, it is tempting to hypothesize an involvement of the three genes in the reproductive development of *Arabidopsis thaliana.*

RESULTS

1. Oryza sativa

1.1 Accepted Manuscript (The Plant Journal) - The *ALOG* family members *OsG1L1* and *OsG1L2* regulate inflorescence branching in rice

***Short title:** *OsG1L1* and *OsG1L2* regulate branching in rice

The *ALOG* family members *OsG1L1* and *OsG1L2* regulate inflorescence branching in rice

Veronica M. Beretta[2,a], Emanuela Franchini[2,a], Israr Ud Din[2a,b], Elia Lacchini[a,c], Lisa Van den Broeck[d], Rosangela Sozzani[d], Gregorio Orozco-Arroyo[a], Elisabetta Caporali [a], Hélène Adam[e], Stefan Jouannic[e], Veronica Gregis[a] and Martin M. Kater[a,3]

Affiliations:

[a] Dipartimento di Bioscienze, Università degli Studi di Milano, Via Celoria 26, 20133, Milano, Italy

[b] Present address: Institute of Biotechnology and Genetic Engineering (IBGE),

University of Agriculture, Peshawar 25130, Pakistan

[c] Present address: VIB Center for Plant Systems Biology, Technologiepark 71, B-9052 Ghent, Belgium

[d] Plant and Microbial Biology Department, North Carolina State University, Raleigh, NC 27695

[e] DIADE, University of Montpellier, IRD, CIRAD, Montpellier, France

[1] This work was supported by MUR PRIN2017_2017N5LBZK

The PhD fellowship of E.F. and V.M.B, were supported by the Doctorate School in Molecular and Cellular Biology, Università degli Studi di Milano. E.F. was supported by H2020-MSCA-RISE-2015 ExpoSEED Proposal Number: 691109.

[2] These authors contributed equally to the article.

[3] Corresponding author: martin.kater@unimi.it

ORCID IDs: 0000-0003-3293-5137 (V.M.B.), 0000-0002-0643-2408 (I.U.D.), 0000-0002-1598-8950 (E.L.), 0000-0001-7509-6244 (G.O.A.), 0000-0003-0226-0757 (L.V.B.), 0000-0003-3316-2367 (R.S.), 0000-0003-0324-6201 (H.A.), 0000-0001-5777-3336 (S.J.), 0000-0003-1876-9849 (V.G.), 0000-0003-1155-2575 (M.K.)

One-sentence summary: *OsG1L1* and *OsG1L2* control panicle architecture by delaying the transition from indeterminate branch- to determinate spikelet-meristem identity.

Author contributions: M.K. and V.G. conceived and designed the research. E.F., V.M.B., E.C., I.U.D., G.O.A., L.V.B., R.S. and E.L. carried out and interpreted the experiments. H.A. and S.J. contributed to experimental design and analysis. V.M.B., E.F., V.G. and M.K. wrote the article with the contribution of all the authors.

Keywords: *Oryza sativa*, transcription factor, inflorescence architecture, meristem identity, transcriptome analysis, CRISPR mutants, gene regulatory network, *ALOG*.

ABSTRACT

The architecture of the rice inflorescence is an important determinant of crop yield. The length of the inflorescence and the number of branches are among the key factors determining the number of spikelets, and thus grains, that a plant will develop. Especially the timing of the identity transition from indeterminate branch meristem to determinate spikelet meristem regulates the complexity of the inflorescence. In this context, the *ALOG* gene *TAWAWA1* (*TAW1*) has been shown to delay the transition to determinate spikelet development in rice. Recently, by combining precise laser microdissection of inflorescence meristems with RNA-seq we observed that two *ALOG* genes, *Oryza sativa OsG1-like 1* (*OsG1L1*) and *OsG1L2,* have an expression profile similar to *TAW1*. Here we report that *osg1l1* and *osg1l2* loss-of-function CRISPR mutants have similar phenotypes as the previously published *taw* mutant, suggesting that these genes might act on related pathways during inflorescence development. Transcriptome analysis of the *osg1l2* mutant suggested interactions of *OsG1L2* with other known inflorescence architecture regulators and the datasets were used for the construction of a gene regulatory network (GRN) proposing interactions among genes potentially involved in controlling inflorescence development in rice. We selected in this GRN the homeodomain-leucine zipper transcription factor encoding gene *OsHOX14* for further characterisation. The spatio-temporal expression profiling and phenotypical analysis of CRISPR loss-of-function mutants of *OsHOX14* suggests that the proposed GRN indeed serves as a valuable resource for the identification of new players involved in rice inflorescence development.

INTRODUCTION

The inflorescences of land plants show a wealth of distinct architectures which evidences their importance for reproductive success. The plant species or family-specific inflorescence shape depends on the identity and activity of meristems which determine the degree of branching and the number of flowers that will ultimately develop. Inflorescence meristems are defined as indeterminate since they continue to develop meristems in the axils of lateral organs, such as bracts. On the contrary, floral meristems are determinate as the development of the floral organs exhausts meristematic activity. In this sense, the formation of flowers can be seen as a developmental endpoint. An extreme example are tulips, where the apical meristem transforms into a floral meristem and forms one single apical flower. It is thus the transition from indeterminate to determinate meristems that defines the complexity of an inflorescence (Hake, 2008).

Oryza sativa, commonly known as rice, develops a complex and determinate inflorescence, named panicle (Bommert et al., 2005; Han et al., 2014). Its architecture is established during early stages of rice reproductive development, and it depends on the activity of different meristem types (Tanaka et al., 2013; Caselli et al., 2020). During the floral transition, the rice Shoot Apical Meristem (SAM) becomes Inflorescence Meristem (IM), also called Rachis Meristem. The IM gives rise to Primary Branch Meristems (PBMs) that produce Axillary meristems (AMs) which could differentiate into indeterminate Secondary Branch Meristems (SBMs) or determinate Spikelet Meristems (SMs). In the same way, SBMs elongate and produce SMs. In rice, the SM develops three floral meristems (FMs), of which one will differentiate into one fertile floret, whereas the other two will develop into empty glumes (sterile lemmas); thus, exhausting the pool of meristematic cells (Bommert et al., 2005; Han et al. 2014). Furthermore, the length of the rice inflorescence, and consequently the number of primary branches that can develop, is also determined by the timing of IM abortion with the formation of an undifferentiated dome.

Rice plants in which early transitions to SM identity occur will develop less complex panicles with fewer grains in contrast to plants in which the transition is delayed. Among the genes that have been identified to control this transition are *ABERRANT PANICLE ORGANIZATION1 (APO1)* and *APO2* (Ikeda-Kawakatsu et al., 2012). Both are mainly expressed in IM and in BMs, where they also promote cellular proliferation. They are orthologs of the *Arabidopsis thaliana* genes *UNUSUAL FLORAL ORGANS* (*UFO*) and *LEAFY* (*LFY*), respectively. However, while the *UFO* and *LFY* promote floral identity, *APO1* and *APO2* repress the transition to determinate spikelet meristem formation (Ikeda-Kawakatsu, et al., 2009; Ikeda-Kawakatsu, et al., 2012). Recently, it was shown that LARGE2, a HECT-domain E3 ubiquitin ligase OsUPL2, interacts directly with APO1 and APO2 to modulate their stability. Genetic analysis of the *large2* mutant, which displays bigger panicles with more branches and grains, confirmed that *LARGE2* functions in a common pathway with *APO1* and *APO2* (Huang et al., 2021). *TAWAWA1* (*TAW1*)/*G1-LIKE 5* (*G1L5*) is another gene that promotes BM identity and suppresses SM specification by activating genes involved in the repression of floral transition (Yoshida et al., 2013). The dominant *taw1-D* gain-of-function mutant shows a delay in spikelet specification

which results in increased branching and higher grain numbers. *TAW1* belongs to the *Arabidopsis LSH1 and Oryza G1* (*ALOG*) gene family, which includes fourteen *ALOG* genes in rice. The ALOG domain is highly conserved among land plants and evolutionary studies propose that it is derived from the N-terminal DNA-binding domain of integrases that belong to the tyrosine recombinase superfamily which are encoded by a distinct type of DIRS1-like LTR retrotransposons that are found in several eukaryotes (Iyer & Aravind, 2012; Naramoto et al., 2020).

Harrop et al. (2016) used laser microdissection microscopy to specifically isolate different rice inflorescence meristem tissues for RNA-seq based expression profiling. Subsequent transcriptome analysis revealed that two *ALOG* genes, *OsG1L1* and *OsG1L2*, have similar expression profiles as *TAW1*. All three genes are highly expressed in the IM and subsequently, their expression gradually decreases in PBM, ePBM/AMs and SM. Phylogenetic analysis showed that *OsG1L1* and *OsG1L2* cluster both in subgroup A and are therefore more distantly related to *TAW1* which belongs to subgroup C (Li et al., 2019).

Here, we describe the functional analysis of *OsG1L1* and *OsG1L2* which provides evidence that both genes play a similar role in rice inflorescence development. Like in the *taw1-3* and *TAW1* RNAi lines, both *osg1l1* and *osg1l2* CRISPR-Cas9 mutants showed a reduced branching phenotype and lower grain numbers. RNA-seq analysis of developing *g1l2* inflorescences was used to compute a gene regulatory network (GRN). Validation of the resulting network by the functional characterization of the homeodomain-leucine zipper transcription factor gene *OsHOX14* suggests that the proposed GRN could serve as a valid resource for the identification of genes controlling inflorescence development in rice.

RESULTS

OsG1L1 and *OsG1L2* expression analysis

Previous transcriptome analysis of laser micro-dissected rice reproductive meristems allowed the identification of two *ALOG* genes, *OsG1L1* and *OsG1L2* that share a similar expression profile with the previously studied *TAW1* gene (Harrop et al., 2016; Yoshida et al. 2013; Fig. 1A). These genes are highly expressed in the Inflorescence Meristem (IM), then mRNA abundance decreases in the Primary Branch Meristem (PBM), and a further reduction is observed in the elongated PBM with axillary meristems (ePBM/AM). In the Spikelet Meristem (SM) there is a slight increase in mRNA levels for all three genes.

To determine in more detail the expression profile of *OsG1L1* and *OsG1L2* and to confirm their expression in reproductive meristems, we performed real-time PCR on different plant tissues such as the root, the root tip (where the Root Apical Meristem (RAM) is localised), young and mature leaves, the Shoot Apical Meristem (SAM), all reproductive meristems enriched tissues, like IM, PBM, ePBM/AM, SM/FM and milk and mature grains, respectively at 8 and 30 days after fertilisation. The different meristem-type enriched tissues were collected following the time points defined for the Nipponbare cultivar as described previously (Harrop et al., 2016) and the correct developmental stage was checked using a stereomicroscope. Since the expression of

TAW1 was already described (Yoshida et al., 2013), it was used as a positive control. This analysis showed that all three genes are preferentially expressed in inflorescence meristem tissues (Fig. 1B).

RNA in situ hybridisation was performed to further investigate and compare the spatiotemporal expression of *OsG1L1*, *OsG1L2* and *TAW1* during different stages of panicle development. We designed for each of the three genes a specific digoxigenin-labelled RNA probe. This analysis revealed that *OsG1L1* and *OsG1L2* have a similar expression profile as *TAW1*. All three genes are expressed in the IM, PBM, ePBM/AM and SM/FM, suggesting *OsG1L1* and *OsG1L2* might have a similar functional role in the reproductive meristems as *TAW1* **(**Fig. 1C**).**

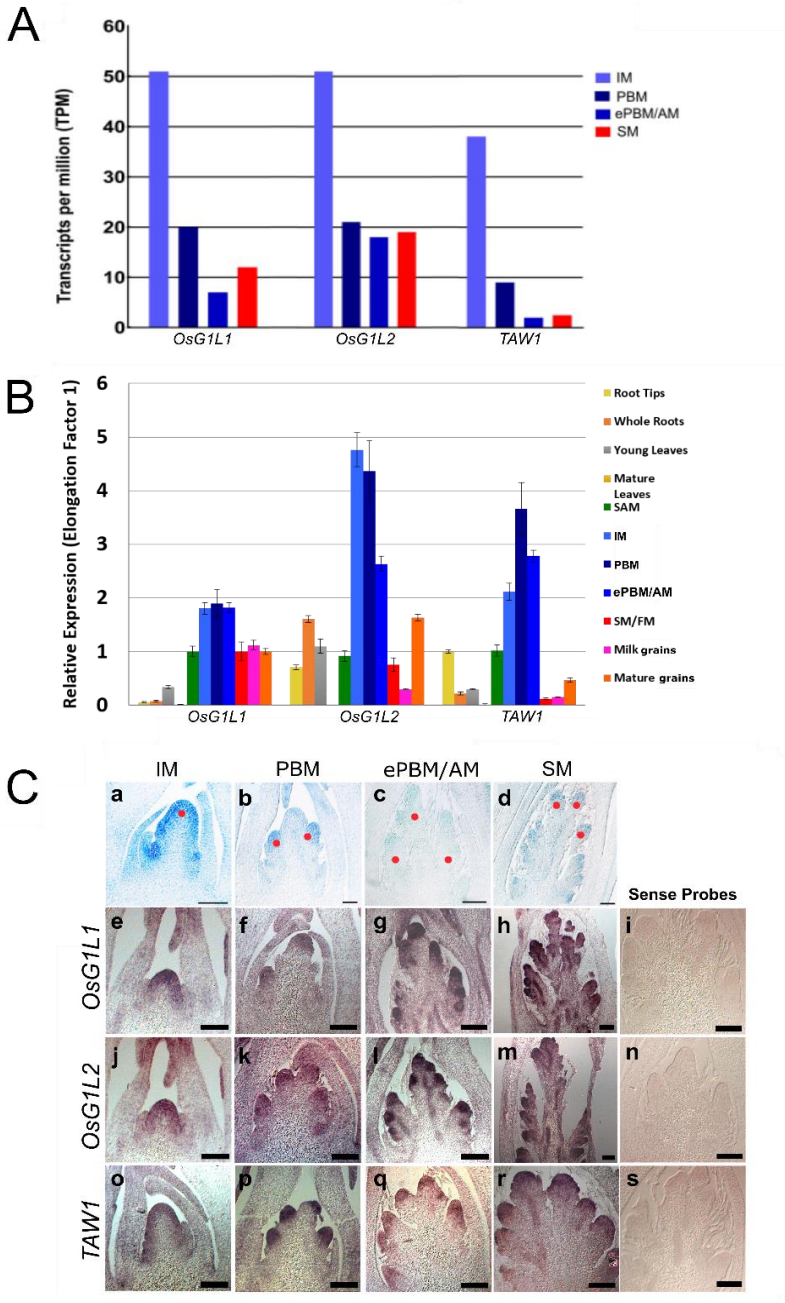

Fig. 1. The *ALOG* family genes *OsG1L1, OsG1L2* and *TAW1* are highly expressed in reproductive meristems. A, *OsG1L1* and *OsG1L2* expression in four reproductive meristem types analysed by RNA-seq (Harrop et al. 2016). Read counts are presented in transcripts per million. B, *OsG1L1, OsG1L2* and *TAW1* expression by qRT-PCR in different tissues: vegetative tissues (roots and leaves), manually dissected IM, PBM, ePBM/AM, SM/FM meristems and grains. C, Expression pattern of *OsG1L1, OsG1L2* and *TAW1* analysed by *in situ* hybridization in the four developmental stages that are presented in panel A and described in the text. Red dots indicate respectively the different meristematic tissues: IM (a), PBM (b), ePBM/AM (c) and SM (d). *OsG1L1* Antisense probe (e-h), *OsG1L1* sense negative control probe (i), *OsG1L2* antisense probe (j-m), *OsG1L2* sense negative control probe (n), *TAW1* antisense positive control probe (o-r), *TAW1* sense negative control probe (s). Scale bars represent 50 μm (a-c) and 100 μm (d-s). [Inflorescence Meristem (IM), Primary Branch Meristem (PBM), elongated PBM with Axillary Meristem (ePBM/AM), Spikelet Meristem (SM), Flower Meristem (FM)].

Analysis of the *osg1l1* and *osg1l2* mutant phenotypes

To functionally characterise *OsG1L1* and *OsG1L2*, CRISPR-Cas9 genome editing technology was used to generate mutations in these genes. A specific single-guide RNA (sgRNA) was designed for each gene and the two CRISPR-constructs (Miao et al. 2013) were used for *Agrobacterium tumefaciens* mediated transformation of rice embryonic calli. The two sgRNAs were designed to create indels in the ALOG domain.

The sgRNA designed for *OsG1L1* targeted the first exon at 397 bp from the ATG start site, whereas the sgRNA for *OsG1L2* was designed to target a region 131 bp downstream from the ATG start site (Supplemental Fig. S1 A; Supplemental Fig. S2 A). For *OsG1L1*, five T0 transgenic plants with different mutations at the sgRNA target site were obtained. Three of these plants present in frame mutations (3 and 6 bp deletions) and were not further analysed. Two independent transformants had a homozygous deletion of 2 bp (AG) at 145 bp from the translation start site. This mutation created a frameshift resulting in the formation of an aberrant protein, characterised by the disruption of the ALOG domain and of the putative nuclear localization signal (NLS). For these reasons, the obtained aberrant protein is most likely not functional (Supplemental Fig. S1 B-C). We used for further analysis the two *osg1l1* mutants that present an AG homozygous deletion and in the T2 generation we obtained homozygous plants without the Cas9 encoding T-DNA insertion.

For the CRISPR-construct targeting *OsG1L2*, eighteen T0 transgenic rice plants were generated. All these plants had a similar frameshift mutation due to the insertion of a single base pair (A, C, G or T) at 148 bp from the start site. The A insertion leads to the formation of a premature stop codon (TGA), resulting in the production of a truncated protein of 49 amino acids (Supplemental Fig. S2 B-C), lacking the ALOG domain and the putative NLS. The insertion of one of the other bases (C, G, T) leads to the formation of a protein of 176 amino acids without the ALOG domain and the putative NLS (Supplemental Fig. S2 C). We selected in the T1 generation two independent *osg1l2* mutant lines having an A or C insertion. In the T2 generation we obtained lines homozygous for these insertions and without the Cas9 encoding T-DNA insertion. For detailed phenotyping we used the line with the A insertion.

Considering that the expression of *OsG1L1* and *OsG1L2* was predominant in the reproductive meristem tissues, a detailed phenotypic analysis of the panicle was performed using Panicle TRAit Phenotyping software (P-TRAP) (Fig. 2; AL-Tam et al., 2013). To obtain a robust statistical analysis, at least 15 plants for each

genotype were analysed. In particular we analysed 15 wild-type plants, 19 *osg1l1* mutants and 20 *osg1l2* mutants. After panicle imaging, the P-TRAP software quantified the traits related to the panicle architecture and grain numbers (Supplemental Table S1).

This analysis showed that *osg1l1* and *osg1l2* produced significantly shorter panicles than wild-type plants. Furthermore, their panicles developed fewer PBs, SBs and spikelets**.** In particular, the *osg1l1* mutants produced panicles that were on average 2 cm shorter than wild type and developed on average 3 PBs and 30 spikelets less than wild-type plants. Interestingly, the number of SBs was not significantly different from wild type (Fig. 2 C-F).

The *osg1l2* mutant plants produced panicles that were on average 1.5 cm shorter than wild type and developed on average 4 PBs, 8 SBs and 51 spikelets less than wild-type plants (Fig. 2 C-F). This analysis confirmed a previous independent experiment in which PBs, SBs and spikelets numbers were compared between wild-type and *osg1l2* plants with a different mutation (a C insertion at 148 bp from the ATG) (Supplemental Fig. S3).

The P-TRAP analysis revealed also that both *osg1l1* and *osg1l2* mutant lines had longer PBs and SBs as well as longer internodes in PBs (Fig. 2 G-I). In detail, the *osg1l1* mutant plants displayed PBs and SBs that were on average respectively 1 cm and 0.5 cm longer than those of wild-type rice plants. The internodes of PBs were on average 0.4 cm longer than in wild type. The *osg1l2* mutant plants instead produced PBs and SBs that were on average 1.6 cm and 1 cm longer than the wild type, respectively. The internodes of PBs were on average 0.7 cm longer than the wild type. Overall, both mutants showed similar aberrations in panicle architecture although the phenotype of the *osg1l2* mutant was more severe.

We also investigated whether the loss-of-function of *OsG1L1* and *OsG1L2* affects grain size. We compared the length, width and surface area of *osg1l1* and *osg1l2* grains to the wild type. This analysis revealed that *osg1l1* and *osg1l2* mutants produced significantly smaller grains than wild type. Both *osg1l1* and *osg1l2* grains had smaller areas, where *osg1l1* grains had a reduced length and width and *osg1l2* grains only showed a reduction in grain width compared to wild type (Supplemental Fig. S4).

Since *OsG1L1* and *OsG1L2* resulted to be preferentially expressed in the inflorescence meristems, we decided to focus our attention on the development of the panicle.

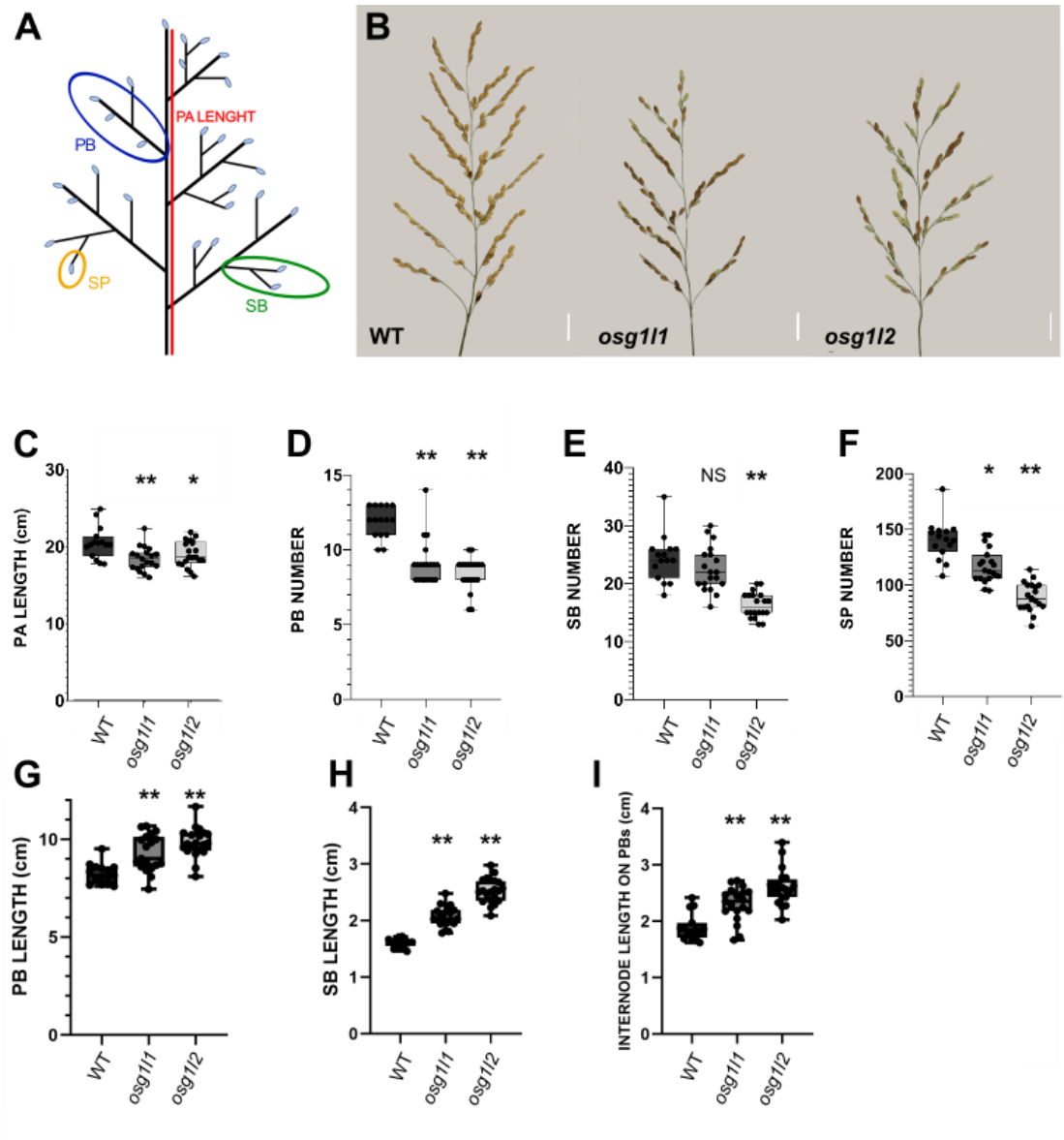

Fig. 2. Phenotypical analysis of panicle architecture in wild type, *osg1l1* and *osg1l2* mutants. A, Schematic representation of panicle structure [PA= panicle; PB= primary branches; SB= secondary branches; SP= spikelets]. B, Main panicles of WT, *osg1l1* and *osg1l2* (2 cm scale bars). Graphs representing the comparison of: (C) Panicle (PA) Length, (D) Primary Branches (PB) number, (E) Secondary Branches (SB) number, (F) Spikelets (SP) number in WT, *osg1l1* and *osg1l2* backgrounds. Graphical representation of the comparison between the: (G) length of Primary Branches (PB), (H) length of Secondary branches (SB) and (I) length of the internodes in PBs. One-Way ANOVA with Tukey test; **p<0,01; * p<0,05.

Comparative analysis of *OsG1L1*, *OsG1L2* and *TAW1* function in reproductive meristems

It has been shown that *TAW1*, which shares with *OsG1L1* and *OsG1L2* a similar expression profile, is a suppressor of the phase change from branch meristems to SMs identity (Yoshida et al., 2013). Since the panicle architecture phenotype of the *osg1l1* and *osg1l2* mutants was similar to the *taw1-3* mutant, we investigated the possibility that these three *ALOG* genes act in the same pathway.

In the dominant overexpression mutant *taw1-D1* three *SHORT VEGETATIVE PHASE* (*SVP*) genes, *OsMADS22*, *OsMADS47* and *OsMADS55*, were upregulated (Yoshida et al., 2013). To investigate whether these genes are deregulated in the *osg1l1* and *osg1l2* mutants, we performed a qRT-PCR analysis using three biological replicates of developing inflorescences enriched in PBMs and ePBM/AMs of wild type, *osg1l1* and *osg1l2*. There were no significant differences in the expression of the three *SVP* genes in the *osg1l1* and *osg1l2* backgrounds compared to the wild type. Only *OsMADS22* seems to present a trend of upregulation just in the *osg1l1* background, which didn't result to be statistically significant (Supplemental Fig. S5).

Yoshida et al. (2013) showed that in the *taw1-D1*, *TAW1* overexpression led to a delay in the phase change from BMs to SMs. To determine whether *OsG1L1* and *OsG1L2* are also involved in this phase transition, we performed an in-situ hybridization using developing panicles at ePBM/AMs stage of wild-type, *osg1l1* and *osg1l2* mutant backgrounds using a digoxigenin-labelled RNA probe specific for *FRIZZY PANICLE* (*FZP*). *FZP* encodes for a protein containing an *APETALA2/ETHYLENE RESPONSE FACTOR* (*AP2/ERF*) domain and has a precise expression pattern that marks the specification of the SM (Bai et al., 2016; Fujishiro et al., 2018; Komatsu et al., 2003). The developing panicles were harvested 16 days after floral induction. In the *osg1l1* and *osg1l2* backgrounds, we observed an increase in *FZP* expression spots that mark the specification of spikelet meristems at the ePBM/AM stage. This suggests that the overall developmental program leading to the switch from indeterminate to determinate meristems in the two mutants occurs earlier with respect to wild type (Fig. 3A-C and Supplemental fig. S6). The earlier specification of the SMs in the *osg1l1* and *osg1l2* mutants was further evidenced by Scanning Electron Microscopy (SEM) (Fig. 3D-I). A whole developing panicle was harvested and scanned from each plant (Fig. 3D-F). Altogether, our analyses clearly demonstrated that both *OsG1L1* and *OsG1L2* are involved in maintaining the indeterminate state of reproductive meristems.

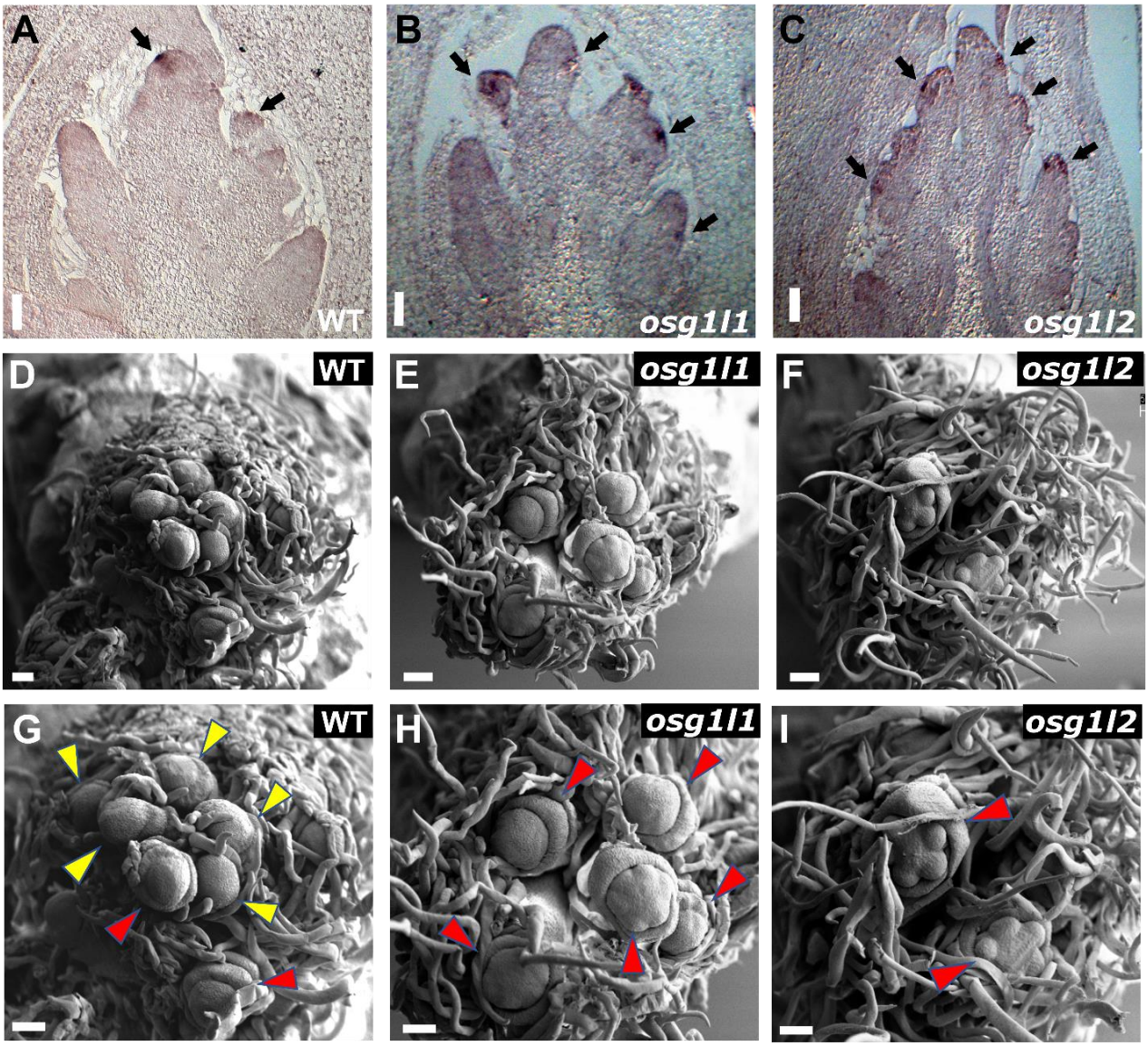

Fig. 3. Expression pattern of *FZP* analysed by *in situ* hybridization at the ePBM/AM stage in wild type (WT, A) *osg1l1* (B) and *osg1l2* (C) backgrounds. [Scale bars represent 50 µm; black arrows indicate *FZP* signal]. **Scanning electron microscopy (SEM) analysis of rice reproductive meristems**, collected at 16 days after the flowering induction in short-day conditions in wild type (D, G); *osg1l1* (E, H) and *osg1l2* (F, I) backgrounds (G, H and I show an enlargement of the meristems that are shown in D, E and F, respectively). Yellow arrows indicate meristems at the indeterminate stage. Red arrows indicate meristems that already reached the determinate stage. In E and F stamen primordia are visible. Scale bars = 50 µm.

Transcriptome analysis of the *osg1l2* mutant at early stages of inflorescence development

The phenotypic analysis of the *osg1l1* and *osg1l2* mutants suggests that both genes may play a similar role during rice inflorescence development. Since inflorescence branching was more severely affected in the *osg1l2*

mutant, this line was selected for RNA-seq transcriptome analysis to obtain deeper insights into the role this *ALOG* gene plays at the early stages of panicle development.

Developing inflorescences enriched in PBMs and ePBM/AMs of the wild type and the *osg1l2* mutant were manually dissected. Four biological replicates were collected, each replicate consisting of 8 to 10 dissected inflorescences. Subsequently, RNA was extracted and used for Illumina sequencing.

The raw RNA-seq files were processed using the TuxNet interface (Spurney et al., 2019). Reads were cleaned, mapped on the *O. sativa* reference genome (IRGSP-1.0), normalised, and FPKMs (Fragment per kilobase of transcript per million mapped reads) were calculated (Supplemental Table S3). Finally, performing a pairwise differential expression analysis between the wild type and mutant, the TuxNet interface generated Differentially Expressed Gene (DEG) datasets (Spurney et al., 2019) (Supplemental Table S4).

After data processing, an average of approximately 13.000.000 reads for each replicate were obtained. The alignment of the reads to the reference genome resulted overall in > 97% coverage. Setting the $\log_2$ (Fold Change (FC)) equal to 1 and the q-value equal to 0.05, a total of 246 differentially expressed genes were identified, of which 128 were downregulated and 118 upregulated in the *osg1l2* mutant compared to the wild type. Among the upregulated genes in the *osg1l2* mutant, we identified *OsMADS37*, a MADS-box transcription factor encoding gene homologous to Arabidopsis *FLOWERING LOCUS C* (*FLC*) (Ruelens et al., 2013), and *OsG1L4*, another member of the *ALOG* gene family. Interestingly, also *EPIGENETIC SHORT PANICLE* (*OsESP*), a putative long-noncoding RNA whose overexpression leads to shorter and denser panicles, was upregulated in the *osg1l2* mutant (Luan et al., 2019). Moreover, the expression of genes involved in hormonal pathways was upregulated, such as *OsRR3*, an A-type response regulator that acts as a negative regulator of cytokinin signalling (Cheng et al., 2010). Among the upregulated genes there are several which encode for Zinc-finger transporter proteins and genes encoding for proteins containing a NB-ARC domain, which is associated to plant disease resistance (Van Ooijen et al., 2008) (Supplemental Table S4 and Table 1).

Among the downregulated genes, we found TFs like *OsNAC120* that is similar to NAM/CUC-2 like proteins, which have been shown to control plant growth and development in response to biotic and abiotic stresses (Ooka et al., 2003) and a member of the TCP family, *OsTB1/FC1* (that henceforth will be referred to as *OsFC1*). Interestingly, *OsFC1* is already known to be a negative regulator of tillering and inflorescence development (Takeda et al., 2003; Cui et al., 2020). Notably, the transcription factors *OsMADS34/PAP2* and *OsGATA7*, which are known to be involved in inflorescence architecture establishment and *OsHOX14*, which has been proposed to be involved in panicle development, were also downregulated (Gao et al. 2010; Kobayashi et al., 2012; Shao et al., 2018; Zhang et al., 2018, Zhu et al., 2022). Additional downregulated genes that have been associated with inflorescence development are *OsRCN1* and *OsRCN4* (Putative phosphatidylethanolamine-binding protein and Rice TFL1/CEN homolog) (Nakagawa et al., 2002). Moreover, genes involved in hormonal pathways like *OsIAA14*, belonging to the Aux/IAA family and involved in auxin-response, resulted deregulated (Jain et al., 2006) (Table 1 and Supplemental Table S4).

Gene name	Gene ID	log2 FC	Q-value	Putative function
OsESP	Os01g0356951	6,55E+04	0,00245724	Involved in the regulation of panicle architecture
OsMADS37	Os08g0531900	1,87E+00	0,00245724	Homolog of *FLC* in rice
OsG1L4	Os04g0516200	1,34E+00	0,00245724	Protein of unknown function DUF640 domain containing protein
OsERF112	Os12g0603300	1,09E+00	0,00245724	Similar to AP2 domain containing protein
OSRR3	Os02g0830200	1,95E+00	0,00245724	A-type response regulator involved in Cytokinin signaling
OsNAC120	Os10g0477600	-2,47E+00	0,00245724	Similar to NAM / CUC2-like protein
OsTB1	Os03g0706500	-1,12E+00	0,00245724	*TCP* family transcription factor, negative regulator of lateral branching
OsMADS34/PAP2	Os03g0753100	-1,13E+00	0,00245724	MADS-box transcription factor, involved in inflorescence and spikelet development
OsRCN1	Os11g0152500	-1,04E+00	0,00245724	Putative phosphatidylethanolamine-binding protein, Rice *TFL1/CEN* homolog. Involved in the control of inflorescence architecture and in the repression of flowering
OsRCN4	Os04g0411400	-1,48E+00	0,00839011	Terminal flower 1-like protein
OsHOX14	Os07g0581700	-1,53E+00	0,00456853	Homeodomain-leucine zipper (HD-Zip) transcription factor, may be involved in the regulation of panicle development
OsGATA7	Os10g0557600	-1,49E+00	0,00245724	*GATA* transcription factor. Involved in brassinosteroids-mediated growth regulation, panicle development and grain shape/number/weight/yield
OsIAA14	Os03g0797800	-1,44E+00	0,00245724	Protein belonging to the AUX/IAA protein family

Table 1. Differentially expressed genes in the *osg1l2* mutant that are involved in inflorescence development. For each gene the Gene Name (column one); the Gene ID (column two); the log2 Fold Change (log2 FC, column three); the q-value (column four; a significance cut-off of 0.05 is applied) and information related to their function (column 5).

Gene regulatory network inference predicts a functional role for *OsHOX14*

To identify major regulatory transcription factors underlying the inflorescence phenotype of *osg1l2*, we built a gene regulatory network (GRN) using a regression tree with random forest approach (Spurney et al., 2019). Specifically, we inferred causal relations between 15 identified differentially expressed transcription factors (TFs) (log_2(FC) > 1 or < -1, q-value < 0.05) and 232 downstream genes in *osg1l2* mutant (log_2(FC) > 1 or < -1, q-value < 0.05). The inferred network contained 79 genes, of which five TFs have more than 10 outgoing regulations, including *OsWRKY80* (Wu et al., 2005), *OsG1L2*, *OsMADS37* (Ruelens et al., 2013), *OsFC1* (Takeda et al., 2003; Cui et al., 2020), and *OsGATA7* (Zhang et al., 2018) (Fig. 4). One of these major regulators is *OsG1L2*, regulating 16 downstream genes, several of which have been shown to be involved in rice inflorescence development (Fig. 4C). For example, *OsESP* is a putative long-noncoding RNA whose gain-of-function mutant leads to a short and denser panicle (Luan et al., 2019) and *OsJAZ4*, also known as *OsTIFY11b*, is a positive regulator of grain-size acting downstream of *TRIANGULAR HULL1* (*OsTH1*), another ALOG factor (Hakata et al., 2012; Wang et al., 2019). Interestingly, thirteen of the predicted OsG1L2 targets are upregulated in the *osg1l2* mutant, ten of which are predicted to be co-regulated by *OsFC1*, a gene known to negatively regulate branching (Takeda et al., 2003; Cui et al., 2020).

To identify regulatory subclusters within the *osg1l2* network, we clustered the network genes into different modules with the Cytoscape plugin clusterMaker2 (see materials and methods) (Fig. 4). A total of four modules were identified, one smaller module of 10 genes (Fig. 4 B), and three larger modules of 24, 23 and 22 genes (Fig. 4 A, C, D). The smaller module contains *CYTOKININ-RESPONSIVE GATA TRANSCRIPTION FACTOR1* (*OsCGA1*), of which constitutive overexpression reduced grain filling (Hudson et al., 2013) and *OsMADS37*, the closest homologues of Arabidopsis *FLC* (Shrestha et al., 2014) (Fig. 4 B). One of the largest modules contains two *GATA* TFs, *OsGATA6* and *OsGATA7*, which were recently reported to influence plant architecture and grain shape by regulating cell proliferation and of which CRISPR/Cas9 lines show a similar phenotype as *osg1l2* (Zhang et al., 2018, Zhang et al., 2022) (Fig. 4 D). As we were interested in the regulatory interactions underlying the *osg1l2* mutant phenotype, we focused on module C, which contains four TF encoding genes: *OsG1L2*, *OsFC1*, *OsMADS34*, and *OsHOX14*. Interestingly, *OsMADS34* has been shown to be necessary for correct inflorescence development, further emphasising the functional importance of this regulatory module (Kobayashi et al., 2012). *OsHOX14* can form heterodimers with *OsHOX12*, a gene that regulates panicle exertion (Gao et al., 2016). Overall, our network analysis allowed the identification of many interesting candidates, of which some have already been described in the context of panicle development and who might be targets of OsG1L2 and other major players in this context. This analysis also provided suggestions for genes that might be involved in the same developmental pathway regulating a similar set of genes.

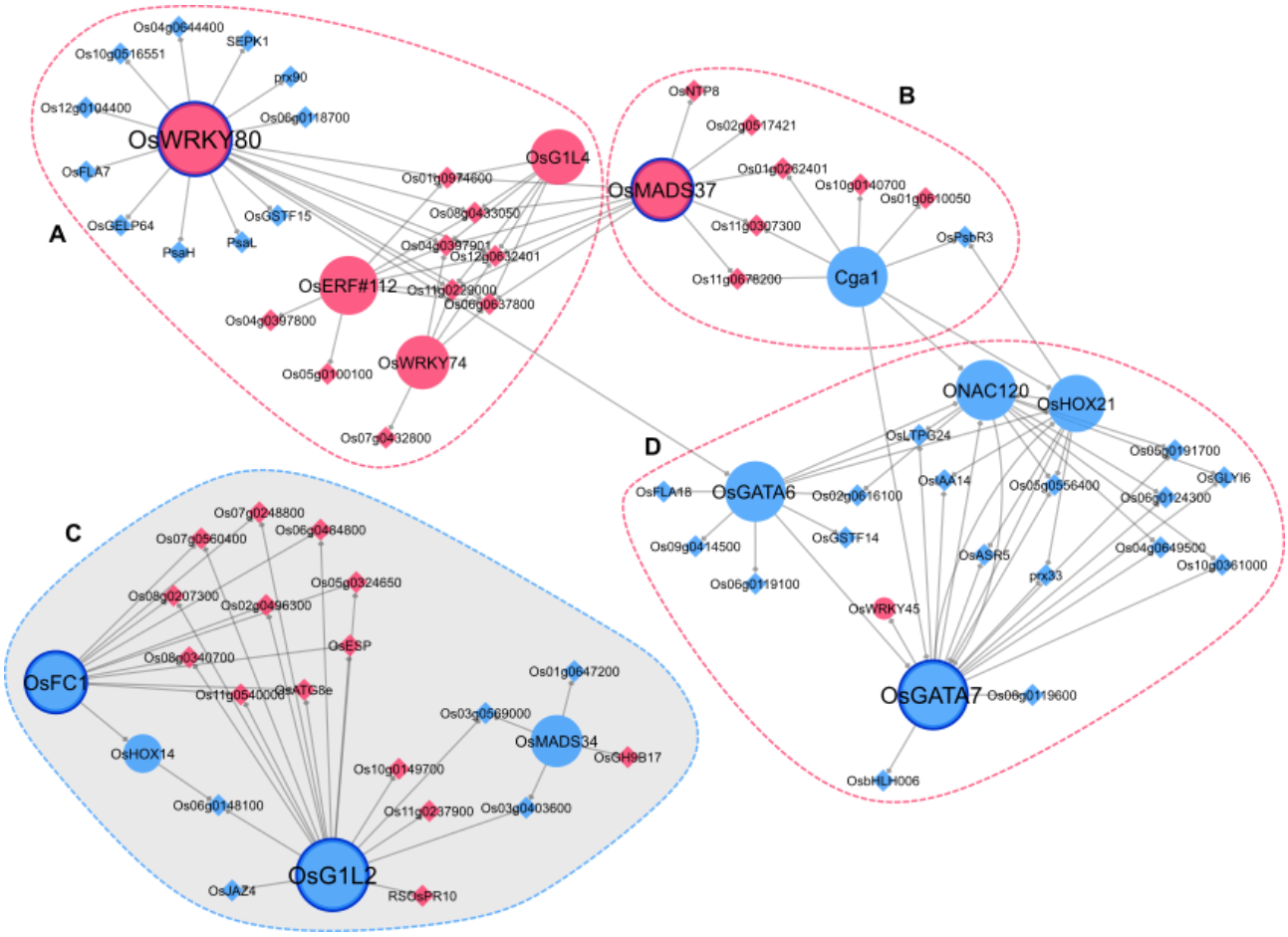

Fig. 4. Graphic representation of the predicted Gene Regulatory Network (GRN). Regulatory interactions were inferred using a regression tree with random forest approach. Transcription factors and other genes are represented in circles and diamonds, respectively. The interactions are represented by a diamond arrow. Upregulated and downregulated genes are highlighted in magenta and light blue respectively**.** Circled with a dotted line, there are the four major subclusters (A to D) in which the network can be divided. Circled in blue with a continuous line there are the five major TFs of the GRN: *OsWRKY80*, *OsG1L2*, *OsMADS37*, *OsFC1*, and *OsGATA7*. The module containing *OsG1L2* is highlighted in grey (C).

Validation of GRNs by qRT-PCR

RT-qPCR experiments were carried out to validate some of the deregulated genes of subcluster C of the predicted GRN (Fig. 5). We focused on those genes that were already proposed to be involved in inflorescence development, such as *OsHOX14, OsMADS34, OsFC1* and *OsESP* (Takeda et al., 2003; Gao et al. 2010; Shao et al., 2018; Luan et al., 2019). *Os03g0569000* was also analysed since the GRN predicted it to be downstream of both *OsMADS34* and *OsG1L2*.

To include the *taw1 CR-1* mutant in this analysis we generated a CRISPR-Cas9 mutant for this gene. The sgRNA was designed to target a region 275 bp downstream from the ATG start site (Supplemental Fig. S7). Two independent transformants had a homozygous insertion of 1 bp (A) at 293 bp from the translation start site. This mutation created a frameshift resulting in the formation of an aberrant protein, characterised by the

disruption of the ALOG domain and of the putative NLS. For these reasons, the obtained aberrant protein is most likely not functional. The *taw1 CR-1* mutants closely resembled the phenotype of the already published missense mutant *taw 1-3* (Yoshida et al., 2013).

The qRT-PCR was performed using three biological replicates of developing inflorescences enriched in PBMs and ePBM/AMs of wild-type, *osg1l1*, *osg1l2* and *taw1 CR-1* plants.

As shown in Fig. 5 (A-E), the qRT-PCR confirmed the downregulation of *OsHOX14, OsMADS34, OsFC1* and *Os03g0569000,* whereas *OsESP* was upregulated in the *osg1l2* mutant.

Expression analysis of the selected genes in the *osg1l1* mutant showed that *OsHOX14*, *OsMADS34, OsFC1* and *Os03g0569000* were also downregulated in this mutant background (Fig. 5B-D)*;* whereas the expression level of *OsESP* was not significantly different from wild-type inflorescences (Fig. 5E). Regarding the expression analysis performed in *taw1 CR-1* mutant, *OsMADS34, OsFC1* and *Os03g0569000* resulted all down regulated in developing panicles, whereas neither *OsESP* nor *OsHOX14* expression resulted significantly changed in respect to wild type. Overall, these results suggest that the analysed genes within the *OsG1L2*-containing subcluster C (Fig. 4) could have a genetic interaction as predicted by the GRN. These analyses suggest that the ALOGs genes under investigation cover partially overlapping pathways regulating the panicle architecture in rice.

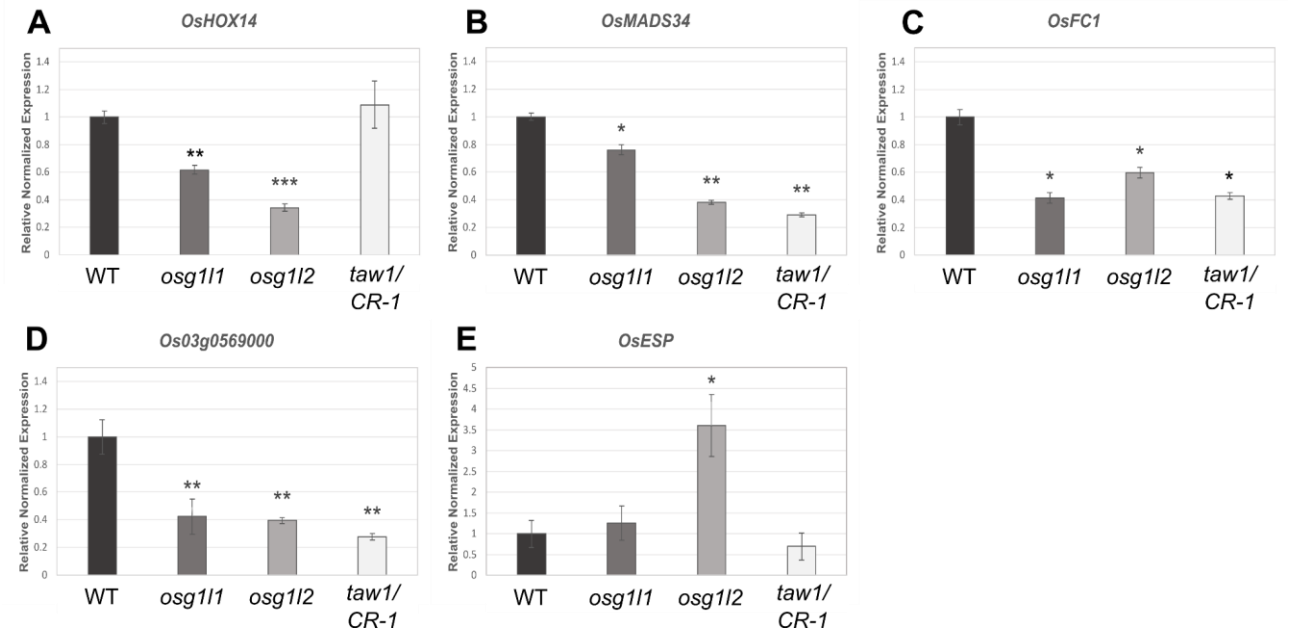

Fig. 5. Expression analysis of subcluster C genes in the *osg1l1, osg1l2 and taw1 CR-1* mutants. Expression analysis of *OsHOX14* (A), *OsMADS34* (B), *OsFC1* (C), *Os03g0569000* (D), *OsESP* (E) by quantitative real-time PCR in wild type (WT), *osg1l1*, *osg1l2* and *taw1 CR-1* mutants. Expression of *OsHOX14, OsMADS34, OsFC1* and *Os03g0569000* was normalised to that of *Elongation Factor 1* and the expression level of wild type was set to 1. The asterisks indicate: *** p< 0,001; **p<0,01; * p<0,05, student's t-test.

Loss-of *OsHOX14* function causes changes in panicle architecture

The GRN subcluster C, that contains *OsG1L2*, shows as major components *OsMADS34*, *OsFC1* and *OsHOX14*. *OsMADS34* and *OsFC1* have been intensively studied for their role in inflorescence development (Takeda et al., 2003; Gao et al. 2010) whereas for *OsHOX14* only an overexpression study has been reported (Shao et al., 2018). Therefore, we selected *OsHOX14* for further functional studies to validate the GRN predicted involvement of this gene in inflorescence architecture. Notably, the RT-qPCR experiments, shown in the previous paragraph, suggest that *OsHOX14* is regulated by *OsG1L1* and *OsG1L2*, whereas *TAW1* doesn't seem to be involved.

OsHOX14 is a member of the homeodomain-leucine zipper (HD-Zip) transcription factor family, and it is the rice orthologue of barley *HvHox2* that, together with its recently diverged paralogue *HvVrs1*, is responsible for the barley's spike architecture (Sakuma et al., 2010). Indeed, *OsHOX14*, like *OsG1L1* and *OsG1L2* was shown to be expressed in the reproductive meristem tissues (PBM, ePBM/AM, SM) (Harrop et al., 2016). The spatiotemporal expression of *OsHOX14* throughout early panicle development was assessed by RNA in situ hybridization analysis. *OsHOX14* resulted to be expressed in PBM, ePBM/AM and SM/FM, suggesting a putative role of this gene during reproductive meristem establishment (Fig. 6 A-C).

We generated a knock-out mutant line for *OsHOX14* using the CRISPR-Cas9 genome editing system (Miao et al., 2013). A specific sgRNA was designed to target the first exon of the *OsHOX14* gene (Supplemental Fig. S8 A). T0 transgenic plants were selected and genotyped. In the T1 generation, three different mutant lines were obtained, having respectively, a homozygous G deletion, a homozygous C insertion, and a biallelic CG deletion and T insertion at 7 bp, 11 bp, and 6 bp downstream of the start site. In all three cases, the different mutations led to a frameshift in the coding sequence and the formation of a premature stop codon, which resulted in the formation of a protein consisting of 22, 27, and 22 amino acids, respectively (Supplemental Fig. S8 B-C).

To evaluate the inflorescence phenotype of *oshox14*, a comparative analysis was performed on panicles belonging to 5 wild-type and 5 T1 *oshox14* mutant plants (1 plant carrying the homozygous C insertion mutation, 1 plant carrying the CG deletion and T insertion mutation and 3 plants carrying the G deletion mutation). This analysis revealed that the *oshox14* mutants developed panicles with less PBs and spikelets than wild type plants. The number of SBs was not significantly different from wild type. In particular, the *oshox14* mutant plants produced panicles that developed on average 3 PBs and 20 spikelets less than the wild-type (Fig. 6 D-G). Overall, this analysis showed that *OsHOX14* plays a role in inflorescence branching as predicted by the GRN.

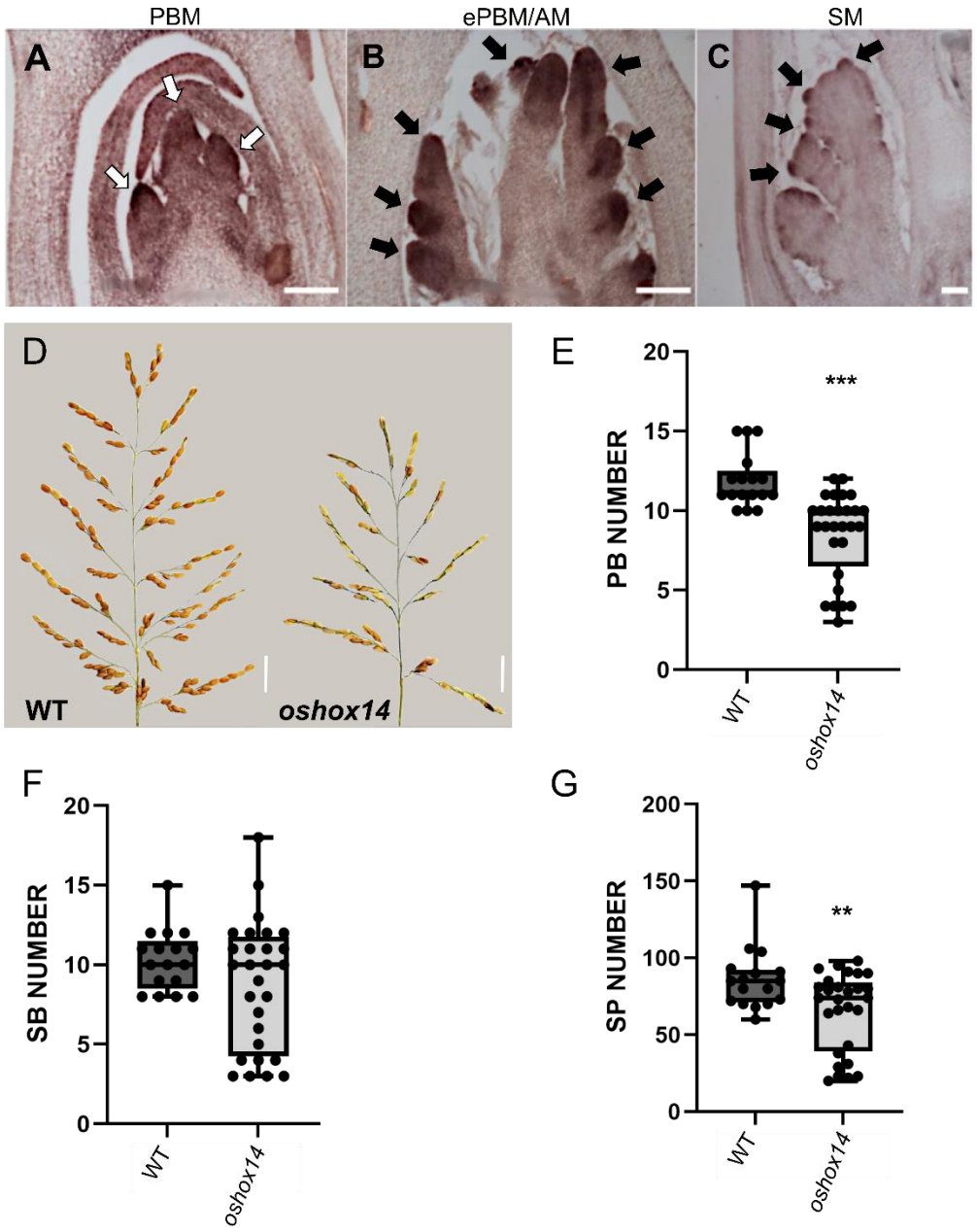

Fig. 6. Expression and functional characterization of *OsHOX14*. *In situ* analysis of three developmental stages: A, PBMs; B, ePBMs/AMs and C, SMs. Scale bars represent 50 μm (C) and 100 μm (A-B). [Primary Branch Meristems (PBMs), elongated PBMs with Axillary Meristems (ePBMs/AMs), Spikelet Meristems (SMs) white (A) and black (B and C) arrows indicate the signal in the corresponding meristem type]. D-G, Phenotypical analysis of panicle architecture in wild type and *oshox14* mutant. D, main panicles of wild type (WT) and *oshox14* (2 cm scale bars). Graphs representing the comparison of: E, Primary Branch (PB) number; F, Secondary Branch (SB) number; G, Spikelets (SP) number in WT and *oshox14* backgrounds. *** = p< 0,001; ** = p<0,01; * = p<0,05, Student's t-test.

Osg1l1 osg1l2 double mutant phenotype

To investigate the genetic relation between *OsG1L1* and *OsG1L2*, we generated the double mutant by crossing the *osg1l1* and *osg1l2* single mutants.

Homozygous double mutant grains presented difficulties in germination. During the vegetative phase, the overall structure of the plant didn't present any obvious defects. However, the propagation of new generations of plants was difficult due to a very high rate of sterility of the *osg1l1 osg1l2* double mutant. We phenotypically compared the architecture of panicles of six wild type and seven *osg1l1 osg1l2* double mutant plants. This comparative phenotypic analysis revealed that the *osg1l1 osg1l2* plants developed panicles that are shorter, with less PBs, extremely reduced SBs and less spikelets than wild type plants. In particular, *osg1l1 osg1l2* double mutant plants produced panicles that were on average 1.5 cm shorter than wild type and developed on average two PBs and 20 spikelets less than wild type plants (Figure 7 B, C, E). Interestingly, concerning the SBs, except the three panicles that developed only one SB each, none of the other panicles of the double mutant produced SBs (Figure 7 D). This analysis indicates that combining the *osg1l1* and *osg1l2* mutants results in an enhancement of the reduction in SB formation, almost completely abolishing the development of these branches.

Furthermore, combining the single mutants caused a high rate of sterility since only 6.2% of the spikelets produce viable grains, suggesting that *OsG1L1* and *OsG1L2* are redundantly involved in plant fertility. Indeed, the analysed panicles each developed on average only two fertile grains.

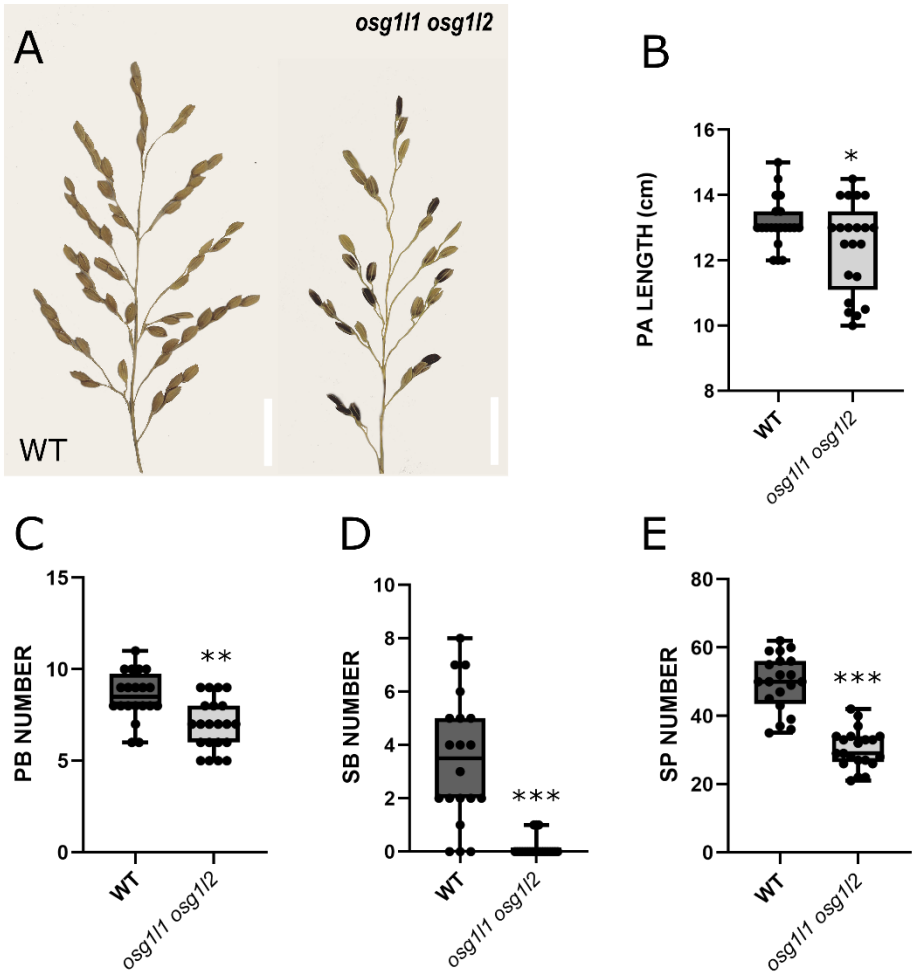

Fig. 7 Phenotypical analysis of panicle architecture in wild type and the *osg1l1 osg1l2* double mutant. A, Main panicles of WT and *the osg1l1 osg1l2 double mutant* (2 cm scale bars). Graphs representing the comparison of: (B) Panicle (PA) Length, (C) Primary Branches (PB) number, (D) Secondary Branches (SB) number, (E) Spikelets (SP) number in WT and *osg1l1 osg1l2* backgrounds. *** = p< 0,001; ** = p<0,01; * = p<0,05, Student's t-test.

DISCUSSION

Inflorescence architecture is a key agronomic trait that influences grain yield, and its development is finely regulated by genes involved in meristem identity specification and in the control of the transition from indeterminate to determinate growth. Therefore, identifying genes involved in inflorescence development promises to contribute to improved crop yield through breeding and biotechnological approaches.

In this study, we functionally characterised *OsG1L1* and *OsG1L2*, two rice genes belonging to the *ALOG* gene family. These two genes are likely to play an important role in the regulation of inflorescence architecture specification acting as positive regulators of primary and secondary branch development. The role of *OsG1L1* and *OsG1L2* in such processes is suggested by their expression in the reproductive meristems in a pattern similar to *TAW1*, an *ALOG* family member already known to be involved in the development of the rice inflorescence by promoting indeterminate meristem identity (Yoshida et al 2013). We compared the protein and promoter sequence of *OsG1L1*, *OsG1L2* and *TAW1* with those of *OsG1* and *OsTH1*, other *ALOG* genes already characterized in rice (Yoshida et al., 2009; Sato et al., 2014). Interestingly, neither *OsG1* nor *OsTH1* shows any meristematic expression. The protein sequence encoded by the five *ALOG* genes is quite conserved, showing an identity spanning from 54% to 79% (Supplemental Fig. S9 B). Of course, if identity calculation is restricted to the ALOG domains, then the percentage will be even higher as shown in Supplemental Fig. S9 A, as well as already described in Naramoto et al. (2020).

Notably, an analysis of the promoter sequence revealed a subset of TFs that are predicted to bind motifs in *OsG1L1*, *OsG1L2* and *TAW1*, but not *OsG1* and *OsTH1* promoters, like members of the *AP2*, *NAM* and *MADS*-domain TF families (Supplemental Table S5). This observation suggests that this subset of TFs might be important for the peculiar meristematic expression pattern of *OsG1L1*, *OsG1L2* and *TAW1*.

Phenotypical analysis of the *osg1l1* and *osg1l2* mutant inflorescences showed that the two single mutants developed shorter panicles with fewer spikelets and smaller grains when compared to wild type. Overall, the inflorescence architecture of *osg1l1* and *osg1l2* single mutants resembled the *taw1* mutant phenotype. Furthermore, SEM analysis revealed that the *osg1l1* and *osg1l2* mutants faced a premature switch from indeterminate ePBMs/AMs to determinate SMs. This observation was confirmed by in situ hybridisation using the *FZP* spikelet identity meristem marker. The expression of *FZP* evidenced that spikelet identity determination happened earlier in the *osg1l1* and *osg1l2* mutants suggesting that, like *TAW1*, both *OsG1L1* and *OsG1L2* repress the transition from indeterminate to determinate phase changes in the inflorescence meristems (Fig. 8). Based on these observations it is tempting to speculate that both *OsG1L1* and *OsG1L2*

might regulate the overall architecture of the panicles in regard to the length of the rice inflorescence, and consequently the number of primary branches that can develop, controlling the timing of IM abortion.

The *osg1l1 osg1l2* double mutant showed an almost complete loss of SB formation suggesting that the two genes act redundantly on the formation of these branches (Figure 2E).

The fact that the double mutant plants were almost completely sterile suggests that *OsG1L1* and *OsG1L2* also play an important role in the fertility of the plant. Indeed, in both RNAseq and qRT PCR analyses (Fig. 1 A-B) the expression of *OsG1L1* and OsG1L2 during FM formation and grain development overlapped whereas *TAW1* was barely expressed in these tissues. It is further interesting to note that the expression of *OsG1L1* and *OsG1L2* overlapped also in mature grain tissues and again *TAW1* was less expressed. These different patterns might be causal to the low germination rate of the *osg1l1 osg1l2* double mutant. Further analysis on fertility and grain development will need to be performed to understand the cause of these observations.

Expression analysis of the putative downstream genes of *TAW1* (Yoshida et al., 2013), *OsMADS22*, *OsMADS47* and *OsMADS55* in the *osg1l1* and *osg1l2* mutant backgrounds didn't evidence any difference when compared to the wild type (Supplemental Figure S5). The DEGs list obtained from our RNA-seq analysis of the *osg1l2* mutant inflorescences are coherent with these data and showed that also other genes proposed to be acting downstream of TAW1 such as *OsMADS7*, *OsMADS8*, *OsMADS16*, *OsMADS3* and *OsMADS58* all presented a level of expression comparable to the wild type (Yoshida et al., 2013). These observations might suggest that, as being part of distinct phylogenetic groups, *OsG1L1* and *OsG1L2* may function in an inflorescence developmental pathway that acts in parallel with *TAW1*. However, since the downstream genes were identified by Yoshida et al. (2013) in the dominant *taw1-D* gain-of-function mutant it might well be possible that in our recessive single mutants we don't see significant changes in the expression of these downstream genes due to redundancy between *TAW1*, *OsG1L1* and/or *OsG1L2*. Future genetic experiments in which the different mutants will be combined in higher-order mutant combinations might clarify this.

The transcriptomic analysis of the *osg1l2* reproductive meristems revealed that some of the differentially expressed genes are indeed factors known to be involved in inflorescence architecture determination. For instance, in previous studies, *OsRCN1* and *OsRCN4* overexpression resulted in plants that produced panicles with an increased number of branches (Nakagawa et al., 2002; Liu et al., 2013) and knocking-down all RCN genes resulted in shorter panicles with fewer secondary branches (Liu et al., 2013). This phenotype is similar to the one observed in the *osg1l2* mutant, where *OsRCN1* and *OsRCN4* are both downregulated. Nakagawa et al. (2002) indicate a role for *RCN* genes in the suppression of spikelet meristem identity which fits well with the evidence we presented for the *OsG1L1* and *OsG1L2* genes as meristematic regulators. Furthermore, it is also interesting to notice that recently it was published that *OsRCN4* is regulated by OsMADS34 (Zhu et al., 2021). In the GRN that we propose, *PAP2/OsMADS34* falls in the same subcluster as *OsG1L2*. *OsMADS34* belongs to the *SEPALLATA* (*SEP*) subfamily of the MADS-box gene family and was previously pointed out as a positive regulator of SM development (Gao et al., 2010; Kobayashi et al., 2012). The phenotype of the

osmads34 osrcn4 double mutant is similar to what we observed in our *osg1l1* and *osg1l2* single mutants (Zhu et al., 2022). Together, all these observations suggest that *OsMADS34*, *OsRCN4*, *OsG1L1*, *OsG1L2* and probably also *TAW1* are involved in the same pathway controlling inflorescence architecture but further analysis will be necessary to clarify the molecular genetic interactions between them.

Other examples to mention are *OsGATA6* and *OsGATA7*, two TFs which were downregulated in the *osg1l2* mutant. Knock-down and knock-out mutants of *OsGATA6* and *OsGATA7* showed alterations in the architecture of the inflorescence; in particular they developed panicles bearing fewer primary and secondary branches (Zhang et al., 2018; Zhang et al. 2022). It is also interesting to mention that *OsGATA6* and *OsGATA7* were proposed to work in the pathway of Brassinosteroid signalling and *OsGATA7* controls cell proliferation. It will be worth further analysing whether the elongation of the primary branches and the modification in the grain size that we observe in our *osg1l2* background is due to a different cell proliferation rate. Moreover, since in the predicted GRN, *OsGATA6* and *OsGATA7* located in a different subcluster than *OsG1L2* (Fig. 4), it could be hypothesised that these two genes regulate inflorescence architecture in a parallel pathway.

Some genes that were upregulated in the *osg1l2* background had an expression level equal to zero in the wild-type background. One of them is *OsESP*, which encodes for a long non-coding RNA (Luan et al., 2019). In the semi-dominant *Epi-sp* mutant, 3' region of the transcribed region was characterised by a loss of DNA methylation resulting in a strong upregulation of the gene causing the development of a denser and shorter panicle. It might well be that the reduction in panicle length observed in *osg1l2* background is linked to the observed upregulation of *ESP*. It would be interesting to investigate whether the loss of *OsG1L2* activity leads to changes in the 3' methylation of the *ESP* gene. *ESP* was one of the predicted putative direct targets of OsG1L2 within the GRN and according to our RT-qPCR experiments, its deregulation seems to be specific only for the *osg1l2* mutant since no upregulation was observed in the *osg1l1* and *taw1 CR-1* mutants. The GRN also indicated that *ESP* (together with eight other genes, still unknown and only expressed in the *osg1l2* mutant developing inflorescences) is a target of both *OsG1L2* and *OsFC1*. It is known that *OsFC1* controls panicle architecture since the null mutant developed shorter panicles (Cui et al.,2020). It might well be that OsFC1 during the reproductive phase represses *ESP* together with OsG1L2.

Among the genes which were selected for real-time PCR validation, *OsHOX14* showed a strong downregulation, in the *osg1l2* mutant and to some extent also in the *osg1l1* mutant but was not deregulated in the *taw1 CR-1* mutant. This result suggests that these ALOG genes regulate rice panicle development through partially overlapping pathways as described in our model (Fig. 8).

Notably, *OsHOX14* is a member of the homeodomain-leucine zipper (HD-Zip) transcription factor family which members are known to play in different species important roles in various aspects of plant development, morphogenesis and in responses to biotic and abiotic stresses (Perotti et al., 2017; Sessa et al., 2018). The specific expression profile obtained through in-situ hybridization, confirmed the expression of *OsHOX14* in reproductive meristems as reported by Harrop et al. (2016) and Shao et al. (2018). Furthermore, it is worth

mentioning that the online RiceXPro tool (https://ricexpro.dna.affrc.go.jp/) showed the expression of *OsHOX14* mainly in developing panicles and pistils, suggesting a specific role of this transcription factor during reproductive development. The CRISPR *oshox14* mutants that we generated, confirmed a role for this gene in inflorescence development, since panicle architecture was impaired in these mutants. The *OsHOX14* overexpression lines generated by Shao et al. (2018) displayed dramatic phenotypes, such as severe delay in growth at the seedling stage and difficulties with panicle exertion through stem and leaves. A mild-overexpression line was analysed for panicle development which showed both a reduction in panicle length and PBs number. Since ectopic expression of *OsHOX14* during the vegetative phase causes growth defects it might well be that this caused pleiotropic effects on reproductive development. However, we cannot rule out the possibility that the knock-out mutant caused a similar phenotype as the overexpression line because of the existence of regulatory loops and dependence on threshold levels that could influence regulatory pathways (Prelich, 2012).

Taking together all these observations, it is tempting to hypothesise that *OsG1L1*, *OsG1L2* and *TAW1* act in partially overlapping pathways. Moreover, *OsG1L2* together with *OsG1L1* seems to act in pathways that include *OsHOX14*, *OsMADS34* and *OsFC1* (Fig. 8). Finally, the functional analysis of *OsHOX14* indicated that the proposed GRN promises to be of value for the identification of new players in the first stages of inflorescence development.

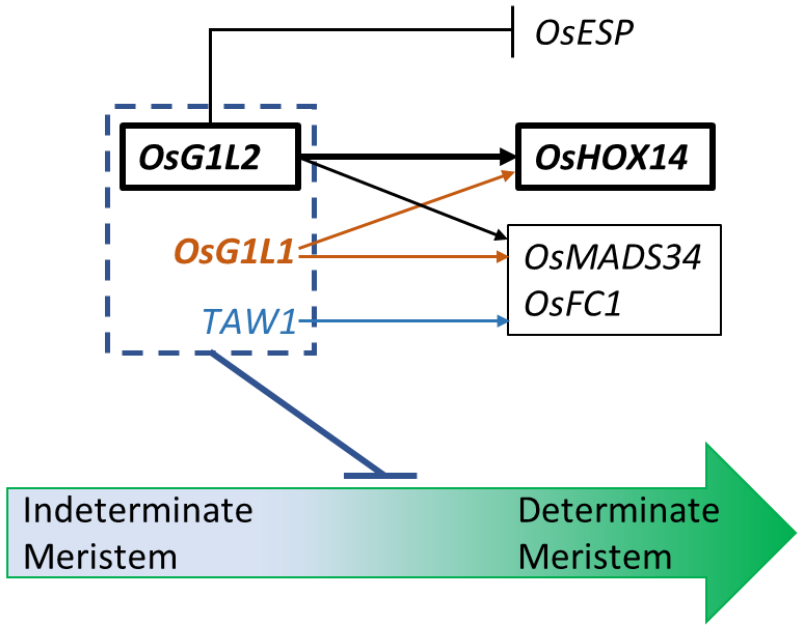

Fig. 8. *ALOGs* Gene Regulatory Network. *OsG1L1*, *OsG1L2* and *TAW1* (dashed box) GRN modulate the phase transition from indeterminate (light blue) to determinate (green) meristems. *ALOGs* regulate both unique (*OsESP*) or shared downstream genes (*OsMADS34 and OsFC1*). *OsHOX14* is a specific putative target of both *OsG1L1* and *OsG1L2*. (⊣ indicates a negative regulation; → indicates a positive regulation, in bold are indicated genes functionally characterised in this work)**.**

MATERIALS AND METHODS

1. Plant material and growth condition

For the experiments we used *Oryza sativa, ssp. japonica, cv Nipponbare*. The plants were grown for 8-10 weeks in LD conditions (70% humidity, 16h light at 28°C/8h dark at 26°C) and then moved in SD conditions (70% humidity, 12h light at 28°C/12h dark at 26°C) to induce flowering. In vitro, plants were germinated on MS-F medium (2,2 g/L MS + vitamins, 15 g/L Sucrose, 1L ddH2O, pH adjusted to 5.6 adding KOH, 2.5 g/L gelrite) and after 15 days were transplanted in soil. Plants used for phenotypic analysis were grown in IRD transgenic greenhouse (Montpellier, France) in spring 2019 (grains have been sown in February 2019 and panicles collected in June) under natural day conditions at 28°C-30°C, and humidity at 60%. Plants used for the RNAseq experiment were grown in the C chamber in NC State University Phytotron.

2. RNA isolation and cDNA synthesis

Total RNA from different tissues (roots, young and mature leaves, milk and mature grains) and from meristematic tissue enriched in Inflorescence Meristems (IM), Primary Branch Meristems (PBMs), Elongated Primary branch meristems and Axillary Meristems (ePBM/AM) and Spikelet Meristems (SM) was extracted with the NucleoSpin® RNA Plant kit (http://www.mn-net.com) and DNA contamination was removed using the TURBO DNA-free™ Kit according to the manufacturer's instructions (https://www.thermofisher.com). The different tissues were sampled in liquid Nitrogen using an optical microscope. The RNA was reverse transcribed using the ImProm-II™ Reverse Transcription System (https://ita.promega.com) and the cDNA was used as a template in RT-PCR reactions.

3.1 Transcriptome analysis

80 plants (40 WT plants and 40 *osg1l2* mutant plants) were sown in growth chamber under LD condition (70% humidity, 16h light at 28°C/8h dark at 26°C), at NC State University Phytotron and, after 12 day of induction in SD conditions, were sampled. Fifty mg of tissue, corresponding to 8-10 meristems at early developmental stages enriched in PBMs and ePBM/AMs, was manually dissected using an optical microscope. RNA was extracted from the samples using RNeasy Plant Mini Kit from Qiagene. cDNA libraries were prepared using NEBNext Ultra DNA Library Prep Kit for Illumina (E7370) according to the manufacturer's instructions. Novaseq6000 Illumina machine was used and sequencing was single-end stranded.

3.2 Data analysis

Raw RNA-seq data in fastq format of wild type and *osg1l2* mutant was processed and subsequently used for gene regulatory network inference with the TuxNet interface (Spurney et al., 2019) (https://github.com/rspurney/TuxNet). For the processing of the raw RNA-seq, the gff and fasta file of the reference genome (IRGSP-1.0) and gene name file was downloaded from The Rice Annotation Project Database (RAP-DB; https://rapdb.dna.affrc.go.jp/download/irgsp1.html) (Supplemental Table S6). The gene IDs from rice transcription factors were downloaded from the plant transcription database v4.0 (http://planttfdb.gao-lab.org/) and converted from MSU to RAP , with the manual addition of the *ALOG* gene family. Next, TuxNet uses ea-utils fastq-mcf (Aronesty, 2013) for pre-processing, hisat2 (Kim et al., 2015) for genome alignment and Cufflinks (Trapnell et al., 2012) for differential expression analysis. The following xlsx files are generated by TuxNet: a file containing the FPKM values for each replicate (Supplemental Table S3), a file with the differentially expressed genes (DEGs) identified with a q-value threshold of 0.05 and a $\log_2$(fold change) of 1 (Supplemental Table S4), and a file containing an average expression, a $\log_2$(fold change), and a q-value (Supplemental Table S7).

The PCA (principal component analysis) was performed in R with the RPKM file from TuxNet using the *prcomp* function from the *stats* package and the *pca3d* package (January Weiner (2020). pca3d: Three Dimensional PCA Plots. R package version 0.10.2. https://CRAN.R-project.org/package=pca3d) (Supplemental Fig. S10).

To infer the gene regulatory network (GRN) in *osg1l2* and predict the causal relationships between and target genes underlying the inflorescence phenotype in *osg1l2*, the differentially expressed TFs and genes identified in *osg1l2* with a q-value threshold < 0.05 and a $\log_2$(fold change) > 1 or < -1 (Supplemental Table S4) were selected. We manually added *OsG1L2* to the DEGs list, since the $\log_2$FC of *OsG1L2* was less than 1 (-0.885798). Within the TuxNet interface, RTP-STAR (Regression Tree Pipeline for Spatial, Temporal and Replicate data) leverages the replicate data of the wild type and *osg1l2* and consists of three parts: spatial clustering using the k-means method, network inference using GENIE3 (regression tree with random forest approach) and edge sign (activation or repression) identification using the first-order Markov method. As options, we used 100 iterations when inferring the GRN and an edge proportion equal to 0.33. The table containing the final predicted network (Supplemental Table S8) has been imported into Cytoscape® 3.8.0 (Shannon et al., 2003), a network visualisation software, to obtain high-quality graphics representation of the predicted GRN. Different node shape, colour, and size were used to represent TFs, the down- or upregulation in *osg1l2*, and the number of interactions, respectively. The nodes within the network were clustered into different modules with the Cytoscape plugin clusterMaker2 according to the available community clustering algorithm, an implementation of the Girvan-Newman fast greedy algorithm that uses connectivity to cluster nodes (Morris et al., 2011).

4. qRT-PCR Analysis

Fresh meristematic tissue enriched in Inflorescence Meristems (IM), Primary Branch Meristems (PBMs), Elongated Primary branch meristems and Axillary Meristems (ePBM/AM) and Spikelet Meristems (SM) was collected in liquid nitrogen using an optical microscope. RNA was extracted with the NucleoSpin® RNA Set for NucleoZOL - MACHEREY-NAGEL KIT for high purity products.

The qRT-PCR analysis was carried out in a final volume of 12 µL in a Biorad C1000™ thermal cycler, using 3 µL of a 1:10 dilution cDNA, 0,2 µM (stock 10mM) Forward and Reverse Primer, 6 µL of Sybr Green Super Mix 2X (Bio-Rad), 2,6 µl MQ H2O.

The expression levels of *OsG1L1(LOC_Os02g07030), OsG1L2 (LOC_Os06g46030)* and *TAW1 (LOC_Os10g33780)* were evaluated using primer pairs RT2541/RT2542, RT1387/ RT1389 and RT2543/ RT2544 respectively. The RT-PCR was performed with the following conditions: 95°C 90'' 40 cycles (95°C 15'', 60°C 10'', 60°C 30'') and 60°C 10''.

The expression levels of *OsESP(Os01g0356951), OsMADS34/PAP2 (LOC_Os03g54170), OsHOX14 (LOC_Os07g39320), OsCEP6 (LOC_Os08g37070.1), OsTB1/FC1 (LOC_Os03g49880)* and *Os03g0569000* in WT and *osg1l2* background were evaluated using primer pairs OSP2055/OSP2056, OSP0855/OSP0856, OSP1400/1401, OSP2043/OSP2044, OSP2045/OSP2046, OSP2059/OSP2060 and using the following condition: 95°C 90'' 40 cycles (95°C 15'', 58°C 10'', 60°C 30'') and 60°C 10''.

Three biological replicates for each experiment were performed.

Rice *Elongation Factor 1* (*EF1*) (*LOC_Os03g08010*) was used as an internal reference during the experiments. Primer sequences are listed in Supplemental Table S9.

5. Tissue fixation and *In situ* Hybridization

Rice reproductive meristems from the main stem at different stages of early panicle development were collected and fixed in FAA [ethanol (Fluka) 50 %; acetic acid (Sigma-Aldrich) 5 %; formaldehyde (Sigma-Aldrich) 3·7 % (v/v)], infiltrated under mild vacuum conditions for 15 min in ice. After 1h 45' the samples were washed 3 times for 10' in EtOH 70% and conserved at 4°C; they were dehydrated in a series of increasing graded ethanol series, transferred to bioclear (Bioptica) and then embedded in Paraplast X-TRA® (Sigma-Aldrich). To generate the sense and antisense probes, gene fragments were amplified from cDNA using gene-specific primers (Supplemental Table S9)**,** cloned into pGEM®-T Easy Vector and confirmed by sequencing. Digoxigenin-labeled antisense and sense RNA probes were transcribed and labelled from pGEM®-T Easy with T7/SP6 RNA polymerase (Promega) according to the manufacturer's instructions and using the DIG RNA labelling mix (Roche). Paraplast-embedded tissues were sliced on an RM2155 microtome (Leica) at 8 μm of thickness and hybridized as described by Caselli et al. (2019) with minor modifications. Immunodetection was carried out with anti-digoxigenin-AP Fab fragment (Roche) and BCIP-NBT colour development substrate (Promega) as specified by the manufacturer. Sample's images were acquired with a Zeiss Axiophot D1 (Zeiss, Oberkochen, Germany) microscope with an Axiocam MRc 5 (Zeiss) at different magnifications.

As regards *FZP*, the probes were designed as already described in Komatsu et al. 2003.

6. Inflorescence meristem analysis by SEM (Scanning Electron Microscopy)

Scanning Electron Microscopy samples were prepared as described (Mizzotti et al., 2015) by gold coating them using a sputter coater (SEMPREP2; Nanotech) followed by observation with a FESEM SIGMA Scanning Electron Microscope (Zeiss).

7. CRISPR-Cas9 construct generation

For the generation of *osg1l1*, *osg1l2* and *oshox14* (LOC_Os07g39320) single knock-out mutants, 20-bp specific protospacers (Supplemental Table S9) for each gene were selected using the CRISPR-P database (*http://cbi.hzau.edu.cn/crispr/)* and cloned into the *BsaI* site of pOs-sgRNA entry vectors under U3 promoter and then combined into the destination vector containing the Cas9 under maize Ubiquitin Promoter using the Gateway® LR Clonase II Enzyme mix following the procedure reported by Miao et al. (2013) and already followed by Lacchini et al., 2020.

8. Bacterial and plant transformation

For bacterial transformation, we used *E. coli* electrocompetent cell (DH10b strains) and *Agrobacterium tumefaciens* electrocompetent cell (EH105 strain).

All final constructs were used to transform embryogenic calli obtained from *Oryza sativa* L. ssp. *japonica cv. Nipponbare* grains according to the methods described by Hiei et al. (1994) and Toki (1997).

9. Mutant screening in transgenic plants

Genomic DNA was extracted from T0-hygromycin-resistant rice plants and genotyped by PCR using primers specific for Cas9 construct, Atp5706/Atp5718 (Supplemental Table S9). Subsequently, from the positive plants, DNA fragments across the target sites were amplified through PCR using gene-specific primer pairs (Supplemental Table S9). The PCR amplicons were purified and sequenced. The obtained chromatograms were analysed and compared with WT sequences with FinchTV searching for mutations.

10. Phenotypical analysis of panicles and grains

To perform phenotypical analysis 15, 19 and 20 panicles from the main tiller were collected respectively from WT, *osg1l1* and *osg1l2* plants. Each panicle was attached on A4 white paper and all panicle branches were spread and blocked with transparent sticks. Each paper with panicle and scale bar was put on an Image capturing system consisting of Portable Camera Stand and two RB 218N HF Lighting Units. The pictures were processed into P-TRAP software. The analysis was done as described in AL-Tam et al., (2013). The results were statistically analysed by One Way ANOVA followed by Tukey test and represented with GraphPad Prism 8.

To perform the phenotypical analysis on wild type and *oshox14* plants, all the panicles produced by 5 wild-type and 5 *oshox14* plants were collected. For each panicle, the number of Primary Branches (PBs), Secondary Branches (SBs) and Spikelets/grains (SP) was manually calculated. The results were statistically analysed with a Student's T-test and graphically represented with GraphPad Prism 8.

At least one hundred grains were analysed for each genotype (*osg1l1, osg1l2* and WT). Images of the grains were acquired using a Leica MZ6 stereomicroscope in conjunction with a Leica DFC280 camera at different magnifications; each image was then processed with Smart Grain (Tanabata et al. 2012). The obtained results were statistically analysed with a One Way ANOVA followed by Tukey test and represented with GraphPad Prism 8.

11. Promoter analysis and protein alignment

The promoter analysis was performed using the Plant Promoter Analysis Navigator (PlantPAN3; http://PlantPAN.itps.ncku.edu.tw/). Specifically, gene group analysis was used to determine the TFs and their binding sites within the promoters of *OsG1*, *OsG1L1*, *OsG1L2*, *TAW1*, and *OsTH1*. The default parameters were used, also for the coordinates of the promoter here defined as 1000 bp upstream and 100 bp downstream of the transcription start site (Chow et al., 2019). The protein alignment was performed using Uniprot (https://www.uniprot.org/align).

Accession Numbers:

Sequence from this article can be found in the GeneBank / EMBL databases under the following accession numbers: *OsG1L1 LOC_Os02g07030, OsG1L2 LOC_Os06g46030, TAW1 LOC_Os10g33780, OsESP Os01g0356951, OsMADS34/PAP2 LOC_Os03g54170, OsHOX14 LOC_Os07g39320, OsCEP6 LOC_Os08g37070.1, OsTB1/FC1 LOC_Os03g49880, Os03g0569000, OsEF1 LOC_Os03g08010*

Supplemental Data

The following supplemental materials are available:

Supplemental Figure S1 Gene structure and wild type and mutant proteins alignment of *OsG1L1*.

Supplemental Figure S2 Gene structure and wild type and mutant proteins alignment of *OsG1L2*.

Supplemental Figure S3 Chromatogram showing the type of mutation and phenotypical analysis of *osg1l2* mutant (C insertion).

Supplemental Figure S4 Size measurements of wild type, *osg1l1* and *osg1l2* grains.

Supplemental Figure S5 Expression analysis of *OsMADS22*, *OsMADS47* and *OsMADS55* in wild type, *osg1l1* and *osg1l2* background.

Supplemental Figure S6. Expression pattern of *FZP* analysed by *in situ* hybridization in wild type, *osg1l1* and *osg1l2*.

Supplemental Figure S7 Gene structure and wild type and mutant proteins alignment of *TAW1*.

Supplemental Figure S8 Gene structure and wild type and mutant proteins alignment of *OsHOX14*.

Supplemental Figure S9 Protein alignment among OsG1 (Os07g0139300), OsG1L1 (Os02g0166800), OsG1L2 (Os06g0672400) OsTH1 (Os02g0811000) and TAW1 (Os10g0478000).

Supplemental Figure S10 PCA output.

Supplemental Table S1 Phenotypical traits analysed in wild type, *osg1l1* and *osg1l2* plants.

Supplemental Table S2 Area, length and width of wild type, *osg1l1* and *osg1l2* grains.

Supplemental Table S3 FPKM values for each replica.

Supplemental Table S4 Differentially expressed genes between wild type and *osg1l2* mutants.

Supplemental Table S5 List of transcription factors that are predicted to bind motifs in *OsG1L1*, *OsG1L2*, and *TAW1* promoters.

Supplemental Table S6 List of gene names.

Supplemental Table S7 Average gene expression, $\log_2$(fold change) and q-value in wild type and *osg1l2* mutant.

Supplemental Table S8 Final predicted GRN.

Supplemental Table S9 Primers used in this article.

ACKNOWLEDGMENTS

We like to thank Andrea Guazzotti, Andrea Finocchio, Stefano Buratti, Cecilia Bertone and Marco Maffei for valuable discussion and technical support. Furthermore, we thank Mario Beretta and Valerio Parravicini for their help in taking care of the rice plants. Part of this work was carried out at NOLIMITS, an advanced imaging facility established by the Università degli Studi di Milano.

REFERENCES

A L-Tam, F., Adam, H., Anjos, A. dos, Lorieux, M., Larmande, P., Ghesquière, A., … Shahbazkia, H. R. (2013). P-TRAP: a Panicle TRAit Phenotyping tool. BMC Plant Biology, 13, 122. https://doi.org/10.1186/1471-2229-13-122

Aronesty, E. (2013). Comparison of Sequencing Utility Programs. The Open Bioinformatics Journal, 7(1), 1–8. https://doi.org/10.2174/1875036201307010001

Bommert, P., Satoh-Nagasawa, N., Jackson, D., Hirano, HY., (2005) Genetic and evolution of grass inflorescence and flower development in grasses. Plant and Cell Physiology 46, 69–78, https://doi.org/10.1093/pcp/pci504

Bai, X., Huang, Y., Mao, D., Wen, M., Zhang, L., & Xing, Y. (2016). Regulatory role of FZP in the

determination of panicle branching and spikelet formation in rice. *Scientific Reports*, *6*(January), 1–11. https://doi.org/10.1038/srep19022

Caselli, F., Zanarello, F., Kater, M. M., Battaglia, R., & Gregis, V. (2020). Crop reproductive meristems in the genomic era: A brief overview. Biochemical Society Transactions, 48(3), 853–865. https://doi.org/10.1042/BST20190441

Cheng, X., Jiang, H., Zhang, J., Qian, Y., Zhu, S., & Cheng, B. (2010). Overexpression of type-A rice response regulators, OsRR3 and OsRR5, results in lower sensitivity to cytokinins. Genetics and Molecular Research : GMR, 9(1), 348–359. https://doi.org/10.4238/vol9-1gmr739

Chow, C. N., Lee, T. Y., Hung, Y. C., Li, G. Z., Tseng, K. C., Liu, Y. H., Kuo, P. L., Zheng, H. Q., & Chang, W. C. (2019). Plantpan3.0: A new and updated resource for reconstructing transcriptional regulatory networks from chip-seq experiments in plants. Nucleic Acids Research, 47(D1), D1155–D1163. https://doi.org/10.1093/nar/gky1081

Cui, Y., Hu, X., Liang, G., Feng, A., Wang, F., Ruan, S., … Qian, Q. (2020). Production of novel beneficial alleles of a rice yield-related QTL by CRISPR/Cas9. Plant Biotechnology Journal, 18(10), 1987–1989. https://doi.org/10.1111/pbi.13370

Fujishiro, Y., Agata, A., Ota, S., Ishihara, R., Takeda, Y., Kunishima, T., … Kitano, H. (2018). Comprehensive panicle phenotyping reveals that qSrn7/FZP influences higher-order branching. Scientific Reports, 8(1), 1–9. https://doi.org/10.1038/s41598-018-30395-9

Gao, X., Liang, W., Yin, C., Ji, S., Wang, H., Su, X., … Zhang, D. (2010). The SEPALLATA-like gene OsMADS34 is required for rice inflorescence and spikelet development. Plant Physiology, 153(2), 728–740. https://doi.org/10.1104/pp.110.156711

Gao, S., Fang, J., Xu, F., Wang, W., & Chu, C. (2016). Rice HOX12 regulates panicle exsertion by directly modulating the expression of ELONGATED UPPERMOST INTERNODE1. Plant Cell, 28(3), 680–695. https://doi.org/10.1105/tpc.15.01021

Hakata, M., Kuroda, M., Ohsumi, A., Hirose, T., Nakamura, H., Muramatsu, M., … Yamakawa, H. (2012). Overexpression of a rice tify gene increases grain size through enhanced accumulation of carbohydrates in the stem. Bioscience, Biotechnology and Biochemistry, 76(11), 2129–2134. https://doi.org/10.1271/bbb.120545

Hake, S. (2008). Inflorescence architecture: the transition from branches to flowers, Current Biology, Volume 18, Issue 23, R1106-R1108, https://doi.org/10.1016/j.cub.2008.10.024.

Han, Y., Yang, H., & Jiao, Y. (2014). Regulation of inflorescence architecture by cytokinins. Frontiers in Plant Science, 5(November), 669. https://doi.org/10.3389/fpls.2014.00669

Harrop, T. W. R., Ud Din, I., Gregis, V., Osnato, M., Jouannic, S., Adam, H., & Kater, M. M. (2016). Gene expression profiling of reproductive meristem types in early rice inflorescences by laser microdissection. Plant Journal, 86(1), 75–88. https://doi.org/10.1111/tpj.13147

Hiei, Y., Ohta, S., Komari, T., & Kumashiro, T. (1994). Efficient transformation of rice (Oryza sativa L.) mediated by Agrobacterium and sequence analysis of the boundaries of the T-DNA. The Plant Journal, 6(2), 271–282. https://doi.org/10.1046/j.1365-313X.1994.6020271.x

Huang, L., Hua, K., Xu, R., Zeng, D., Wang, R., Dong, G., … Li, Y. (2021). The LARGE2-APO1/APO2

regulatory module controls panicle size and grain number in rice. The Plant Cell, 1–17. https://doi.org/10.1093/plcell/koab041

Hudson, D., Guevara, D., Hand, A., Xu, Z., Hao, L., Chen, X., Zhu, T., Bi, Y., Rothstein, S. (2013). Rice cytokinin GATA transcription Factor1 regulates chloroplast development and plant architecture. Plant Physiology PMID: 23548780 PMCID: PMC3641198 DOI: 10.1104/pp.113.217265

Ikeda-Kawakatsu, K., Maekawa, M., Izawa, T., Itoh, J. I., & Nagato, Y. (2012). ABERRANT PANICLE ORGANIZATION 2/RFL, the rice ortholog of Arabidopsis LEAFY, suppresses the transition from inflorescence meristem to floral meristem through interaction with APO1. Plant Journal, 69(1), 168–180. https://doi.org/10.1111/j.1365-313X.2011.04781.x

Ikeda-Kawakatsu, K., Yasuno, N., Oikawa, T., Iida, S., Nagato, Y., Maekawa, M., & Kyozuka, J. (2009). Expression level of ABERRANT PANICLE ORGANIZATION1 determines rice inflorescence form through control of cell proliferation in the meristem. Plant Physiology, 150(2), 736–747. https://doi.org/10.1104/pp.109.136739

Iyer, L. M., & Aravind, L. (2012). ALOG domains: Provenance of plant homeotic and developmental regulators from the DNA-binding domain of a novel class of DIRS1-type retroposons. Biology Direct, 7(1), 1. https://doi.org/10.1186/1745-6150-7-39

Jain, M., Kaur, N., Garg, R., Thakur, J. K., Tyagi, A. K., & Khurana, J. P. (2006). Structure and expression analysis of early auxin-responsive Aux/IAA gene family in rice (Oryza sativa). Functional and Integrative Genomics, 6(1), 47–59. https://doi.org/10.1007/s10142-005-0005-0

Kim, D., Langmead, B., & Salzberg, S. L. (2015). HISAT: A fast spliced aligner with low memory requirements. Nature Methods, 12(4), 357–360. https://doi.org/10.1038/nmeth.3317

Kobayashi, K., Yasuno, N., Sato, Y., Yoda, M., Yamazaki, R., Kimizu, M., … Kyozukaa, J. (2012). Inflorescence meristem identity in rice is specified by overlapping functions of three AP1/FUL-Like MADS box genes and PAP2, a SEPALLATA MADS Box gene. Plant Cell, 24(5), 1848–1859. https://doi.org/10.1105/tpc.112.097105

Komatsu, M., Chujo, A., Nagato, Y., Shimamoto, K., & Kyozuka, J. (2003). Frizzy panicle is required to prevent the formation of axillary meristems and to establish floral meristem identity in rice spikelets. Development, 130(16), 3841–3850. https://doi.org/10.1242/dev.00564

Lacchini, E., Kiegle, E., Castellani, M., Adam, H., Jouannic, S., Gregis, V., & Kater, M. M. (2020). CRISPR-mediated accelerated domestication of African rice landraces. PLoS ONE, 15(3), 1–12. https://doi.org/10.1371/journal.pone.0229782

Li, N., Wang, Y., Lu, J., & Liu, C. (2019). Genome-wide identification and characterization of the ALOG domain genes in rice. International Journal of Genomics, 2019. https://doi.org/10.1155/2019/2146391

Liu, C., Teo, Z. W. N., Bi, Y., Song, S., Xi, W., Yang, X., … Yu, H. (2013). A conserved genetic pathway determines inflorescence architecture in Arabidopsis and rice. Developmental Cell, 24(6), 612–622. https://doi.org/10.1016/j.devcel.2013.02.013

Luan, X., Liu, S., Ke, S., Dai, H., Xie, X. M., Hsieh, T. F., & Zhang, X. Q. (2019). Epigenetic modification of ESP, encoding a putative long noncoding RNA, affects panicle architecture in rice. Rice, 12(1), 20. https://doi.org/10.1186/s12284-019-0282-1

Miao, J., Guo, D., Zhang, J., Huang, Q., Qin, G., Zhang, X., … Qu, L.-J. (2013). Targeted mutagenesis in rice

using CRISPR-Cas system. Cell Research, 23(10), 1233–1236. https://doi.org/10.1038/cr.2013.123

Mizzotti, C., Fambrini, M., Caporali, E., Masiero, S., & Pugliesi, C. (2015). A CYCLOIDEA-like gene mutation in sunflower determines an unusual floret type able to produce filled achenes at the periphery of the pseudanthium. Botany, 93(3), 171–181. https://doi.org/10.1139/cjb-2014-0210

Morris, J. H., Apeltsin, L., Newman, A. M., Baumbach, J., Wittkop, T., Su, G., … Ferrin, T. E. (2011). ClusterMaker: A multi-algorithm clustering plugin for Cytoscape. BMC Bioinformatics, 12, 1–14. https://doi.org/10.1186/1471-2105-12-436.

Nakagawa, M., Shimamoto, K., & Kyozuka, J. (2002). Overexpression of RCN1 and RCN2, rice TERMINAL FLOWER 1 CENTRORADIALIS homologs, confers delay of phase. 29.

Naramoto, S., Hata, Y., & Kyozuka, J. (2020). The origin and evolution of the ALOG proteins, members of a plant-specific transcription factor family, in land plants. Journal of Plant Research, 133(3), 323–329. https://doi.org/10.1007/s10265-020-01171-6

Ooka, H., Satoh, K., Doi, K., Nagata, T., Otomo, Y., Murakami, K., … Kikuchi, S. (2003). Comprehensive Analysis of NAC Family Genes in Oryza sativa and Arabidopsis thaliana. DNA Research, 10(6), 239–247.

Perotti, M. F., Ribone, P. A., & Chan, R. L. (2017). Plant transcription factors from the homeodomain-leucine zipper family I. Role in development and stress responses. IUBMB Life, 69(5), 280–289. https://doi.org/10.1002/iub.1619

Prelich, G. (2012). Gene overexpression: Uses, mechanisms, and interpretation. Genetics, 190(3), 841–854. https://doi.org/10.1534/genetics.111.136911

Ruelens, P., De Maagd, R. A., Proost, S., Theißen, G., Geuten, K., & Kaufmann, K. (2013). FLOWERING LOCUS C in monocots and the tandem origin of angiosperm-specific MADS-box genes. Nature Communications, 4. https://doi.org/10.1038/ncomms3280

Sakuma, S., Pourkheirandish, M., Matsumoto, T., Koba, T., & Komatsuda, T. (2010). Duplication of a well-conserved homeodomain-leucine zipper transcription factor gene in barley generates a copy with more specific functions. Functional and Integrative Genomics, 10(1), 123–133. https://doi.org/10.1007/s10142-009-0134-y

Sato, D. S., Ohmori, Y., Nagashima, H., Toriba, T., & Hirano, H. Y. (2014). A role for TRIANGULAR HULL1 in fine-tuning spikelet morphogenesis in rice. Genes and Genetic Systems, 89(2), 61–69. https://doi.org/10.1266/ggs.89.61

Sessa, G., Carabelli, M., Possenti, M., Morelli, G., & Ruberti, I. (2018). Multiple links between HD-Zip proteins and hormone networks. International Journal of Molecular Sciences, 19(12). https://doi.org/10.3390/ijms19124047

Shannon, P., Markiel, A.,Ozier, O., Baliga, N., Wang, J., Ramage, D., Amin, N., Schwikowski, B., Ideker T. (2003). Cytoscape: A Software Environment for Integrated Models. Genome Research, 13(22), 426. https://doi.org/10.1101/gr.1239303.metabolite

Shao, J., Haider, I., Xiong, L., Zhu, X., Hussain, R. M. F., Övernäs, E., … Ouwerkerk, P. B. F. (2018). Functional analysis of the HD-Zip transcription factor genes Oshox12 and Oshox14 in rice. PLOS ONE, 13(7), e0199248. https://doi.org/10.1371/journal.pone.0199248

Shrestha, R., Gómez-Ariza, J., Brambilla, V., & Fornara, F. (2014). Molecular control of seasonal flowering in rice, arabidopsis and temperate cereals. Annals of Botany, 114(7), 1445–1458.

https://doi.org/10.1093/aob/mcu032

Spurney, R. J., Van den Broeck, L., Clark, N. M., Fisher, A. P., de Luis Balaguer, M. A., & Sozzani, R. (2019). tuxnet: a simple interface to process RNA sequencing data and infer gene regulatory networks. In Plant Journal (Vol. 101). https://doi.org/10.1111/tpj.14558

Takeda, T., Suwa, Y., Suzuki, M., Kitano, H., Ueguchi-Tanaka, M., Ashikari, M., … Ueguchi, C. (2003). The OsTB1 gene negatively regulates lateral branching in rice. The Plant Journal : For Cell and Molecular Biology, 33(3), 513–520. https://doi.org/10.1046/j.1365-313x.2003.01648.x

Tanabata, T., Shibaya, T., Hori, K., Ebana, K., Yano, M., (2012).

SmartGrain: High-Throughput Phenotyping Software for Measuring Seed Shape through Image Analysis. Plant Physiology, 160 (4) 1871-1880; https://doi.org/10.1104/pp.112.205120

Tanaka, W., Pautler, M., Jackson, D., & Hirano, H.-Y. (2013). Grass Meristems II: Inflorescence Architecture, Flower Development and Meristem Fate. Plant and Cell Physiology, 54(3), 313–324. https://doi.org/10.1093/pcp/pct016

Toki, S. (1997). Rapid and efficient Agrobacterium-mediated transformation in rice. Plant Molecular Biology Reporter, 15(1), 16–21. https://doi.org/10.1007/BF02772109

Trapnell, C., Roberts, A., Goff, L., Pertea, G., Kim, D., Kelley, D. R., … Pachter, L. (2012). Differential gene and transcript expression analysis of RNA-seq experiments with TopHat and Cufflinks. Nature Protocols, 7(3), 562–578. https://doi.org/10.1038/nprot.2012.016

Van Ooijen, G., Mayr, G., Kasiem, M. M. A., Albrecht, M., Cornelissen, B. J. C., & Takken, F. L. W. (2008). Structure-function analysis of the NB-ARC domain of plant disease resistance proteins. Journal of Experimental Botany, 59(6), 1383–1397. https://doi.org/10.1093/jxb/ern045

Wu, K. L., Guo, Z. J., Wang, H. H., & Li, J. (2005). The WRKY family of transcription factors in rice and arabidopsis and their origins. DNA Research, 12(1), 9–26. https://doi.org/10.1093/dnares/12.1.9

Yoshida, A., Suzaki, T., Tanaka, W., & Hirano, H. Y. (2009). The homeotic gene long sterile lemma (G1) specifies sterile lemma identity in the rice spikelet. Proceedings of the National Academy of Sciences of the United States of America, 106(47), 20103–20108. https://doi.org/10.1073/pnas.0907896106

Yoshida, A., Sasao, M., Yasuno, N., Takagi, K., Daimon, Y., Chen, R., … Kyozuka, J. (2013). TAWAWA1, a regulator of rice inflorescence architecture, functions through the suppression of meristem phase transition. Proceedings of the National Academy of Sciences of the United States of America, 110(2), 767–772. https://doi.org/10.1073/pnas.1216151110

Zhang, Y. J., Zhang, Y., Zhang, L. L., Huang, H. Y., Yang, B. J., Luan, S., … Lin, W. H. (2018). OsGATA7 modulates brassinosteroids-mediated growth regulation and influences architecture and grain shape. Plant Biotechnology Journal, Vol. 16, pp. 1261–1264. https://doi.org/10.1111/pbi.12887

Zhang, Y. J., Zhang, Y., Zhang, L., He, J., Xue, H., Wang, J., Lin, W. *OsGATA6* regulates rice heading date and grain number per panicle, *Journal of Experimental Botany*, 2022;, erac247, https://doi.org/10.1093/jxb/erac247

Zhu, W., Yang, L., Wu, D., Meng, Q., Deng, X., Huang, G., … Zhang, D. (2022). Rice SEPALLATA genes OsMADS5 and OsMADS34 cooperate to limit inflorescence branching by repressing the TERMINAL FLOWER1-like gene RCN4. New Phytologist, 233(4), 1682–1700. https://doi.org/10.1111/nph.1785

1.2 Generation of an overexpression line and of a reporter line for *G1L2*

The single mutant *g1l2* was showing the most drastic phenotype. Indeed, according to the phenotypical analysis performed on the panicle of the single mutants *g1l1* and *g1l2*, the knock-out of *G1L2* seems to also affect the production of secondary branches, that resulted to be fewer with respect to the wild type. This could indicate that *G1L2* plays a predominant role with respect to *G1L1* in the context of regulating the timing of the transition from an indeterminate to a determinate stage of the reproductive meristem.

It will be interesting to determine if, like it happens expressing constitutively *TAW1*, the overexpression of *G1L2* is sufficient to delay the transition of the reproductive meristem to a determinate stage, leading to the production of more branched panicles (Yoshida et al., 2013). To this purpose, I've generated a construct to obtain the expression of *G1L2* under the control of the rice *ACTIN* constitutive promoter (*pACT*). From the *A. tumefaciens* mediated transformation of rice wild type calli I obtained five independent T0 regenerant transgenic plants. In each of these five T0 plants the expression level of *G1L2* was evaluated in mature leaves tissue (were normally *G1L2* is almost not expressed) by means of qRT-PCR. The results indicate that *G1L2* presents different levels of overexpression in each of the five T0 plants with respect to the wild type control. The five T0 pants will then be propagated and their panicles will be phenotypically analyzed.

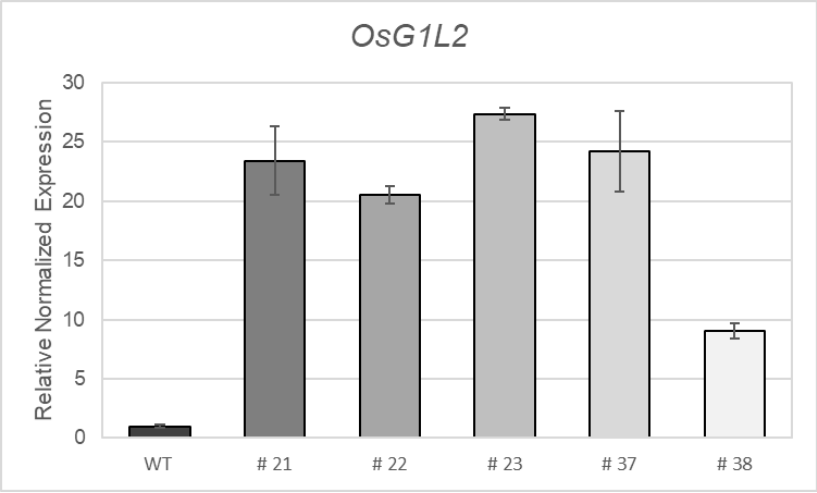

Figure 1. Expression analysis of *G1L2* in five independent *pACT:G1L2* overexpression lines. Quantitative real-time PCR performed in wild type (WT), and *pACT:G1L2 #21, #22, #23, #37, #38* lines . Expression of *G1L2* was tested in mature leaf tissue samples. The expression of *G1L2* was normalized to that of *Elongation Factor 1* and the expression level of wild type was set to 1.

To better investigate the expression pattern and the cellular localization of G1L2 protein in the rice plant, I generated the construct *pG1L2:G1L2:YFP*, that I have transformed in *g1l2* calli. Obtaining this line will be useful also to perform experiments like chromatin immunoprecipitation (ChIP), and

to determine if *G1L2* is able to directly bind the putative targets individuated by means of the RNA-seq on the *g1l2* single mutant. At the moment, the calli are in regeneration.

Collectively, these transgenic lines will help in elucidating the role played by *G1L2* in the context of rice plant development.

1.3 Generation of different mutant combinations among *G1L1, G1L2* and *TAW1*

To better investigate the relationship among *G1L1, G1L2* and *TAW1*, I am performing crosses among the mutant lines *g1l1*, *g1l2* and *taw1 CR-1*. In this way, I will obtain the different combinations of double mutants (I already obtained the *g1l1 g1l2* line, and I will generate also the double mutant lines *g1l1 taw1 CR-1* and *g1l2 taw1 CR-1*) and the triple mutant *g1l1 g1l2 taw1 CR-1*.

At the moment I am analyzing the F1 generation. The phenotypical and molecular analysis of these transgenic lines will help understanding how the three *ALOG* genes are related among each other in the context of rice plant development.

2. *Arabidopsis thaliana*

Role of *LSH1*, *LSH3* and *LSH4* in the inflorescence development of *Arabidopsis thaliana*

An analysis of RNA-seq data performed on reproductive meristems in Arabidopsis showed that *LSH1*, *LSH3* and *LSH4* present a similar expression profile in the analyzed tissues: all three genes show a high expression in the inflorescence meristem and progressively lower expression levels in FM and in flowers at stage 3 (ST3) (Mantegazza, Gregis, Chiara, et al., 2014). It has already been reported that *LSH3* and *LSH4* are expressed in the IM and in the boundary cells between the meristem and the developing floral primordia (Bencivenga et al., 2016; Cho & Zambryski, 2011a; S. Takeda et al., 2011).

Taking together these data it is tempting to hypothesize that *LSH1*, *LSH3* and *LSH4* could be involved in the reproductive development of *Arabidopsis thaliana*.

2.1 Determination of ALOG proteins' DNA-binding specificity

Despite the numerous studies that show the importance of the *ALOG* gene family in different developmental processes and species, little is known about the ALOG protein's structure and mechanism of action. Their role as transcription factors was already hypothesized in tomato and in rice (X. Huang et al., 2021; Peng et al., 2017), but the ALOG DNA-binding specificity wasn't established in any species. The ALOG proteins show a common overall organization: a conserved region, called ALOG domain, is proposed to be the DNA-binding-domain (DBD) (Iyer & Aravind, 2012), and it is flanked by non-conserved disordered regions of variable lengths. Studies have shown that the ALOG domain originates from the DBD of bacterial recombinases (Iyer & Aravind, 2012). The DNA binding mechanism however is still unclear.

Our collaborators from the group of Francois Parcy, at the Laboratoire Physiologie Cellulaire et Végétale, in Grenoble (France), were interested in understanding more about the ALOG proteins. They confirmed the role of the ALOG proteins as transcription factors and, thanks to an amplified DNA affinity purification sequencing (ampDAP-seq, O'Malley et al., 2016) performed using full-length in-vitro produced ALOG proteins and Arabidopsis genomic DNA, were able to determine the DNA binding specificity and subsequently the motif bound by the ALOG proteins. The identified binding motif was then validated using Electrophoretic Mobility Shift Assay (EMSA).

The structure of the ALOG DBD bound to the identified binding motif was then determined using crystallization tests.

The clarification of the protein structure of the DBD and of the motif bound by the ALOG proteins is helpful to determine the possible direct targets of the ALOG transcription factor and consequently to better understand the pathways in which they are involved (unpublished data).

2.2 Expression analysis of *LSH1*, *LSH3* and *LSH4* across different plant tissues

As already mentioned, *LSH1*, *LSH3* and *LSH4* are expressed in the reproductive meristems of Arabidopsis.

To better determine the expression profile of the three *LSHs*, a qRT-PCR analysis was performed on different plant tissues. This analysis showed that *LSH1*, *LSH3* and *LSH4* were expressed in different vegetative (i.e., roots, hypocotyls, cotyledons, rosette leaves and cauline leaves), reproductive (inflorescences) and fruit (siliques) tissues. All three genes showed a similar expression pattern across all plant tissues. They are strongly expressed in the hypocotyls and also expressed in cotyledons, roots and inflorescences (**Figure 1**).

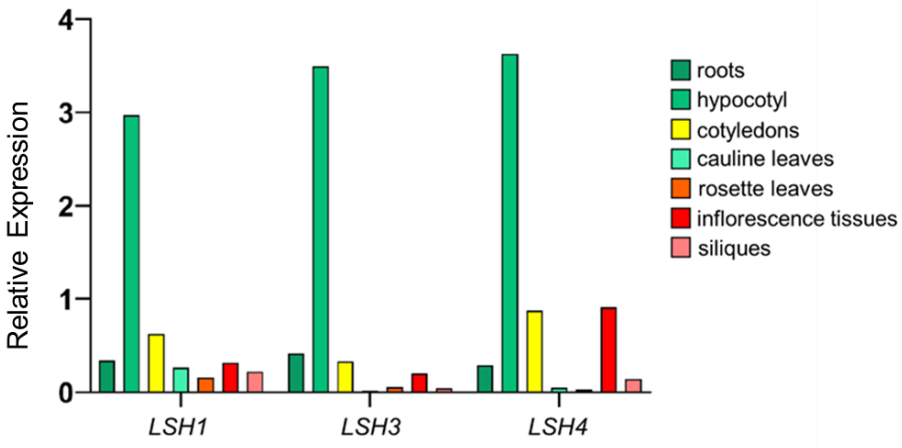

Figure 1. *LSH1*, *LSH3* and *LSH4* expression by qRT-PCR in different tissues: vegetative (roots, hypocotyl, cotyledons, cauline and rosette leaves) and reproductive tissues (inflorescence and siliques).

The expression profile of *LSH1*, *LSH3* and *LSH4* was also investigated specifically in the reproductive meristems by means of in situ hybridization. *LSH1* signal was present especially in the boundary region between the IM and the growing primordia (**Figure 2** A, D, G). *LSH3* expression is localized in the boundary region and in the region of the cryptic bract (**Figure 2** B, E, H). The expression of *LSH4* was specifically localized in the boundary region of the inflorescence (**Figure 2** C, F, I). The expression profile of *LSH3* and *LSH4* in Arabidopsis inflorescence matches the already published data by Takeda et al. (2011) and Bencivenga et al. (2016). These data suggest the involvement of *LSH1*, *LSH3* and *LSH4* in the inflorescence development of Arabidopsis.

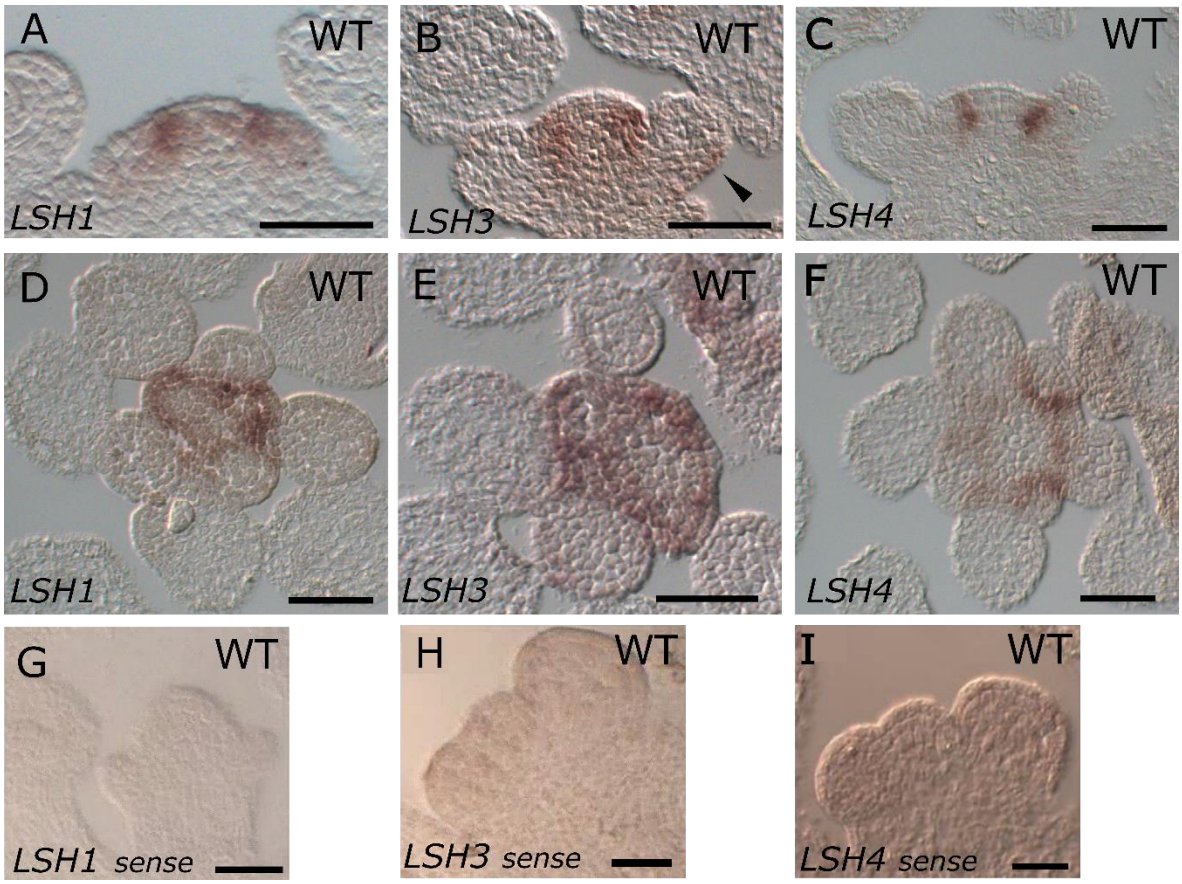

Figure 2. Expression profile of *LSH1* (A, D, G), *LSH3* (B, E, H) and *LSH4* (C, F, I) analyzed by in situ hybridization in the reproductive tissue in wild type (WT) background. A, B, C, G, H, I are longitudinal sections and D, E, F are transversal section of wild type reproductive tissue. Wild type sections in G, H and I were hybridized with the sense negative control probes for *LSH1*, *LSH3* and *LSH4* respectively (Scale bars = 50 μm; black arrow in B indicates LSH3 signal in the cryptic bract region)

2.3 Generation of mutants for *LSH1*, *LSH3* and *LSH4*

LSH3 and *LSH4* were already published to be involved in the specification of the organ boundaries and in reproductive meristem development. Indeed, the overexpression of *LSH3* and *LSH4* causes the formation of ectopic organs and the over-proliferation of meristematic tissues (Cho & Zambryski, 2011a; S. Takeda et al., 2011). On the other hand, neither the single mutants for *LSH3* and *LSH4*, nor the double mutant *lsh3 lsh4* showed any obvious phenotype. This could be due to redundancy among *LSH3*, *LSH4* and other factors. Considering the similar expression pattern shared by *LSH1*, *LSH3* and *LSH4* in the reproductive tissues, it is tempting to hypothesize that these three *ALOG* genes could be involved in the reproductive development of Arabidopsis and that they can also have a redundant function.

The starting point was to check for the availability of T-DNA insertional mutant on the SALK database. For *LSH1* a knockdown line obtained by miRNA-induced gene silencing (MIGS) was only recently published (Lee et al., 2020). For *LSH3*, an unpublished line SALK_123953C, with an insertion in the 5'-UTR (300 base pairs upstream the ATG start codon), was available. To evaluate if the T-DNA insertion was interfering with the expression of *LSH3*, a qRT-PCR was performed. The result showed a mild reduction in *LSH3* expression, that was around 50% of the wild type. The mutant plants weren't showing any phenotype.

For *LSH4* the line SALK_067722C, which presented the T-DNA insertion in an intron, was available. This *lsh4-1* T-DNA line was already published as a strong knockdown mutant, showing a remaining 3% expression of *LSH4* with respect to the wild type (Takeda et al., 2011). Even if the *lsh4-1* mutant line didn't show any aberrant phenotype, it proved, when combined with the *rpl* mutant, to partially restore the *rpl* phenotype (Bencivenga et al., 2016).

The two SALK lines for *LSH3* and *LSH4* were crossed to obtain the double mutant *lsh3 lsh4*. This double mutant wasn't showing any evident phenotype.

Since no mutant lines were available for *LSH1* and since none of the T-DNA insertion lines for *LSH3* and *LSH4* were complete knock-out mutants, we decided to generate new mutants using a CRISPR-Cas9 approach.

Specific sgRNA were designed to target *LSH1*, *LSH3* and *LSH4* and generate insertions or deletions in the *ALOG* domain. Each CRISPR-construct was then used to transform Arabidopsis plants by *Agrobacterium* mediated floral dipping.

A sgRNA was designed to target *LSH1* sequence at 153 base pairs from the ATG start site (**Figure 3** A). Out of thirty transgenic plants obtained, one presented a homozygous biallelic A/T insertion at 156 base pairs from the ATG start site. Either A or T insertion causes a frameshift and the consequent formation of a premature stop codon at 160 bp from the ATG that results in a truncated protein of 53 amino acids, disrupting the ALOG domain and the putative NLS (**Figure 3** B). For this reason, the obtained protein is most likely not functional. After segregation of the Cas9 construct, a homozygous line carrying the A insertion was propagated for further analysis.

A

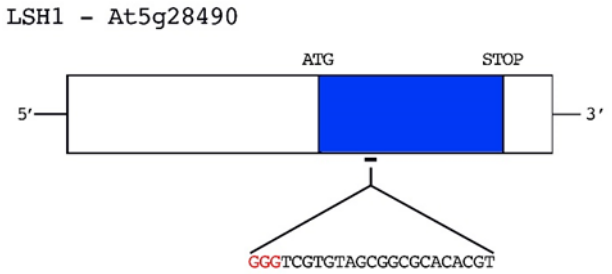

B

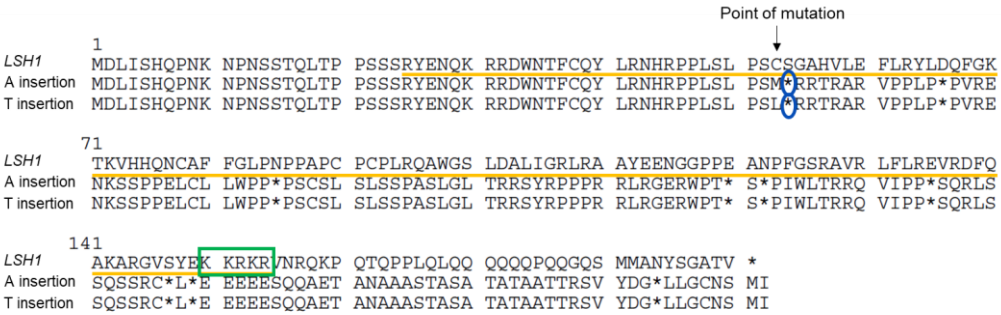

Figure 3. A, *LSH1* gene structure. The blue rectangle represents the exons, the black line represents the introns, and the white rectangle represents the 5' and 3' UTRs respectively. The position and the target sequence of the sgRNA, which targets *LSH1* exon, 153 bp downstream the ATG site are indicated. The PAM sequence is indicated in red. B, Amino acid sequence alignments of *LSH1* and the *lsh1* mutants. On the left are indicated the different base pairs insertions obtained in mutant plants. The ALOG domain is underlined in yellow; the green rectangle indicates the putative NLS and premature stop codons (*) are circled in blue. The A and T insertions cause a frameshift and the formation of a premature stop codon. In all cases, the ALOG domain and the NLS result to be disrupted.

For *LSH3*, the sgRNA was designed to target this gene at 24 base pairs from the ATG start site (**Figure 4** A). Out of twenty-one transgenic plants obtained, one presented a homozygous biallelic A/T insertion at 41 base pairs from the ATG start site. The A insertion causes a frameshift resulting in the formation of a premature stop codon at 40 base pairs from the ATG start site. The T insertion determines a frameshift and the formation of a premature stop codon at 109 base pairs from the ATG start site. Both A and T insertions led to the formation of a truncated protein of 13 or 36 amino acids respectively (**Figure 4** B). In both cases the truncated proteins didn't present the ALOG domain or the NLS and are therefore most likely not functional. The line presenting an A insertion was selected for further analysis.

A

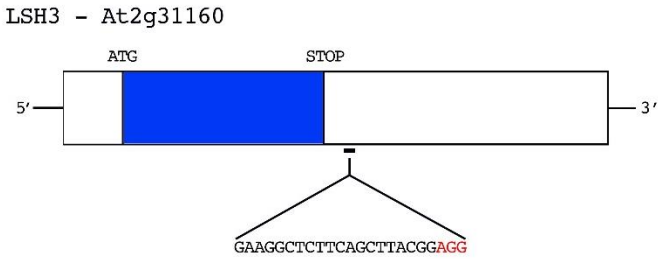

B

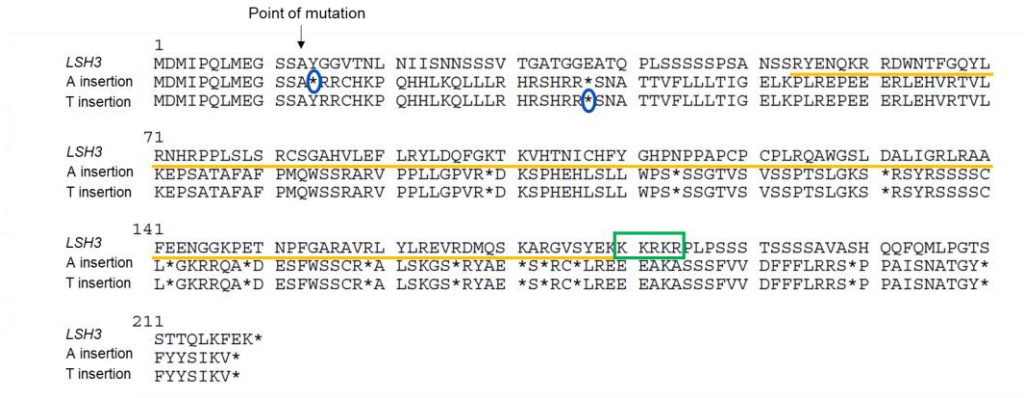

Figure 4. A, *LSH3* gene structure. The blue rectangle represents the exons, the black line represents the introns, and the white rectangle represents the 5' and 3' UTRs respectively. The position and the target sequence of the sgRNA, which targets *LSH3* exon, 24 bp downstream the ATG site are indicated. The PAM sequence is indicated in red. B, Amino acid sequence alignments of *LSH3* and the *lsh3* mutants. On the left are indicated the different base pairs insertions obtained in mutant plants. The ALOG domain is underlined in yellow; the green rectangle indicates the putative NLS and premature stop codons (*) are circled in blue. The A and T insertions cause a frameshift and the formation of a premature stop codon. In both cases, the ALOG domain and the NLS result to be disrupted.

For *LSH4* the sgRNA was designed to target the first exon at 121 base pairs from the ATG start site (**Figure 5** A). Out of six transgenic plants obtained, one presented a heterozygous A insertion at 139 base pairs from the ATG start site. This plant was then propagated to obtain a homozygous line. The A insertion causes a frameshift and the formation of a premature stop codon at 248 base pairs from the ATG start site, resulting in the formation of a truncated protein of 82 amino acids (**Figure 5** B). In this truncated version of the protein there is the disruption of the ALOG domain and of the NLS.

A

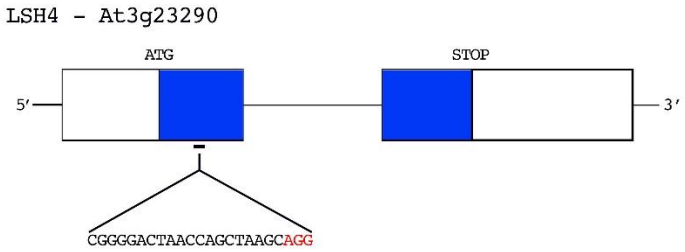

B

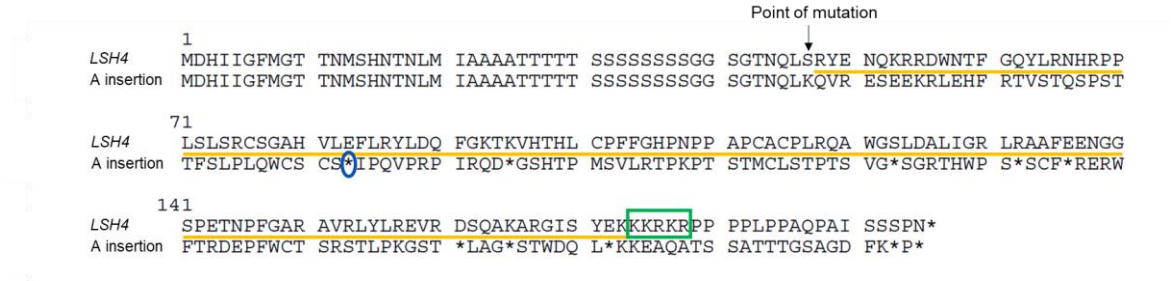

Figure 5. A, *LSH4* gene structure. The blue rectangle represents the exons, the black line represents the introns, and the white rectangle represents the 5' and 3' UTRs respectively. The position and the target sequence of the sgRNA, which targets *LSH4* first exon, 121 bp downstream the ATG site are indicated. The PAM sequence is indicated in red. B, Amino acid sequence alignments of *LSH4* and the *lsh4* mutant. On the left is indicated the base pairs insertion obtained in mutant plants. The ALOG domain is underlined in yellow; the green rectangle indicates the putative NLS and premature stop codons (*) are circled in blue. The A insertion causes a frameshift and the formation of a premature stop codon. The ALOG domain and the NLS result to be disrupted.

The single mutants *lsh1*, *lsh3* and *lsh4* didn't present any visible aberrant phenotype if compared to the wild type, coherently with the absence of phenotype showed by the published knockdown lines for *LSH1*, *LSH3* and *LSH4* (Cho & Zambryski, 2011a; Lee et al., 2020; S. Takeda et al., 2011). This could be due to the redundant effect among the three *LSHs*.

For this reason, we proceeded with the generation of the different double mutant combinations (*lsh1 lsh3*, *lsh1 lsh4*, *lsh3 lsh4*) by crossing the single mutant lines. Also, the different combinations of double mutants didn't present any visible aberrant phenotype when compared to wild type plants.

We then generated the triple mutant. The triple mutant lines *lsh1 lsh3 lsh4* and *lsh1 lsh3 LSH4/lsh4* present a phenotype that was not presented by any of the single or double mutant combinations. Indeed, in the triple mutant each flower is subtended by a well-developed bract, an organ which growth is usually suppressed in wild type Arabidopsis plants.

This phenotype suggests a role for *LSH1*, *LSH3* and *LSH4* in the development of Arabidopsis inflorescence and in the specification of the identity of different areas of the reproductive meristems.

2.4 Analysis of *lsh1 lsh3 lsh4* triple mutant phenotype

As already described above, the different combinations of double mutants (*lsh1 lsh3*, *lsh1 lsh4* and *lsh3 lsh4*) didn't show any visible phenotypical aberration.

Notably, the triple mutant *lsh1 lsh3 lsh4* develops bracts that subtend the flowers. This organ is absent in wild type Arabidopsis plants, where its outgrowth is repressed (**Figure 6** A, B).

lsh1 lsh3 lsh4 plants can develop bracts that subtend each one of the flower primordia. We wanted to determine if the presence of an additional leaf-like structure was somehow impacting the overall productivity of the plant, with an effect on flower structures or seed production. To do so, the flowers of the *lsh1 lsh3 lsh4* mutant were observed at the stereomicroscope. They present a normal number of sepals, petals, stamen and carpels. Furthermore, ten siliques of *lsh1 lsh3 lsh4* plants and ten siliques of wild type plants were analyzed for length, the number of ovules and the number of aborted ovules and no significative differences between the triple mutant and the wild type were recorded (**Figure 6** C-E).

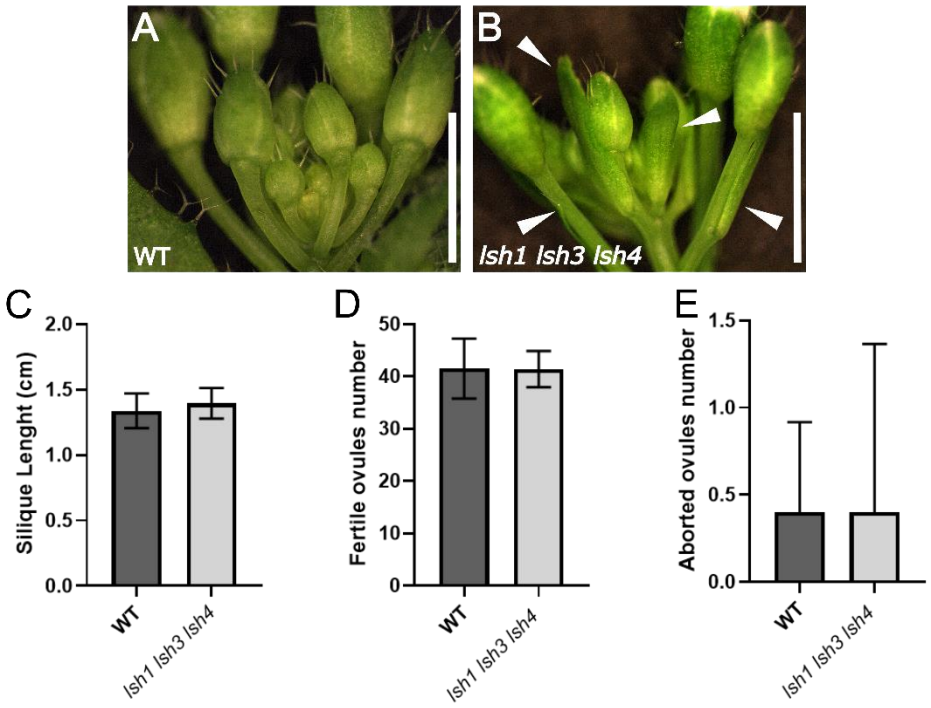

Figure 6. A, B, pictures collected with a stereomicroscope of the inflorescences of wild type (WT, A) and *lsh1 lsh3 lsh4* (B). White arrows in B indicate the bracts (scale bars = 3 mm). Analysis of silique length (C) and fertile (D) and aborted (E) ovules number in wild type (WT) and *lsh1 lsh3 lsh4* background. Ten siliques for each genotype were analyzed.

To analyze more in dept the morphological structure of the bracts, we performed a Scanning Electron Microscopy (SEM) analysis. Inflorescences of *lsh1 lsh3 lsh4* and wild type plants were scanned and compared.

This analysis allowed us to investigate the cell structure of the bract organs developed by *lsh1 lsh3 lsh4*. The bracts emerge from the pedicel of each flower and present the cell structure that is typical of the sepals (**Figure 7** A-D). Furthermore, these organs can also develop structures that resemble stigmatic papillae (**Figure 6** B, C). This could indicate the misexpression of floral organ identity genes, such as *AP1*, *AP2* or *AG*, which can confer the sepal and carpel features to the bracts.

In literature, other mutants are reported to develop bracts with these same floral organ features. For example, it is published that the single mutant *lfy*, as well as the double mutant *lfy ap1*, can develop bracts that present carpelloid characteristics, such as the development of stigmatic papillae or ovules (Weigel et al., 1992b). The triple mutant *puchi bop1 bop2* can as well develop bracts that resemble the organs developed by *lsh1 lsh3 lsh4* mutant, with sepal-like cell structure and stigmatic papillae tissue (**Figure 7** E, Karim et al., 2009).

Taking together these observations we hypothesize that the correct expression of genes that determine FM identity (like *LFY* and *AP1*) and of genes that allow boundaries maintenance (like *PUCHI*, *BOP1*, *BOP2*, but also *LSH1*, *LSH3* and *LSH4*) is necessary for the development of the different areas of the shoot apex. When one or more of the players are absent, the balance among the different factors is perturbed and the outgrowth or the miss specification of the organs occurs.

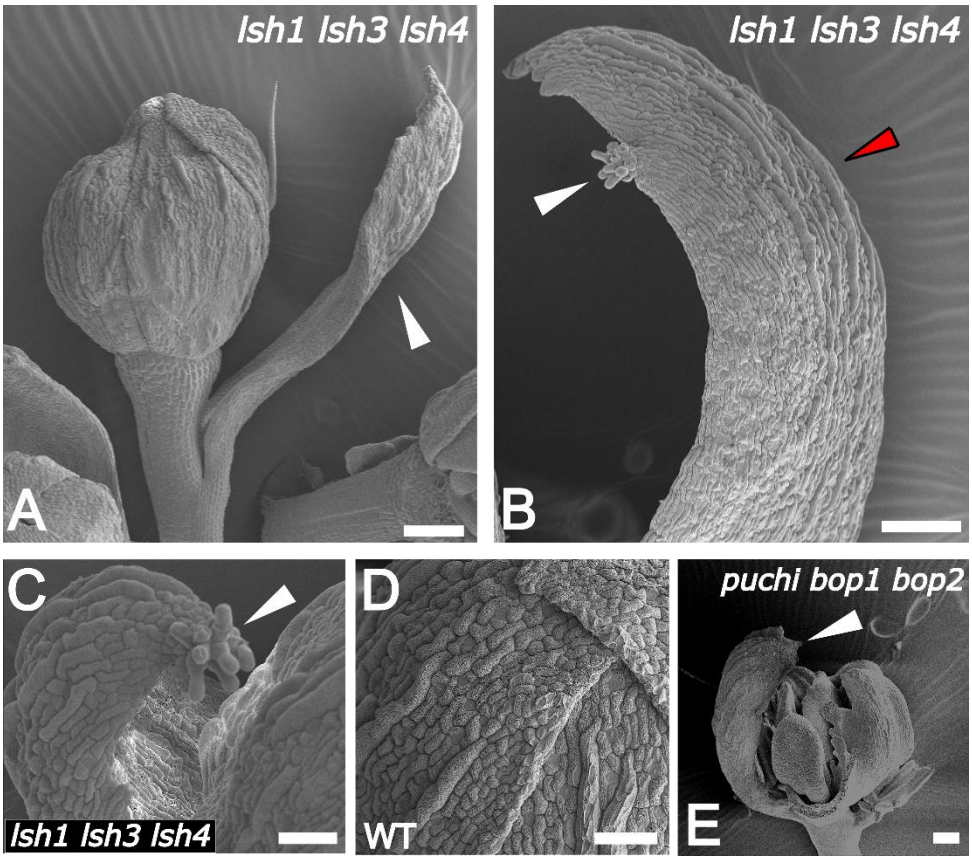

Figure 7. Pictures collected with a scanning electron microscope (SEM) showing the phenotype of wild type (WT), *lsh1 lsh3 lsh4* and *puchi bop1 bop2* plants. A, enlargement of a floral bud of a *lsh1 lsh3 lsh4* plant. The white arrow indicates the bract (scale bar = 100 µm). B and C, enlargement of the bracts developed by the triple mutant *lsh1 lsh3 lsh4*. The white arrows indicate the stigmatic papillae developed by the bracts. The red arrow indicates the sepal-like cells (scale bars in D = 100 µm; E = 50 µm). D, enlargement of a wild type (WT) sepal (scale bar = 50 µm). E, floral bud developed by the triple mutant *puchi bop1 bop2*. The white arrow indicates a bract (scale bar = 100 µm).

2.5 Transcriptome analysis of the *lsh1 lsh3 lsh4* mutant inflorescence

To better understand the pathway underneath the bract phenotype shown by the triple mutant *lsh1 lsh3 lsh4*, we performed an RNA-seq transcriptome analysis on the inflorescences of the triple mutant *lsh1 lsh3 lsh4*. Tissue enriched in IM, FM and flowers primordia until stage 5 (Smyth et al., 1990) was collected for both *lsh1 lsh3 lsh4* and wild type plants. We collected four biological replicates, each replicate consisting of 7 inflorescences. The RNA was then extracted and used for Illumina sequencing. The raw RNA-seq files were processed with Rsem. The reads were mapped on *Arabidopsis thaliana* genome (assembly version TAIR10, annotation version Araport11). The alignment of the reads to the reference genome resulted overall in > 90% mapping rate. Setting the $\log_2$ Fold Change (FC) equal to 0 and the q-value equal to 0.05, a total of 822 differentially expressed genes (DEGs) were identified, of which 338 were downregulated and 484 upregulated in the *lsh1 lsh3*

lsh4 mutant compared to the wild type. On the set of DEGs obtained, we performed a Gene Ontology (GO) enrichment analysis. Among the top twenty enriched Biological Process terms in which the DEGs are involved, there are processes like the cellular response to stresses such as hypoxia or water deprivation, or the response to hormones (**Figure 8**). It is also interesting to notice that among other biological processes that were found enriched, there are different aspects of plant development, like the regulation of plant morphogenesis, especially for the aspects that involve shoot, leaves, bracts and flower development but also meristem maintenance.

Our collaborators from the group of Francois Parcy, at the Laboratoire Physiologie Cellulaire et Végétale, in Grenoble (France) were able to establish a DNA-binding motif for the ALOG proteins, thanks to an ampDAP-seq analysis.

Combining the data obtained from the two experiments, we could select interesting genes, involved in the processes of reproductive meristems development that are deregulated in the triple mutant *lsh1 lsh3 lsh4*, that present the motif recognized by the ALOG proteins in their promoter or both (**Table 1**).

Indeed, among the deregulated genes found thanks to the RNA-seq, we found *BOP1* and *BOP2*. It is published that *BOP1*, together with its close homolog *BOP2*, is already proposed to be involved in the specification and maintenance of the boundary region (Karim et al., 2009; M. Xu et al., 2010). *BOP1* and *BOP2* act together with *PUCHI*, another boundary gene that, according to the results of the ampDAP-seq, presents the ALOG binding motif in its promoter region, but seems to be not deregulated in the *lsh1 lsh3 lsh4* background.

Among the genes that resulted to be bound by the ALOG proteins according to the ampDAP-seq there are also *LFY* and *AP1*, the flower meristem identity genes. Their correct expression and localization are necessary for the identity acquisition of the flower meristem.

Other two factors whose promoter region resulted to be bound by the ALOG proteins, according to the ampDAP-seq, and that resulted to be downregulated in the *lsh1 lsh3 lsh4* background according to the RNA-seq are *SVP* and *STM*. Both these genes have a very important role in specifying the flower meristem and maintaining its identity.

These observations reinforce the hypothesis that *LSH1*, *LSH3* and *LSH4* are involved in the development of the reproductive meristems of *Arabidopsis thaliana*, and that they could participate in the pathways that lead to the correct specification of the different areas of the meristems. To better understand how the three *LSHs* are involved in these processes, we decided to investigate the pattern

of expression of the selected interesting genes (**Table 1**) in the triple mutant *lsh1 lsh3 lsh4* background. Furthermore, we tested the possible interaction among the LSHs and known players in the process of bract outgrowth suppression.

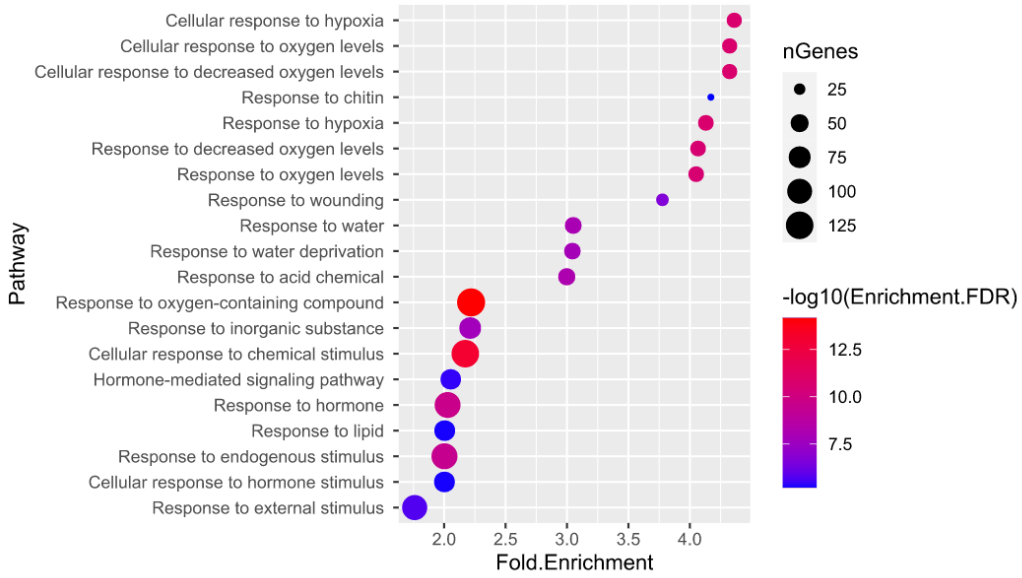

Figure 8. Gene Ontology enrichment analysis on the set of 219 DEGs. Top 20 enriched Biological Process terms. x axis: Fold enrichment. Dot size: Number of genes annotated to the enriched term. Color: Significance level (FDR).

		RNA-seq results			
Gene Name	**Locus**	**log2 FC**	**padj**	**Promoter region bound by the ALOG proteins**	**Putative function**
BOP1	AT3G57130	2.271	6.02E-06	no	Has a role in growth and development, leaf complexity, organ abscission and bract suppression.
BOP2	AT2G41370	1.270	0.00373	no	Has a role in growth and development, leaf complexity, organ abscission and bract suppression.
SVP	AT2G22540	-0.564	0.01628	yes	Floral repressor in the thermo-sensory pathway. Maintains meristematic activity and prevents the induction of ectopic floral meristem formation.
STM	AT1G62360	-0.384	0.00745	yes	Prevents the incorporation of cells of the meristem center into differentiating organ primordia
PUCHI	AT5G18560	not significantly deregulated		yes	Required for early floral meristem growth and for bract suppression.
LFY	AT5G61850	not significantly deregulated		yes	Involved in flower meristem development by promoting the transition to flowering.
AP1	AT1G69120	not significantly deregulated		yes	Specifies floral meristem and sepal identity

Table 1. List of interesting genes selected for further analysis according to the results of the RNA-seq and of the ampDAP-seq. For each gene the Gene Name (column one); the Gene Locus (column two); RNA-seq results divided in log2 FC (column three) and padj (column four); if the promoter region is bound by the ALOG proteins (column five) and information related to their function (column six) are indicated.

2.6 LSH1, LSH3 and LSH4 interact with BOP1 and BOP2 and may determine the expression profile of *PUCHI*

As previously mentioned, *BOP1* and *BOP2*, according to the results of the RNA-seq, resulted upregulated in the *lsh1 lsh3 lsh4* background. *BOP1*, with is homolog *BOP2*, is proposed to be involved in the specification and maintenance of the boundary region. Furthermore, the interaction among *ALOG* and *BOP* factors was previously reported in tomato, where *TERMINATING FLOWER* (*TMF*), a member of the *ALOG* gene family, is able to interact with *SlBOP1*, *SlBOP2* and *SlBOP3* to determine leaf patterning. For this reason, to better characterize the pathway in which *LSH1*, *LSH3* and *LSH4* are involved, we decided to perform a Yeast-Two-Hybrid (Y2H) essay to test whether the interaction among ALOG and BOP factors is conserved also in Arabidopsis.

Since it is reported that in Arabidopsis the double mutant *bop1 bop2* is able to develop bracts, and since it is published that also mutants for other genes like *LFY*, *AP1*, *PUCHI*, *JAG* and *JGL* are reported to develop bracts, we decided to test also the interaction among the LSHs and the other players involved in bract suppression pathway (Dinneny et al., 2004; V. F. Irish & Sussex, 1990; Karim et al., 2009; Norberg et al., 2005; Ohno et al., 2004; Weigel et al., 1992b). We also tested if LSH1, LSH3 and LSH4 can interact among themselves, to assess if they can act as monomers, dimers or heterodimers. We tested with a Y2H essay the interaction among LSH1, LSH3, LSH4 and: LSH1, LSH3, LSH4, BOP1, BOP2, PUCHI, LFY, AP1, JAG and JGL.

Interestingly, from our analysis, resulted that LSH1, LSH3 and LSH4 can't form homo or heterodimers, but can all three interact with both BOP1 and BOP2. Among the interaction that we tested these were the only positive ones (**Figure 9**).

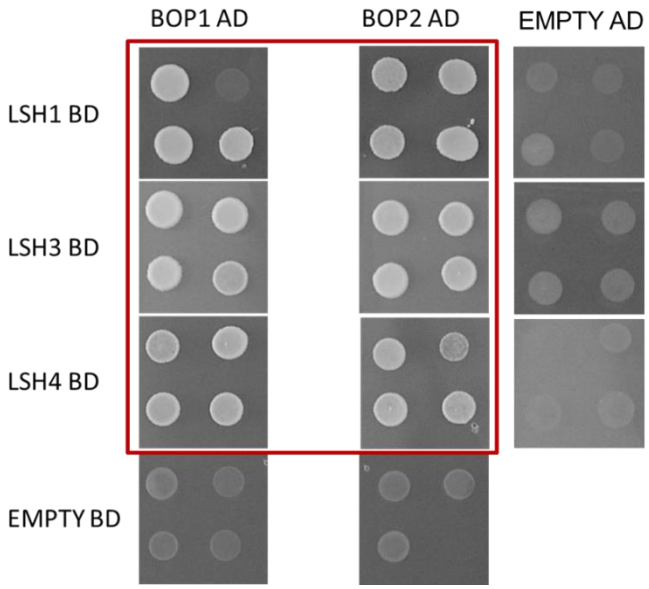

Figure 9. Yeast two hybrid (Y2H) assay showing the interactions among LSH1, LSH3, LSH4 and BOP1 and BOP2, on –L-W-H + 2.5 3-AT selective media. Empty pGADT7 and pGBKT7 vectors were employed as negative controls.

It is published that *BOP1* and *BOP2*, acting together with *PUCHI*, can promote the specification of the determinate FM, and participate in the pathway of bract outgrowth suppression (Karim et al., 2009; M. Xu et al., 2010). Indeed, while the single mutant *puchi-1* can develop rudimentary bracts, as well as the double mutant *bop1 bop2* can occasionally develop bracts that subtend the flowers; the triple mutant *puchi bop1 bop2* shows a drastic enhancement of the bract phenotype (Karim et al., 2009). In the double mutant *bop1 bop2*, *PUCHI* is expressed in a broader domain with respect to the wild type. According to the data from the ampDAP-seq performed by our collaborators, the promoter region of *PUCHI* seems to be bound by the LSHs, allowing us to hypothesize that the LSHs could directly regulate the area of expression of *PUCHI*. To test if the expression pattern of *PUCHI* changes in the inflorescences of *lsh1 lsh3 lsh4* we performed an in-situ hybridization using a digoxigenin-labelled RNA probe specific for *PUCHI* (**Figure 10** A-C). Our analyses showed that the expression of *PUCHI* is different in *lsh1 lsh3 lsh4* background with respect to the wild type. Indeed, the expression of *PUCHI* in the wild type is very specific and localized on the adaxial side of the flower meristem (Karim et al., 2009; Figure 4 A). In *lsh1 lsh3 lsh4* background, *PUCHI* expression it's not confined anymore to the adaxial side of the flower meristem but results also diffused in the abaxial side of the flower meristem (**Figure 10** B, C).

The expression profiles of *BOP1* and *BOP2* were also evaluated in inflorescences of *lsh1 lsh3 lsh4* background with in-situ hybridization using a digoxigenin-labelled RNA probe specific for

BOP1(**Figure 10** D, E) and *BOP2* (**Figure 10** F, G). Overall, the expression profile of *BOP1* and *BOP2* is comparable between *lsh1 lsh3 lsh4* and wild type background.

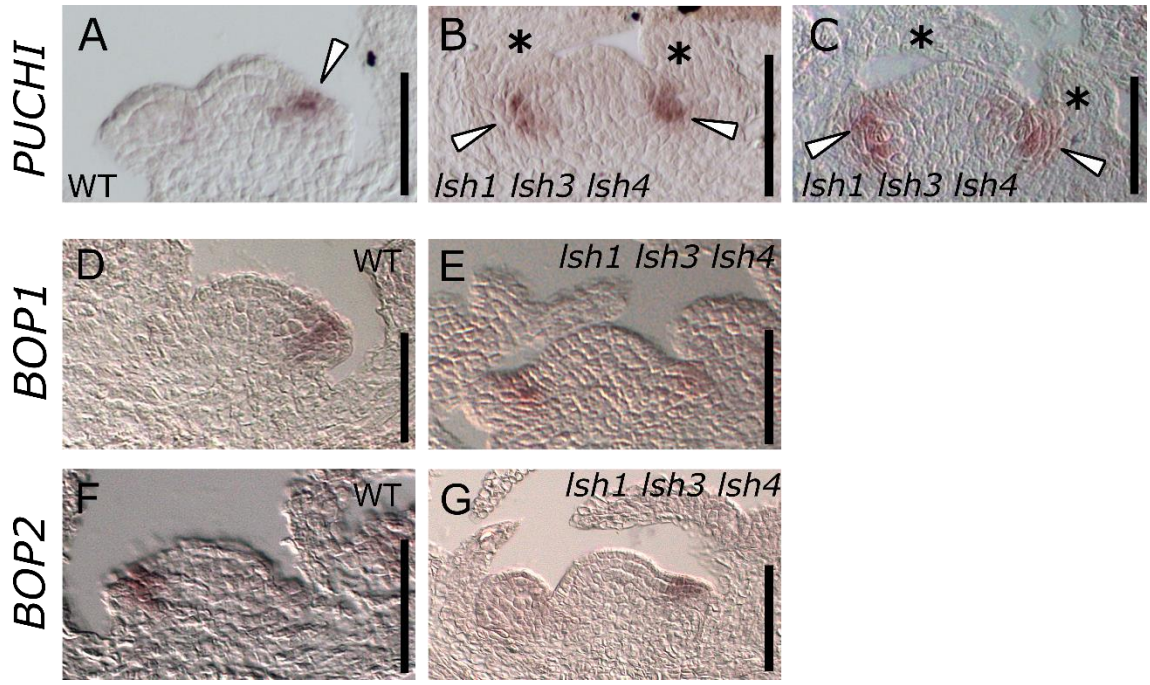

Figure 10. Expression profile of *PUCHI* (A, B, C), *BOP1* (D, E) and *BOP2* (F, G) analyzed by in situ hybridization in the reproductive tissue in wild type (WT, A, D, F) and *lsh1 lsh3 lsh4* (B, C, E, G) backgrounds (Scale bars represent 50 μm; black asterisks indicate the bracts that subtend the primordia, and the white arrows indicate *PUCHI* signal).

These results allow us to speculate that the correct expression, localization and interaction among *LSH1*, *LSH3*, *LSH4*, *BOP1* and *BOP2* is necessary to promote the precise localization of *PUCHI*, which is one of the fundamental players in bract outgrowth suppression. When either *BOP1* and *BOP2* or *LSH1*, *LSH3* and *LSH4* are absent, the balance among the different factors is lost, and this results in defects in the maintenance of the different areas of the meristems and the outgrowth of bracts. *BOP1* and *BOP2*, according to the RNA-seq, resulted upregulated in *lsh1 lsh3 lsh4* background. This upregulation could rely on independent pathways of regulation that are necessary to maintain the balance among the different factors.

I crossed the mutant line *lsh1 lsh3 lsh4* with the reporter line *PUCHI:GFP*, and with the single mutant *puchi-1* (kindly provided by Mitsuhiro Aida; Hirota et al., 2007; Karim et al., 2009). I now obtained the F2 generation. These crosses will be useful to better investigate the relationship among *LSH1*, *LSH3*, *LSH4* and *PUCHI*.

2.7 The correct expression of *SVP* and *STM* in the reproductive meristems is determined by *LSH1, LSH3* and *LSH4*

According to the data obtained from the RNA-seq and the ampDAP-seq, *STM* and *SVP* appear to be both deregulated in the *lsh1 lsh3 lsh4* triple mutant and bounded by the ALOG proteins.

Given the important role played by both *STM* and *SVP* in the context of Arabidopsis' reproductive meristems development, we performed an in-situ hybridization using a digoxigenin-labelled RNA probe specific for *STM* and *SVP* to assess their expression pattern in the inflorescence tissue of the triple mutant *lsh1 lsh3 lsh4.*

The expression of *STM* in wild type inflorescences is localized in the inflorescence meristem and in the flower meristems, except for the area of the cryptic bract (Chung et al., 2019; Long & Barton, 2000; Figure 5 A). During the reproductive development of Arabidopsis, the function of *STM* is to maintain an undifferentiated state of the meristems by preventing the incorporation of cells of the meristem center into differentiating organ primordia (Endrizzi et al., 1996). It was also published that the downregulation of *STM* promotes the initiation of flower primordia (Chung et al., 2019).

In the triple mutant *lsh1 lsh3 lsh4* background, the signal indicating *STM* expression seems lower than in the wild type (**Figure 11 B**). This result is coherent with the downregulation of *STM* according to the RNA-seq. This allows us to hypothesize that, in absence of the three *LSHs*, the expression of *STM* is not sufficient to ensure the maintenance of an undifferentiated stage of the developing primordia's cells, that will therefore develop the bracts.

The expression pattern of *STM* doesn't seem to change in the *lsh1 lsh3 lsh4* background. However, the expression profile of *STM* should be analyzed more carefully, also performing in situ hybridizations of transversal sections of the triple mutant *LSH* reproductive meristems. This will allow a better overview of the developing primordia at different stages of development (Long & Barton, 2000) and consequently an improved definition of STM expression pattern in this mutant background.

To further characterize the expression profile of *STM* in the triple mutant *lsh1 lsh3 lsh4* background, I performed crosses between *lsh1 lsh3 lsh4* and two reporter lines for *STM* [*pSTM::STM-Venus* and *pSTM::ALcR AlcA::GFP*, kindly provided by professor Olivier Hamant, ENS de Lyon (France); Landrein et al., 2015]. I obtained the F2 generation for all the crosses, that will be analysed soon in our laboratory.

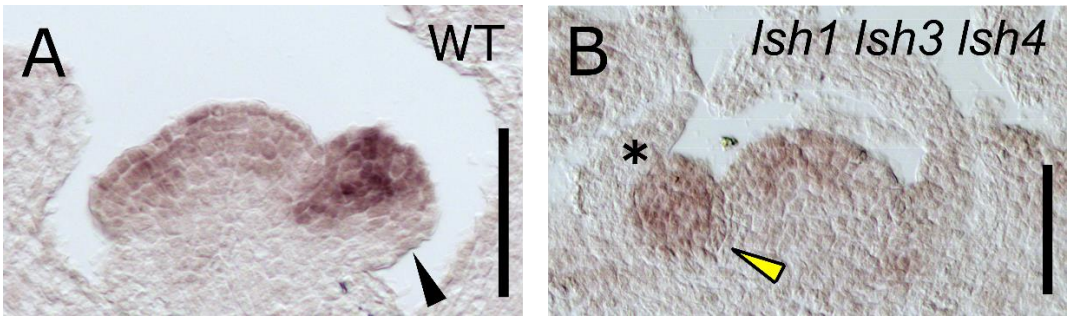

Figure 11. Expression profile of *STM* analyzed by in situ hybridization in the reproductive tissue in wild type (WT, A) and *lsh1 lsh3 lsh4* (B) backgrounds (Scale bars represent 50 μm; black asterisk indicates the bract that subtends the primordia, the black arrow in A indicates the absence of *STM* signal in the cryptic bract, the yellow arrow in B indicates *STM*).

SVP expression in wild type reproductive tissues has a very specific pattern, in a restricted area of the flower primordium (Gregis et al., 2008; Figure 6 A). *SVP* function during the transition to the reproductive phase is to act as a floral repressor in the thermo-sensory pathway (Hartmann et al., 2000). During the reproductive phase, *SVP* has the function to maintain meristematic activity at the level of FM and to prevent the expression of homeotic genes which leads to the precocious differentiation of the FM. In particular, *SVP* represses the class B and C floral homeotic genes (Gregis et al., 2006, 2008, 2009; Porri et al., 2014). Interestingly, in the triple mutant *lsh1 lsh3 lsh4* the signal of *SVP* expression is undetectable in the reproductive meristem tissues (**Figure 12** B). This fact suggests that *LSH1*, *LSH3* and *LSH4* could act as promoters of the expression of *SVP*. In this scenario, when the *LSHs* are absent, *SVP* expression is no longer promoted and the activity of the part of the meristem that gives rise to the bract is no longer repressed, as well as the activation of the floral organ identity genes. The lack of activation of the expression of *SVP* and the consequent misexpression of the floral organ identity genes could explain the mixed floral organ identity of the bracts developed by the triple mutant *lsh1 lsh3 lsh4*, that present for example stigmatic papillae, that could develop due to the lack of repression of the class C homeotic gene *AGAMOUS* operated by *SVP*.

To have a complete overview of the expression pattern of *SVP* in the *lsh1 lsh3 lsh4* background, I performed crosses between *lsh1 lsh3 lsh4* and the reporter line *pSVP:SVP::GFP* (from (Gregis et al., 2009).

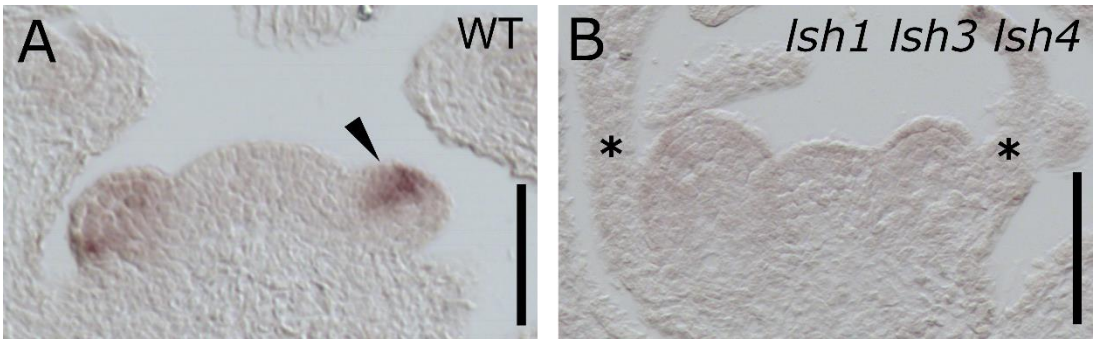

Figure 12. Expression profile of *SVP* analyzed by in situ hybridization in the reproductive tissue in wild type (WT, A) and *lsh1 lsh3 lsh4* (B) backgrounds (Scale bars represent 50 μm; black asterisks indicate the bracts that subtends the primordia, the black arrow in A indicates *SVP* signal in the FM).

In the context of flower meristem development, it is worth mentioning that also *AP1* can act with *SVP* to regulate the expression of floral organ identity genes. Also *AP1* seems to be bound by the *LSHs* according to the results of the ampDAP-seq, and for this reason, it will be interesting to also analyse the expression of *AP1* in the triple mutant background. To do so, I performed a cross between *lsh1 lsh3 lsh4* and an *AP1::GUS* line [provided by Francois Parcy, Laboratoire Physiologie Cellulaire et Végétale, Grenoble (France)].

I obtained the F2 generation for all the crosses, that will be analysed soon in our laboratory and will be useful to further elucidate the pathway in which *LSH1*, *LSH3* and *LSH4* are involved.

2.8 *LFY* controls the spatiotemporal expression of *LSH1*, *LSH3* and *LSH4*

Our collaborators from the group of Francois Parcy, at the Laboratoire Physiologie Cellulaire et Végétale are studying the flower meristem identity gene *LFY* for a long time. Analyzing the results obtained from different ChIP-seq and DAP-seq performed on LFY, they found that this transcription factor is able to bind the promoter region of *LSH1* and *LSH3*, suggesting that *LFY* may be involved in the regulation of the *LSHs*. Also, from the ampDAP-seq that they performed to determine the ALOG proteins binding motif, it resulted that the promoter region of *LFY* is bound by the LSHs, making *LFY* a possible target. As already mentioned before, *LFY* is involved in the pathway of bract outgrowth suppression (Dinneny et al., 2004; Norberg et al., 2005; Weigel et al., 1992b).

Starting from these interesting observations, we decided to further investigate the possible pathways that involve *LFY*, *LSH1*, *LSH3* and *LSH4*.

According to the results obtained from the RNA-seq that we performed on *lsh1 lsh3 lsh4* inflorescences, *LFY* isn't deregulated in the triple mutant background. We decided to investigate the expression pattern of *LFY* in the triple mutant *lsh1 lsh3 lsh4* inflorescences. Since also the promoter

region of *LSH1* and *LSH3* seems to be bound by LFY, we decided to investigate the expression pattern of *LSH1*, *LSH3* and *LSH4* in the *lfy-2* weak mutant line. *lfy-2* early arising inflorescences produce flowers with vegetative characteristics, while the late arising flowers are similar to wild type ones (Grandi et al., 2012). For our analysis, we selected *lfy-2* early arising inflorescences (**Figure 13**).

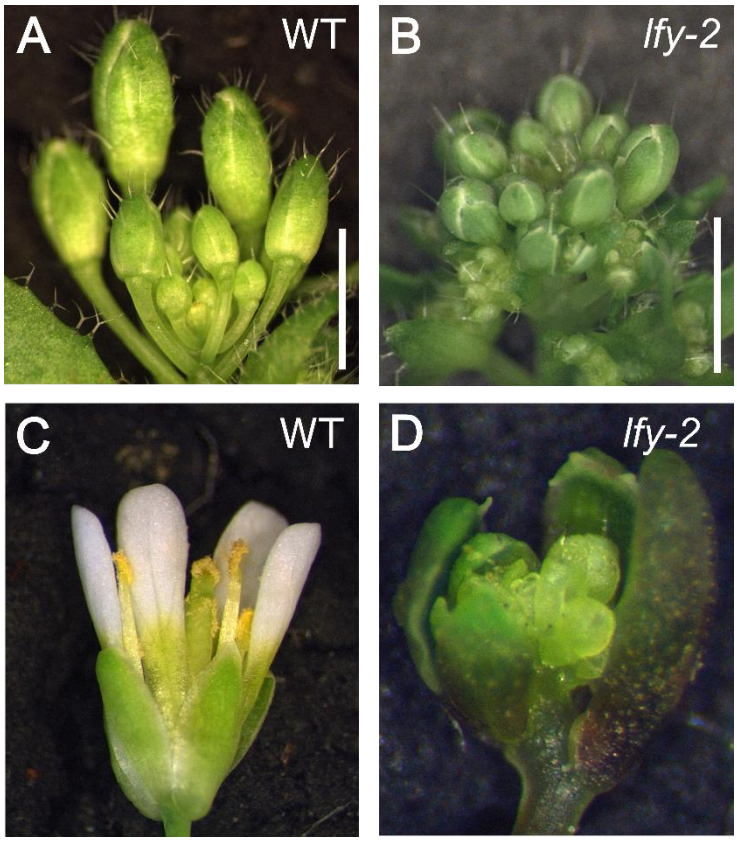

Figure 13. Phenotype of wild type (A, C) and *lfy-2* mutant early arising inflorescences (B, D). *lfy-2* inflorescences present vegetative characteristics (B), as it is visible also in D, where the flower doesn't develop any recognizable floral organ (scale bars in A and B = 3 mm).

The expression of *LFY* in the inflorescences of *lsh1 lsh3 lsh4* was investigated in longitudinal and transversal sections with an in-situ hybridization using a digoxigenin-labelled RNA probe specific for *LFY*. In the triple mutant background, the expression of *LFY* was overall comparable with the wild type (Torti et al., 2012; Figure 14).

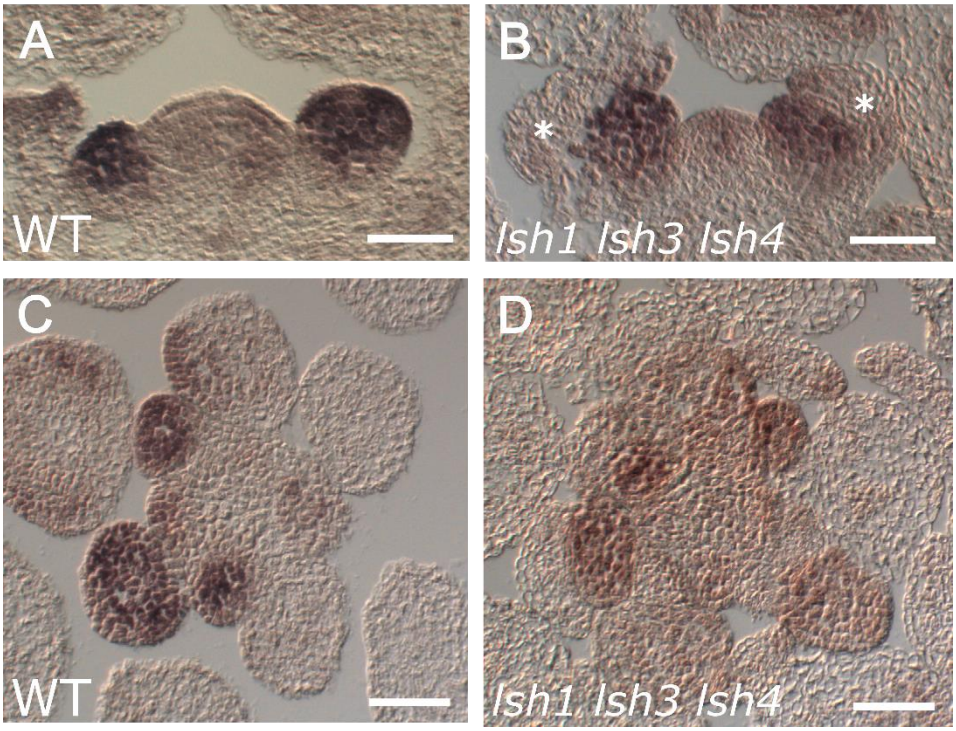

Figure 14. Expression profile of *LFY* analyzed by in situ hybridization in the reproductive tissue in wild type (WT, A, C) and *lsh1 lsh3 lsh4* (B, D) backgrounds. A and B are longitudinal sections of wild type and *lsh1 lsh3 lsh4* reproductive tissue respectively; C and D are transversal section of the reproductive tissue of wild type and *lsh1 lsh3 lsh4* reproductive tissue respectively (Scale bars = 50 μm; white asterisks indicate the bracts that subtends the primordia).

We then investigated the expression of *LSH1*, *LSH3* and *LSH4* in longitudinal and transversal sections of the inflorescences of *lfy-2* mutant line (**Figure 15**). Interestingly, the expression pattern of all three *LSHs* was altered in the *lfy-2* mutant background with respect to the wild type. In particular, *LSH1* expression was almost undetectable in *lfy-2* background (**Figure 15** A-D). The expression of *LSH3* resulted in a more diffused pattern in *lfy-2* background, indeed it was localized also in the flower meristem, an area in which is normally not expressed in wild-type plants (**Figure 15 E-H**). *LSH4* expression, that in the wild type marks precisely the boundary region, in *lfy-2* background is widely detectable in all the inflorescence (**Figure 15 I-N**).

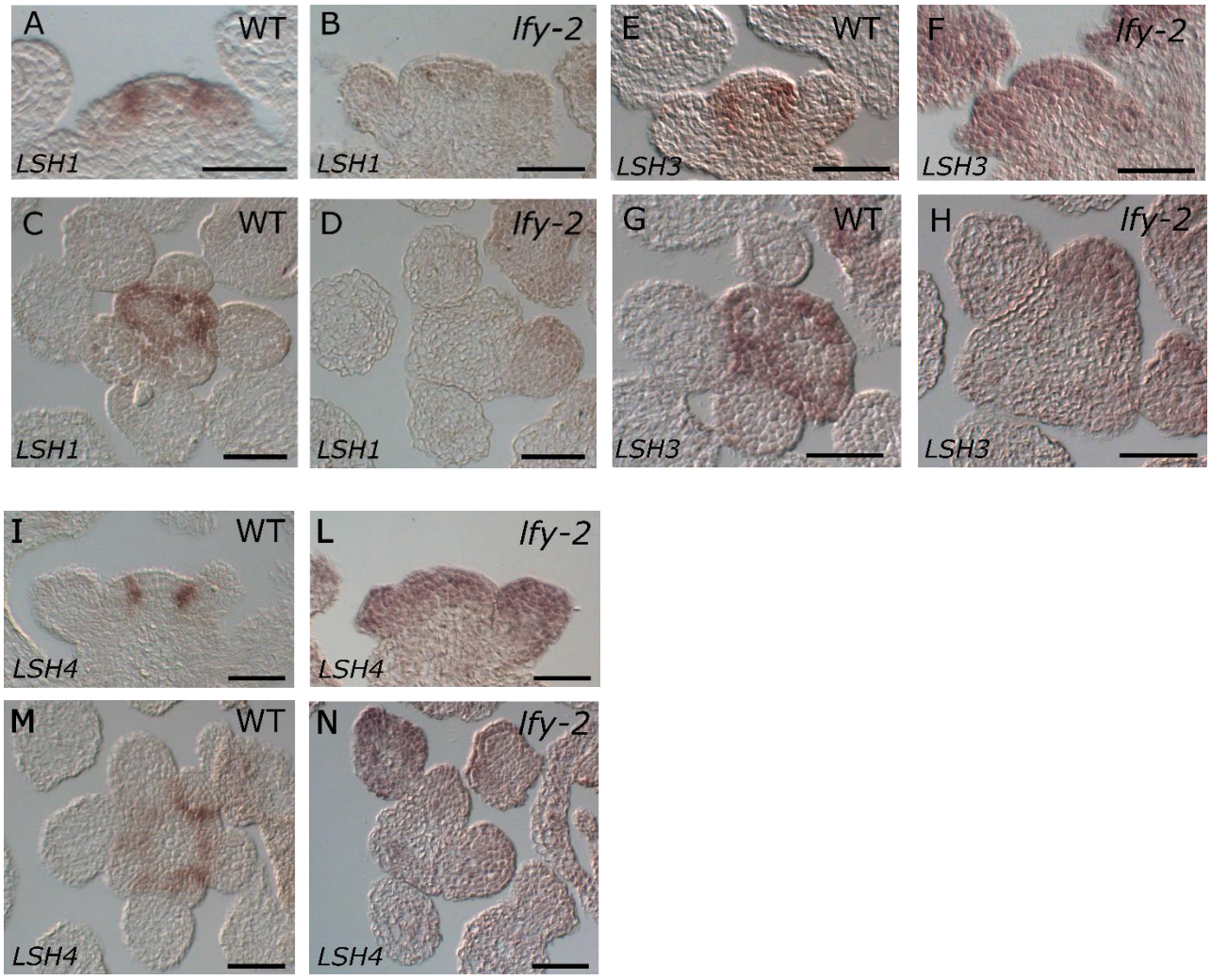

Figure 15. Expression profile of *LSH1* (A-D), *LSH3* (E-H) and *LSH4* (I-N) analyzed by in situ hybridization in the reproductive tissue in wild type (WT, A, C, E, G, I, M) and *lfy-2* (B, D, F, H, L, N) backgrounds. A, E, I are longitudinal sections of wild type reproductive tissue; B, F, L are longitudinal sections of *lfy-2* reproductive tissue; C, G, M are transversal section of the reproductive tissue of wild type and D, H, N are transversal section of *lfy-2* reproductive tissue. (Scale bars = 50 μm).

Taking together these observations, we can propose that *LFY* can regulate *LSH1*, *LSH3* and *LSH4* expression in the reproductive meristems. Indeed, *LFY* can promote the expression of *LSH1*, while it modulates the expression of *LSH3* and confines the expression of *LSH4* in the boundary region.

Further experiments are needed to better uncover the relationship existing among *LFY*, *LSH1*, *LSH3* and *LSH4*. It will be interesting to better investigate the pattern of expression of *LFY* in the *lsh1 lsh3 lsh4* background by means of a reporter line. For this reason, we performed a cross between the triple mutant *lsh1 lsh3 lsh4* and a reporter line *LFY:GFP* [kindly provided by Francois Parcy, Laboratoire Physiologie Cellulaire et Végétale, Grenoble (France)]

2.9 DISCUSSION

LSH1, *LSH3* and *LSH4* were found to be expressed in the reproductive meristem tissues of *Arabidopsis thaliana* with a similar pattern (Mantegazza, Gregis, Chiara, et al., 2014). Their expression profile suggests a probably redundant role in the inflorescence development of Arabidopsis.

They belong to the *ALOG* gene family that, despite its diffusion among the plant kingdom, is still poorly studied. Just recently, our collaborators from the group of Francois Parcy, at the Laboratoire Physiologie Cellulaire et Végétale, in Grenoble (France) were able to confirm that the ALOGs are indeed transcription factors, and they defined the structure of their DNA-binding domain (called ALOG domain) and also the binding motif of these proteins (unpublished data).

Given the overlapping expression profile of *LSH1*, *LSH3* and *LSH4* in the reproductive meristems of Arabidopsis, it is possible to hypothesize that these three *ALOG* genes play a redundant role in the inflorescence development of Arabidopsis.

To better uncover the pathway in which the three *LSHs* are involved, we started with the generation of mutants. However, due to the possible redundancy of the three genes neither the single mutants nor any of the double mutant combinations showed visible defects in the inflorescence architecture. The triple mutant *lsh1 lsh3 lsh4* can develop bracts, leaf-like organs that subtend each flower. The bracts of the triple mutant present sepal-like cells and present stigmatic papillae. This suggests the development of an organ with a mixed identity that emerges from an area of the flower meristem that in wild type plants is kept silent. Indeed, in wild type Arabidopsis plants, the bracts are cryptic, and their outgrowth is repressed (Long & Barton, 2000).

To understand how *LSH1*, *LSH3* and *LSH4* are involved in the pathway of bract suppression, we performed an RNA-seq on the inflorescences of *lsh1 lsh3 lsh4* and wild type plants. To analyze the dataset to obtain a list of differentially expressed genes (DEGs), we decided to apply a log2 Fold Change (log2 FC) equal to 0 to obtain an adequate number of DEGs to analyze the GO terms in which *LSH1*, *LSH3* and *LSH4* are involved in. Then we compared the RNA-seq results with the ampDAP-seq performed by our collaborators. In this way, we were able to make a list of interesting genes to further analyze in the *lsh1 lsh3 lsh4* background. We then investigated the expression pattern of the selected putative targets, and furthermore, we tested the possible interactions among LSH1, LSH3 and LSH4 and the other known players in the pathway of bract suppression. We focused our analysis on *BOP1*, *BOP2*, *PUCHI*, *STM*, *SVP* and *LFY*.

Our analysis indicates that LSH1, LSH3 and LSH4 are likely to interact with BOP1 and BOP2, encoded by two boundary genes that, together with *PUCHI*, are able to promote FM development and that are involved in the pathway of bract suppression (Karim et al., 2009). Since in the *lsh1 lsh3 lsh4* background the expression of *PUCHI* is not confined anymore in the adaxial side of the boundary region, as it happens in the double mutant *bop1 bop2*, we propose that the interaction among LSH1, LSH3, LSH4, BOP1 and BOP2 is necessary for the boundary region to maintain its identity, by confining the expression of *PUCHI* (Karim et al., 2009; Figure 10, B).

STM, according to the results obtained from the ampDAP-seq, presents in its promoter region the binding domain of the ALOG proteins. Furthermore, it resulted to be downregulated in the *lsh1 lsh3 lsh4* background according to the RNA-seq results. Given the role of STM in maintaining an undifferentiated state of the meristem and in preventing the cells to be incorporated in growing primordia, it is tempting to hypothesize that *LSH1*, *LSH3* and *LSH4* can promote and maintain the expression of *STM* in the reproductive meristems. If the three *LSHs* are absent, *STM* is downregulated and its expression is not sufficient to maintain the meristematic cells in an undifferentiated stage, allowing the outgrowth of the bracts (**Figure 16**, A). The expression pattern of *STM* in the triple mutant background will be analyzed more in detail in our laboratory by means of in situ hybridization on transversal sections of the reproductive meristem and thanks to the crosses with the marker lines.

Like *STM*, *SVP* resulted to be both downregulated in the *lsh1 lsh3 lsh4* background and bounded by the ALOG proteins. *SVP* expression appears to be regulated by *LSH1*, *LSH3* and *LSH4.* Indeed, in the triple mutant *lsh1 lsh3 lsh4* the signal of *SVP* expression is undetectable. *SVP* is involved in the maintenance of the meristematic activity at the level of FM and in the repression of the precocious expression of the floral organ identity genes, such as *AG*. We can hypothesize that, in absence of the *LSHs*, the expression of *SVP* is no longer promoted. This probably allows the development of the bracts with sepal-like cell composition and the development of stigmatic papillae (**Figure 16**, A).

Interestingly, the expression of *LSH1*, *LSH3* and *LSH4* seems to be regulated by the FM identity gene *LFY*, as suggested by the fact that LFY seems to be able to bind the promoter region of *LSH1* and *LSH3*. From the analysis of the expression of *LSH1*, *LSH3* and *LSH4* in the inflorescences of *lfy-2* mutant plants, we could conclude that *LFY* regulates in a different way the three *LSHs*: *LFY* can act as a promoter of the expression of *LSH1*, can modulate the spatial expression of *LSH3* and is a repressor of *LSH4* (**Figure 16**, B).

The crosses that I am performing between *lsh1 lsh3 lsh4* and the reporter lines for *LFY*, *AP1*, *PUCHI*, *STM* and *SVP* and with the single mutant *puchi-1* will allow in the future a better characterization of the pathway in which *LSH1*, *LSH3* and *LSH4* are involved.

Overall, the results that we obtained indicated that *LSH1*, *LSH3* and *LSH4* have overlapping functions in the pathway that leads to the correct specification and maintenance of the different areas of the reproductive meristems of Arabidopsis. Indeed, in wild type Arabidopsis plants the inflorescence meristem maintains its indeterminate stage and develops flower meristems on its flanks. Between the IM and the FMs there are the boundary regions, where cell proliferation is suppressed to allow the development of separate organs. The specification of the FMs depends on the activity of different factors expressed in the FM itself or also in the boundary regions. Arabidopsis flowers are not subtended by bracts, which instead remain cryptic. The correct development of the FM and of the boundary areas represses bract growth. If the balance among all the factors is maintained, Arabidopsis inflorescence will develop in the correct way. If one or more factors are impaired, the balance is perturbed and the plant can present organ fusion, but also defects in organ development and altered phyllotactic patterning. In other cases, the plants can develop extra-organs, like bracts as happens in the triple mutant *lsh1 lsh3 lsh4*.

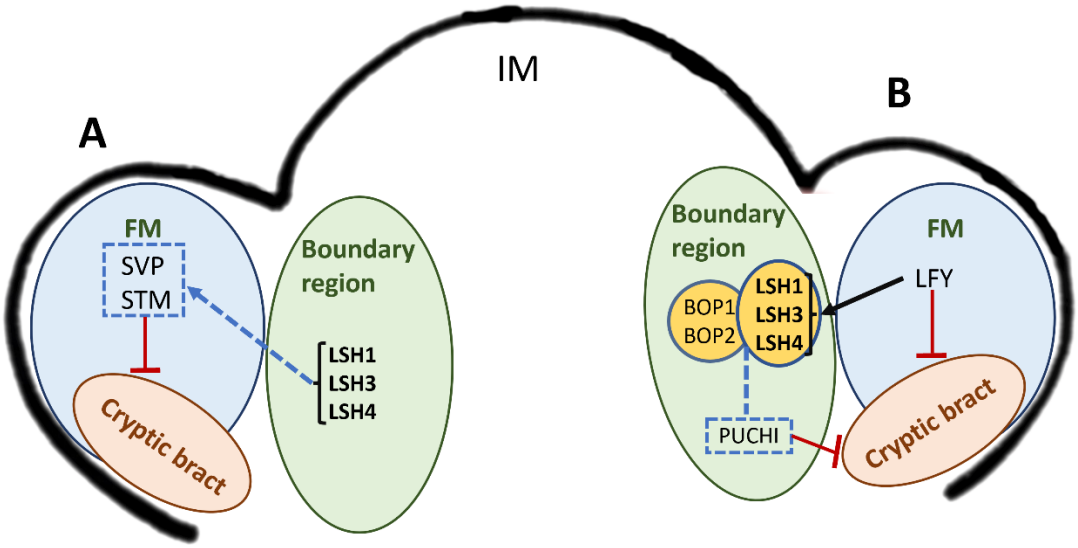

Figure 16. Model of the pathways in which *LSH1, LSH3* and *LSH4* are involved in the context of reproductive meristem maintenance and bract suppression. A, in the boundary region, LSH1, LSH3 and LSH4 promote the expression of *SVP* and *STM* in the flower meristem (FM), that in turn can prevent the outgrowth of the bracts (blue dotted arrow and square indicate putative positive regulation of the expression; ⊣ represents negative regulation). **B**, LSH1, LSH3 and LSH4, interacting with BOP1 and BOP2 can determine the correct expression domain of *PUCHI* in the boundary region. *PUCHI* is one of the players involved in bract outgrowth suppression. Also, *LFY*, expressed in the FM, can determine the correct expression

of *LSH1*, *LSH3* and *LSH4* in the boundary region, allowing the correct balance among the different players involved in bract suppression (Blue dotted line and square indicate the spatial confinement of expression; the yellow circles represent protein interaction; ⟶ indicates regulation of expression; ⊣ represents negative regulation)

CONCLUSIONS AND FUTURE PERSPECTIVES

Inflorescence architecture is one of the key agronomical traits which determines grain yield. Knowing the gene pathways that lead to its development is of extreme interest to improve crop production.

In this context, to identify new players involved in inflorescence architecture development, our group performed a transcriptomic analysis on the different reproductive meristem types of both the model plants *Oryza sativa* and *Arabidopsis thaliana* (Harrop et al., 2016; Mantegazza, Gregis, Chiara, et al., 2014).

From this analysis, it resulted that some members of the *ALOG* gene family resulted to be expressed with a similar pattern in the different reproductive meristem types of both rice and Arabidopsis. This result could indicate an involvement of these genes in the reproductive development of both plant species. These genes are *G1L1*, *G1L2* and *G1L5/TAW1* in rice and *LSH1*, *LSH3* and *LSH4* in Arabidopsis. Interestingly, *G1L5/TAW1* was already characterize as one of the fundamental regulators of panicle development in rice, reinforcing the hypothesis of an involvement of the *ALOGs* in the reproductive development of rice and Arabidopsis (Yoshida et al., 2013).

During my Ph.D. I focused my research activity on elucidating the role played by the *ALOG* genes that we selected during the inflorescence development of both rice and Arabidopsis.

In rice, we focused our analysis on understanding the role played by *G1L1* and *G1L2* in the context of panicle development. Indeed, the two single mutants *g1l1* and *g1l2* produce shorter panicles, with fewer primary branches, fewer secondary branches, and fewer spikelets than the wild type. Also, the grains resulted to be smaller respect to the wild type. Overall, *g1l1* and *g1l2* single mutant phenotype resembles *taw1* mutant phenotype (Yoshida et al., 2013). Further analysis performed with the SEM and by means of in situ hybridization using a probe specific for *FZP*, a marker for the determinate stage of the meristem, suggest that *G1L1* and *G1L2* are involved in the crucial process of phase change of the reproductive meristems, preventing the indeterminate branch meristem from reaching the determinate stage of spikelet meristem too soon, stopping any branching potential.

An RNA-seq performed on the early stages of panicle development in the *g1l2* background allowed us to generate a gene regulatory network and to individuate putative direct targets of *G1L2*. We then tested the expression of interesting genes also in *g1l1* and *taw CR-1* mutants. We also analyzed the panicles of the *g1l1 g1l2* double mutant, that shows a most severe phenotype with respect to the two single mutants. Overall, our analysis allowed us to conclude that *G1L1*, *G1L2* and *TAW1* seem to

work in partially overlapping pathways that control the phase change transition from an indeterminate to a determinate stage of the meristem.

Since the single mutant *g1l2* was the one showing the most drastic phenotype, it will be interesting to better characterize the role played by *G1L2* in the context of panicle development by the analysis of the overexpression line *pACT:G1L2* and the reporter line *pG1L2:G1L2:YFP* that I am generating.

Further analysis of the *g1l1 g1l2* double mutant, as well as of the other combination of double and the triple mutant among *G1L1, G1l2* and *TAW1* will be helpful to clarify the relationship existing among these three genes. Also, the role of *G1L1* and *G1L2* in the context of plant fertility and grain quality should be better investigated.

In Arabidopsis, we focused our work on *LSH1*, *LSH3* and *LSH4*. *LSH3* and *LSH4* were already published as involved in the reproductive development of Arabidopsis (Cho & Zambryski, 2011a; S. Takeda et al., 2011). Since also *LSH1* resulted to be expressed in the reproductive meristems of Arabidopsis with a similar pattern, we hypothesize an involvement of all three genes in the context of Arabidopsis inflorescence development.

Interestingly, nor the single mutants or the different combination of double mutants for *LSH1*, *LSH3* and *LSH4* showed visible alterations in inflorescence development, indicating a possible redundancy among the three genes. The triple mutant *lsh1 lsh3 lsh4* can develop bracts under each flower. Analyzing more in deep the phenotype of the bracts, we noticed that they present floral features, such as sepal-like cells and stigmatic papillae. Since this phenotype could indicate a perturbation in the specification of the different areas of the reproductive meristems, we performed further experiments to determine the pathway in which *LSH1*, *LSH3* and *LSH4* are involved.

We were able to conclude that LSH1, LSH3 and LSH4 are likely to interact with BOP1 and BOP2, two factors already known to be involved in the maintenance of the boundary region, the specification of the FMs and the suppression of bract outgrowth (Karim et al., 2009; Pouteau et al., 2004; M. Xu et al., 2010). The three *LSHs* and *BOP1/2* probably cooperate in confining the expression of *PUCHI* for the correct specification of the boundary region and the consequent suppression of bract outgrowth. We also perform a cross between *lsh1 lsh3 lsh4* and the single mutant *puchi-1* and the reporter line *PUCHI:GFP*, to better determine the possible relationship existing between the *LSHs* and *PUCHI* (Karim et al., 2009; Norberg et al., 2005; M. Xu et al., 2010).

According to the results of in situ hybridization experiments using probes specific for *SVP* and *STM*, we can hypothesize that the *LSHs* are necessary to promote the expression of *SVP* and *STM*. Both

SVP and *STM* are necessary for the correct identity maintenance of the flower meristem (Endrizzi et al., 1996; Chung et al., 2019; Gregis et al., 2006; Porri et al., 2014). It will be interesting to further analyze the expression pattern of *SVP* and *STM* in the *lsh1 lsh3 lsh4* background. To do so, crosses between the triple mutant *lsh1 lsh3 lsh4* and reporter lines for *SVP* and *STM* were performed.

LSH1, *LSH3* and *LSH4* are also regulated by the flower meristem identity gene *LFY*, that seems to be necessary to maintain the correct expression pattern of the three *LSHs*. Furthermore, the LSHs seem to bind the promoter regions of both the flower meristem identity genes *LFY* and *AP1*. It will be informative to deepen the analysis of expression of *LFY* and *AP1* in the triple mutant *lsh1 lsh3 lsh4*. To do so, we performed crosses between the triple mutant and reporter lines for *LFY* and *AP1*.

We will also analyze how the hormones auxin and cytokinin, fundamental for the correct development of the inflorescence, are distributed in the *lsh1 lsh3 lsh4* background by means of crosses between *lsh1 lsh3 lsh4* and the reporter lines *DR5:GFP/DR5v2:Tomato* and *DII:VENUS* (that allow to visualize auxin maxima and auxin minima respectively) and *TCSn:GFP* (a reporter for cytokinins).

Overall, our results indicate the importance of the *ALOG* gene family in the specification and maintenance of the reproductive meristems of rice and Arabidopsis and their consequent involvement in the development of both plant species. Their study will help in increasing the knowledge about the gene pathways that lead to inflorescence development and so to understand how we can improve crop yield.

MATERIALS AND METHODS

1. *Oryza sativa*

1.1 Transgenic lines generation

To generate the construct *pACT:G1L2*, the CDS of *G1L2* was amplified using primers Osp1893/Osp1894 respectively using high-fidelity polymerase Q5 (NEB) following the protocol described on NEB website (https://www.neb.com) and using High GC enhancer buffer and 0,03 ul GoTaq (Promega). The CDS was cloned first into pDNR207(Invitrogen) entry vector and then into pH2GW7 destination vector containing rice actin promoter (*pACT1*) (provided by Fabio Fornara, Università degli studi di Milano) by the Gateway® LR reaction. Each Plasmid was checked by PCR and by sequencing and then transformed into rice calli using *Agrobacterium tumefaciens* (EH105 strain) mediated transformation.

To generate the construct *pG1L2:G1L2:YFP*, a promoter region of 2500 bp upstream *G1L2* ATG start site, and the CDS of *G1L2* minus the stop codon were amplified using high-fidelity polymerase Q5 (NEB) following the protocol described on NEB website (https://www.neb.com) and using High GC enhancer buffer and 0,03 ul GoTaq (Promega) and the primer pairs Osp2075/Osp2101 and Osp1893/Osp2076 respectively. The promoter region and the CDS of *G1L2* were cloned in the pDONR™221 P1-P5r (Invitrogen) and pDONR™221 P5-P2 (Invitrogen) entry vectors respectively by the Gateway® BP reaction. The promoter region and the CDS of *G1L2* were then inserted into the destination vector pGWB540 (provided by Fabio Fornara, Università degli studi di Milano) by the Gateway® LR reaction. Each Plasmid was checked by PCR and by sequencing and the destination vector was then transformed into rice calli obtained from *g1l2* single mutant seeds using *Agrobacterium tumefaciens* (EH105 strain) mediated transformation.

1.2 Crosses between rice plants

Oryza sativa, ssp. japonica, cv Nipponbare plants were grown for 8-10 weeks in LD conditions (70% humidity, 16h light at 28°C/8h dark at 26°C) and then moved in SD conditions (70% humidity, 12h light at 28°C/12h dark at 26°C) to induce flowering. When the panicle emerged from thee flag leaf, from each spikelets the male organs were manually removed to leave only the ovary, that was subsequently manually pollinated with anthers in the correct stage of development taken from spikelets from plants of the desired genotype. To genotype the obtained plants, the following primer pairs were used: *G1L1* Osp1840/Osp1841; *G1L2* Osp1362/Osp1363; *TAW1* Osp2075/Osp2101.

1.3 List of primers used

Primers used for amplification		
GENE	OLIGOS-ID	SEQUENCE
G1L2 CDS with stop codon	Osp1893 (fw)	GGGGACAAGTTTGTACAAAAAAGCAGGCTagGACGTCATGCAGGGAGG
	Osp1894 (rv)	GGGGACCACTTTGTACAAGAAAGCTGGGTgCTAGTTAAACACGGACAGCG
G1L2 CDS without stop codon	Osp1893 (fw)	GGGGACAAGTTTGTACAAAAAAGCAGGCTagGACGTCATGCAGGGAGG
	Osp2076 (rv)	GGGGACCACTTTGTACAAGAAAGCTGGGTcGTTAAACACGGACAGCGGCA
G1L2 2500 bp promoter region	Osp2075 (fw)	GGGGACAAGTTTGTACAAAAAAGCAGGCTGAGACACGGACGATGTATAC
	Osp2101 (rv)	GGGGACAACTTTTGTATACAAAGTTGTGACGTCCTAGCACAAGCAGC

Primers used to genotype transgenic plants		
G1L1	Osp1840 (Fw)	GGAGATGGACATGATCGGCATGG
	Osp1841 (Rv)	GAAGTGCGCCGGGAACAAGAAGTG
G1L2	Osp1362 (Fw)	AGGTTTGCTGCTGCTTGTGC
	Osp1363 (Rv)	TGAGACGAAGACGAGGAGGTG
TAW1	Osp1837 (Fw)	GCAGATCGACGATGGAGTTCGTG
	Osp1838 (Rv)	GCTTCTTGCGCTTCTTCTTCTCG

2. *Arabidopsis thaliana*

2.1 Plant material and growth conditions

All experiments were performed in Arabidopsis thaliana ecotype Columbia-0 (Col-0). Plants were grown in a controlled environment at 20–22°C either under long day conditions (16 h light/8 h dark) or under short day (8 h light/16 h dark) conditions for 4 weeks after germination and then transferred to long day conditions. When necessary, seeds of Arabidopsis were germinated on MS plates (Murashige & Skoog Medium, supplemented with 1% sucrose and solidified with 0,7% Plant Agar) with the appropriate selection. The reporter line *PUCHI:GFP* and the single mutant line *puchi-1* were kindly provided by Mitsuhiro Aida, Nara Institute of Science and Technology, Nara (Japan). The *AP1::GUS* and *LFY:GFP* plant lines were kindly provided by Francois Parcy, Laboratoire Physiologie Cellulaire et Végétale, Grenoble (France). The reporter line *pSVP:SVP::GFP* was generated by Veronica Gregis, Università degli studi di Milano; and the two reporter lines for *STM* (*pSTM::STM-Venus* and *pSTM::ALcR AlcA::GFP*) were kindly provided by professor Olivier Hamant, ENS de Lyon (France). The reporter lines for the hormone auxin *DR5:GFP/DR5v2:Tomato* and *DII:VENUS* were kindly provided by Dolf Weijers (Wageningen University, Netherlands). The reporter line *TCSn:GFP* was provided by Jiří Friml (Ghent University, Belgium).

2.2 RNA isolation and cDNA synthesis

In Arabidopsis, 100 mg per plant tissues (roots, hypocotyl, cotyledon, rosette and cauline leaves, inflorescence, siliques) were harvested and ground with liquid nitrogen for total RNA extraction. Total RNA was extracted from three biological replicates of each tissue sample using the LiCl extraction method as previously described by Gregis et al., 2008. The RNA was reverse transcribed using the iScript™ cDNA Synthesis Kit (BIO-RAD, https://www.bio-rad.com/), and the obtained cDNA was used as a template in RT-PCR reactions.

2.3 qRT-PCR analysis

The RT- PCR analysis was carried out in a final volume of 12 µL using a Biorad C1000™ thermal cycler and using 3 µL of a 1:10 dilution cDNA, 0,2 µM (stock 10mM) Forward and Reverse Primer, 6 µL eQ Sybr Green Super Mix 2X (Bio-Rad), 2,6 µl MQ H2O.

The expression levels of *LSH1*, *LSH3* and *LSH4* were evaluated using the primer pairs RT2250/RT2251, RT2254/RT2255 and RT2252/RT2253 respectively and was performed with the following conditions: 95°C 90'' 40 cycles (95°C 15'', 58°C 10'', 60°C 30'') and 60°C 10''.

Three biological replicates for each experiment were performed.

Arabidopsis reference gene *UBIQUITIN* (*At4g36800*) was used as an internal reference during the experiments. Primer sequences are listed in paragraph 2.10.

2.4 CRISPR-Cas9 mutant generation

For generation of *lsh1*, *lsh3* and *lsh4* single knock- out mutants, 20-bp specific protospacers (see the list of primers used "2.10 Protospacers for CRISPR-Cas9 editing system") for each gene were selected using CRISPR-P v2 database (http://crispr.hzau.edu.cn/CRISPR2/) and cloned into *BbsI* site of pEN-Chimera entry vector under the Arabidopsis U6-26 promoter and then combined into the destination vector containing the Cas9, by single site Gateway® LR reaction.

2.5 Silique Length, Seed Number Evaluation, and Crosses

For at least 3 plants for each line, 10 siliques were dissected in order to evaluate the number of seeds, aborted seeds, and non-fertilized ovules employing a Leica® MZ 6 microscope. To perform the crosses, stage 11-13 buds were emasculated, removing all floral organs except for the ovary. Anthers in the correct stage of development were than taken from other flowers and used to pollinate the stigma.

2.6 Scanning Electron microscopy (SEM)

Scanning Electron Microscopy samples were prepared as described (Mizzotti et al., 2015) by gold coating them using a sputter coater (SEMPREP2; Nanotech) followed by observation with a FESEM SIGMA Scanning Electron Microscope (Zeiss).

2.7 Transcriptome analysis

Sequencing libraries were prepared by NovoGene with poly-A enrichment in order to select for messenger RNA and sequenced with Illumina platform in paired end, 2x150 bp mode. Reads were trimmed with fastq-mcf v1.05 (https://github.com/ExpressionAnalysis/ea-utils) with options -l 50 -q 30 and adapters specified by Novogene. Quality was assessed with FastQC v0.11.5 (https://www.bioinformatics.babraham.ac.uk/projects/fastqc/) and MultiQC v1.12 (Ewels et al., 2016).

Arabidopsis thaliana genome assembly TAIR10 with annotation Araport11 (Cheng et al., 2017) was downloaded from the JGI data portal https://data.jgi.doe.gov/refine-download/phytozome?organism=Athaliana&expanded=447 (accessed on 2022/10/12).

Rsem v1.2.31 (Parrish et al., 2014) was used to prepare the reference sequences for mapping from the transcript file and transcript-to-gene information in order to obtain gene-level abundance estimates. Rsem and Bowtie2 v2.3.4.1 (Langmead & Salzberg, 2012) were used to map the reads on the Arabidopsis thaliana transcripts.

Mapping statistics and differential gene expression analysis were conducted in R version 4.0.2 [R Core Team (2020) https://www.R-project.org/.] on RStudio Desktop 2022.02.3+492 for Windows (http://www.rstudio.com/.). The Bioconductor environment was used (Biobase v2.48.0) (Huber et al., 2015). Package Tximport v1.16.1 (Soneson et al., 2015) was used to import count tables and differential gene expression analysis was performed with DESeq2 v1.28.1 (Love et al., 2014). P-values for differential expression were adjusted with the Benjamini-Hochberg method and the cutoffs for differential expression were set at $|\log2(\text{Fold Change})| > 0$ and $\text{padj} < 0.05$. Plots were obtained with ggplot2 v3.3.5 (Wickham, 2016; https://ggplot2.tidyverse.org).

Differentially expressed genes were analysed for Gene Ontology term enrichment in ShinyGO v0.76 setting Arabidopsis thaliana as species (Ge et al., 2020). Fold enrichment and number of genes was plotted for the 20 most significant terms belonging to Biological Process.

2.8 Yeast two Hybrid (Y2H) essay

The AH109 yeast strain was used for the Yeast-2-Hybrid assay, and yeast transformation was performed as described by de Folter and Immink, 2011. The coding sequences of LSH1, LSH3, LSH4, BOP1, BOP2, PUCHI, LFY, AP1, JAG and JGL were cloned in the GAL4 system Gateway® vectors (pGADT7 and pGBKT7; Clontech Laboratories, Inc.). The protein-protein interaction assays were performed on selective yeast synthetic dropout medium lacking Leu, Trp, Ade, and His, and supplemented with different concentrations of 3-aminotriazole (1, 2.5, or 5 mm of 3-AT). Plates were grown for 5 days at 20°C. The CDS of the genes of interest were cloned with the following primer pairs: LSH1 Atp6397/Atp6398, LSH3 Atp7426/Atp6400, LSH4 Atp6401/Atp6402, BOP1 Atp7372/Atp7373, BOP2 Atp7374/Atp7375, PUCHI Atp7398/Atp7399, LFY Atp7390/Atp7391, JAG Atp7376/Atp7377 and JGL Atp7378/Atp7379. AP1 coding sequence was recovered from a plasmid provided by Martin F. Yanofsky, University of California at San Diego, La Jolla (California, USA); and inserted in the pGADT7 using the restriction enzymes EcoRI/SalI (NEB). As positive and negative controls, the already published interactions between REM35 and REM35; and between REM34 and REM34 respectively were used (Caselli et al., 2019). the primers used are listed in 2.10.

2.9 In situ hybridization

In situ hybridization analyses on *LSH1*, *LSH3*, *LSH4*, *BOP1*, *BOP2*, *PUCHI*, *SVP*, *STM* and *LFY* were performed as described in Caselli et al., 2019. The plant material was obtained growing the plants for 4 weeks in short day conditions and then in long day conditions. The whole inflorescence was sampled after bolting when the plant height reached approximately 5 cm. To generate RNA antisense probes, gene fragments were amplified using the primer pairs listed in paragraph 2.7. Evaluation of the expression profile in the inflorescence and flower meristems, which was previously published for *BOP1*, *BOP2*, *PUCHI*, *SVP*, *STM* and *LFY* was used as a positive control (Chung et al., 2019; Gregis et al., 2008; Hepworth et al., 2005; Karim et al., 2009; Long & Barton, 2000; Torti et al., 2012). The antisense and sense RNA probes for *LSH1*, *LSH3* and *LSH4* were transcribed from pGEM®-T Easy with T7/SP6 RNA polymerase (Promega) according to the manufacturer's instructions.

2.10 List of primers used

Primers used to genotype transgenic plants		
GENE	OLIGOS-ID	SEQUENCE
LSH1	Atp6515 (fw)	GGCTAGACATCTGCTTTGGCTTC
	Atp6516 (rv)	GAACTGGTCAAGGTAGCGGAGG
LSH3	Atp6131 (fw)	CAGCTCCTCCATATCCATCAAG
	Atp6132 (rv)	TTGAGTTCGCCGATGGTGAG
LSH4	Atp6134 (fw)	CAAGCCTCCTCTCATCTTCACC
	Atp6520 (rv)	CTTAGTCTTGCCGAATTGGTCG
Protospacers for CRISPR-Cas9 editing system		
LSH1	Atp6677 (fw)	attgACGTGTGCGCCGCTACACGA
	Atp6678 (rv)	aaacTCGTGTAGCGGCGCACACGT
LSH3	Atp6679 (fw)	attgGAAGGCTCTTCAGCTTACGG
	Atp6680 (rv)	aaacCCGTAAGCTGAAGAGCCTTC
LSH4	Atp6374 (fw)	attgCGGGGACTAACCAGCTAAGC
	Atp6375 (rv)	aaacGCTTAGCTGGTTAGTCCCCG
Primers for qRT-PCR		
LSH1	RT2250 (fw)	AACAGGCAGAAACCGCAAAC
	RT2251 (rv)	AGTACAGAAACAAAAGCATCAGTAG
LSH3	RT2254 (fw)	AGCGTCCTCTTCCTTCGTCG
	RT2255 (rv)	GAAAACCCTACCTTCCTCC
LSH4	RT2252 (fw)	GACTCACAAGCCTCCTCTCATC
	RT2253 (rv)	TGCTTAGCTGGTTAGTCCC
Ubiquitin	RT147 (fw)	CTGTTCACGGAACCCAATTC
	RT148 (rv)	GGAAAAAGGTCTGACCGACA
Primers for *in-situ* hybridization		
LSH1	Atp6128 (fw)	TCAACAGGCAGAAACCGCAAAC
	Atp6420 (rv)	CAACTAGTACAGAAACAAAAGCATC
LSH3	Atp6131 (fw)	CAGCTCCTCCATATCCATCAAG
	Atp6421 (rv)	TTGAGTTCGCCGATGGTGAG
LSH4	Atp6134 (fw)	CAAGCCTCCTCTCATCTTCACC
	Atp6422 (rv)	TTAGCTGGTTAGTCCCCGAG
BOP1	RT3192 (fw)	GCATTGGTTATATCACGCGA
	RT3193 (rv+T7)	TAATACGACTCACTATAGGGTGATGATGCAGATTCATTCC
BOP2	RT3194 (fw)	CTCATATGAATGAGGAGCAC
	RT3195 (rv+T7)	TAATACGACTCACTATAGGGGACTCATACCTTCCCTCTGA
PUCHI	RT3190 (fw)	CTCCACAGTTTGTCATCGATC
	RT3191 (rv+T7)	TAATACGACTCACTATAGGGGACTGAGTAGAAGCCTGTAG
STM	Atp3735 (fw)	GTTGCTTCTTCTTCTTCTCC
	Atp3736 (rv+T7)	TAATACGACTCACTATAGGGACGAGCATTTCACAGTAAGC
SVP	Atp277 (fw)	GCAACTAACGGAAGAGAACGAG
	Atp500 (rv+T7)	TAATACGACTCACTATAGGGCCAGAAATGCAGTGAAGAGAGATC
LFY	RT3461 (fw)	GGAGCGAGTTACATAAACAAGC
	RT3462 (rv+T7)	TAATACGACTCACTATAGGGGCATCCACCACGTCCAGA
Primers used to amplify the CDSs		
LSH1	Atp6397 (fw)	GGGGACAAGTTTGTACAAAAAAGCAGGCTTCATGGATTTGATCTCTCACCAACCA
	Atp6398 (rv)	GGGGACCACTTTGTACAAGAAAGCTGGGTTCATACTGTTGCACCCGAGTAATTAGC
LSH3	Atp7426 (fw)	GGGGACAAGTTTGTACAAAAAAGCAGGCCCAATGGATATGATTCCCCAATTGATG
	Atp6400 (rv)	GGGGACCACTTTGTACAAGAAAGCTGGGTCTTACTTCTCAAACTTTAATTGAGTAG
LSH4	Atp6401 (fw)	GGGGACAAGTTTGTACAAAAAAGCAGGCTCTATGGATCATATCATCGGCTTTATGG
	Atp6402 (rv)	GGGGACCACTTTGTACAAGAAAGCTGGGTGTTAATTAGGGCTACTTGAAATCGC
BOP1	Atp7372 (fw)	GGGGACAAGTTTGTACAAAAAAGCAGGCTccATGAGCAATACTTTCGAAG
	Atp7373 (rv)	GGGGACCACTTTGTACAAGAAAGCTGGGTCTAGAAATGGTGGTGGTGG
BOP2	Atp7374 (fw)	GGGGACAAGTTTGTACAAAAAAGCAGGCTccATGAGCAATCTTGAAGAATC
	Atp7375 (rv)	GGGGACCACTTTGTACAAGAAAGCTGGGTCTAGAAGTGATGTTGATGATG
PUCHI	Atp7398 (fw)	GGGGACAAGTTTGTACAAAAAAGCAGGCTccATGTCAACCTCCAAAACCC
	Atp7399 (rv)	GGGGACCACTTTGTACAAGAAAGCTGGGTCTAAAAGACTGAGTAGAAGC
LFY	Atp7390 (fw)	GGGGACAAGTTTGTACAAAAAAGCAGGCTccATGGATCCTGAAGGTTTCAC
	Atp7391 (rv)	GGGGACCACTTTGTACAAGAAAGCTGGGTCTAGAAACGCAAGTCGTCGC
JAG	Atp7376 (fw)	GGGGACAAGTTTGTACAAAAAAGCAGGCTccATGAGGCATGAGGAGAATTAC
	Atp7377 (rv)	GGGGACCACTTTGTACAAGAAAGCTGGGTTCAGAGCGAGTGATGATCTTG
JGL	Atp7378 (fw)	GGGGACAAGTTTGTACAAAAAAGCAGGCTccATGAGAGCTGATGAAAATAAC
	Atp7379 (rv)	GGGGACCACTTTGTACAAGAAAGCTGGGTTTATAGCCCATGATGTGGAG

BIBLIOGRAPHY

Abe, M. (2009). *FD , a bZIP Protein Mediating Signals from the Floral Pathway Integrator FT at the Shoot Apex FD , a bZIP Protein Mediating Signals from the Floral Pathway Integrator FT at the Shoot Apex*. *1052*(2005), 1052–1057. https://doi.org/10.1126/science.1115983

Aida, M., Ishida, T., Fukaki, H., Fujisawa, H., & Tasaka, M. (1997). <1997_The Plant Cell …_Genes lnvolved in Organ Separation in Arabidopsis An Analysis of the cup-shaped cotyledon Mutant_Aida, Ishida, Fukaki.pdf>. *The Plant Cell*, *9*(June), 841–857.

Aida, M., Ishida, T., & Tasaka, M. (1999). Shoot apical meristem and cotyledon formation during Arabidopsis embryogenesis: Interaction among the CUP-SHAPED COTYLEDON and SHOOT MERISTEMLESS genes. *Development*, *126*(8), 1563–1570. https://doi.org/10.1242/dev.126.8.1563

Alvarez-Buylla, E. R., Benítez, M., Corvera-Poiré, A., Chaos Cador, Á., de Folter, S., Gamboa de Buen, A., Garay-Arroyo, A., García-Ponce, B., Jaimes-Miranda, F., Pérez-Ruiz, R. V., Piñeyro-Nelson, A., & Sánchez-Corrales, Y. E. (2010). Flower Development. *The Arabidopsis Book*, *8*(1), e0127. https://doi.org/10.1199/tab.0127

Bellande, K., Trinh, D. C., Gonzalez, A. A., Dubois, E., Petitot, A. S., Lucas, M., Champion, A., Gantet, P., Laplaze, L., & Guyomarc'H, S. (2022). PUCHI represses early meristem formation in developing lateral roots of Arabidopsis thaliana. *Journal of Experimental Botany*, *73*(11), 3496–3510. https://doi.org/10.1093/jxb/erac079

Bencivenga, S., Serrano-Mislata, A., Bush, M., Fox, S., & Sablowski, R. (2016). Control of Oriented Tissue Growth through Repression of Organ Boundary Genes Promotes Stem Morphogenesis. *Developmental Cell*, *39*(2), 198–208. https://doi.org/10.1016/j.devcel.2016.08.013

Bommert, P., Satoh-Nagasawa, N., Jackson, D., & Hirano, H. Y. (2005). Genetics and evolution of inflorescence and flower development in grasses. *Plant and Cell Physiology*, *46*(1), 69–78. https://doi.org/10.1093/pcp/pci504

Boss, P. K. (2004). Multiple Pathways in the Decision to Flower: Enabling, Promoting, and Resetting. *The Plant Cell Online*, *16*(suppl_1), S18–S31. https://doi.org/10.1105/tpc.015958

Caselli, F., Beretta, V. M., Mantegazza, O., Petrella, R., Leo, G., Guazzotti, A., Herrera-Ubaldo, H., de Folter, S., Mendes, M. A., Kater, M. M., & Gregis, V. (2019). REM34 and REM35 Control Female and Male Gametophyte Development in Arabidopsis thaliana. *Frontiers in Plant Science*, *10*(October), 1–17. https://doi.org/10.3389/fpls.2019.01351

Caselli, F., Zanarello, F., Kater, M. M., Battaglia, R., & Gregis, V. (2020). Crop reproductive meristems in the genomic era: A brief overview. *Biochemical Society Transactions*, *48*(3), 853–865. https://doi.org/10.1042/BST20190441

Chahtane, H., Zhang, B., Norberg, M., LeMasson, M., Thévenon, E., Bakó, L., Benlloch, R., Holmlund, M., Parcy, F., Nilsson, O., & Vachon, G. (2018). LEAFY activity is post-transcriptionally regulated by BLADE ON PETIOLE2 and CULLIN3 in Arabidopsis. *New Phytologist*, *220*(2), 579–592. https://doi.org/10.1111/nph.15329

Chandler, J. W. (2012). Floral meristem initiation and emergence in plants. *Cellular and Molecular Life Sciences*, *69*(22), 3807–3818. https://doi.org/10.1007/s00018-012-0999-0

Cheng, C. Y., Krishnakumar, V., Chan, A. P., Thibaud-Nissen, F., Schobel, S., & Town, C. D. (2017). Araport11: a complete reannotation of the Arabidopsis thaliana reference genome. *Plant Journal*, *89*(4), 789–804. https://doi.org/10.1111/tpj.13415

Cho, E., & Zambryski, P. C. (2011a). ORGAN BOUNDARY1 defines a gene expressed at the junction between the shoot apical meristem and lateral organs. *Proceedings of the National Academy of Sciences of the United States of America*, *108*(5), 2154–2159. https://doi.org/10.1073/pnas.1018542108

Cho, E., & Zambryski, P. C. (2011b). ORGAN BOUNDARY1 defines a gene expressed at the junction between the shoot apical meristem and lateral organs. *Proceedings of the National Academy of Sciences of the United States of America*, *108*(5), 2154–2159. https://doi.org/10.1073/pnas.1018542108

Chung, Y., Zhu, Y., Wu, M. F., Simonini, S., Kuhn, A., Armenta-Medina, A., Jin, R., Østergaard, L., Gillmor, C. S., & Wagner, D. (2019). Auxin Response Factors promote organogenesis by chromatin-mediated repression of the pluripotency gene SHOOTMERISTEMLESS. *Nature Communications*, *10*(1). https://doi.org/10.1038/s41467-019-08861-3

Cui, Y., Hu, X., Liang, G., Feng, A., Wang, F., Ruan, S., Dong, G., Shen, L., Zhang, B., Chen, D., Zhu, L., Hu, J., Lin, Y., Guo, L., Matsuoka, M., & Qian, Q. (2020). Production of novel beneficial alleles of a rice yield-related QTL by CRISPR/Cas9. *Plant Biotechnology Journal*, *18*(10), 1987–1989. https://doi.org/10.1111/pbi.13370

Dennis, L., & Peacock, J. (2019). Genes directing flower development in arabidopsis. *Plant Cell*, *31*(6), 1192–1193. https://doi.org/10.1105/tpc.19.00276

Dinneny, J. R., Yadegari, R., Fischer, R. L., Yanofsky, M. F., & Weigel, D. (2004). The role of JAGGED in shaping lateral organs. *Development*, *131*(5), 1101–1110. https://doi.org/10.1242/dev.00949

Ejaz, M., Bencivenga, S., Tavares, R., Bush, M., & Sablowski, R. (2021). Arabidopsis Thaliana Homeobox Gene 1 controls plant architecture by locally restricting environmental responses. *Proceedings of the National Academy of Sciences of the United States of America*, *118*(17), 1–8. https://doi.org/10.1073/pnas.2018615118

Ewels, P., Magnusson, M., Lundin, S., & Käller, M. (2016). MultiQC: Summarize analysis results for multiple tools and samples in a single report. *Bioinformatics*, *32*(19), 3047–3048. https://doi.org/10.1093/bioinformatics/btw354

Gao, X., Liang, W., Yin, C., Ji, S., Wang, H., Su, X., Guo, C., Kong, H., Xue, H., & Zhang, D. (2010). The SEPALLATA-like gene OsMADS34 is required for rice inflorescence and spikelet development. *Plant Physiology*, *153*(2), 728–740. https://doi.org/10.1104/pp.110.156711

Ge, S. X., Jung, D., Jung, D., & Yao, R. (2020). ShinyGO: A graphical gene-set enrichment tool for animals and plants. *Bioinformatics*, *36*(8), 2628–2629. https://doi.org/10.1093/bioinformatics/btz931

Grandi, V., Gregis, V., & Kater, M. M. (2012). Uncovering genetic and molecular interactions among floral meristem identity genes in Arabidopsis thaliana. *Plant Journal*, *69*(5), 881–893. https://doi.org/10.1111/j.1365-313X.2011.04840.x

Gregis, V., Sessa, A., Colombo, L., & Kater, M. M. (2006). AGL24, SHORT VEGETATIVE PHASE, and APETALA1 redundantly control AGAMOUS during early stages of flower development in Arabidopsis. *Plant Cell*, *18*(6), 1373–1382. https://doi.org/10.1105/tpc.106.041798

Gregis, V., Sessa, A., Colombo, L., & Kater, M. M. (2008). AGAMOUS-LIKE24 and SHORT VEGETATIVE PHASE determine floral meristem identity in Arabidopsis. *Plant Journal*, *56*(6), 891–902. https://doi.org/10.1111/j.1365-313X.2008.03648.x

Gregis, V., Sessa, A., Dorca-Fornell, C., & Kater, M. M. (2009). The Arabidopsis floral meristem identity genes AP1, AGL24 and SVP directly repress class B and C floral homeotic genes. *Plant Journal*, *60*(4), 626–637. https://doi.org/10.1111/j.1365-313X.2009.03985.x

Hake, S. (2008). Inflorescence Architecture: The Transition from Branches to Flowers - ScienceDirect. *Current Biology*, *18*(23), R1106–R1108. https://www.sciencedirect.com/science/article/pii/S0960982208013559

Han, Y., Yang, H., & Jiao, Y. (2014). Regulation of inflorescence architecture by cytokinins. *Frontiers in Plant Science*, *5*(NOV), 1–4. https://doi.org/10.3389/fpls.2014.00669

Harrop, T. W. R., Ud Din, I., Gregis, V., Osnato, M., Jouannic, S., Adam, H., & Kater, M. M. (2016). Gene expression profiling of reproductive meristem types in early rice inflorescences by laser microdissection. *Plant Journal*, *86*(1), 75–88. https://doi.org/10.1111/tpj.13147

Hartmann, U., Höhmann, S., Nettesheim, K., Wisman, E., Saedler, H., & Huijser, P. (2000). Molecular cloning of SVP: A negative regulator of the floral transition in Arabidopsis. *Plant Journal*, *21*(4), 351–360. https://doi.org/10.1046/j.1365-313X.2000.00682.x

Hepworth, S. R., Zhang, Y., McKim, S., Li, X., & Haughn, G. W. (2005). Blade-on-Petiole-dependent signaling controls leaf and floral patterning in Arabidopsis. *Plant Cell*, *17*(5), 1434–1448. https://doi.org/10.1105/tpc.104.030536

Hibara, K. I., Karim, M. R., Takada, S., Taoka, K. I., Furutani, M., Aida, M., & Tasaka, M. (2006). Arabidopsis CUP-SHAPED COTYLEDON3 regulates postembryonic shoot meristem and organ boundary formation. *Plant Cell*, *18*(11), 2946–2957. https://doi.org/10.1105/tpc.106.045716

Hirota, A., Kato, T., Fukaki, H., Aida, M., & Tasaka, M. (2007). The auxin-regulated AP2/EREBP gene PUCHI is required for morphogenesis in the early lateral root primordium of Arabidopsis. *Plant Cell*, *19*(7), 2156–2168. https://doi.org/10.1105/tpc.107.050674

Huang, H., Ji, H., Ju, S., Lin, W., Li, J., Lv, X., Lin, L., Guo, L., Qiu, D., Yan, J., & Ma, X. (2022). Pantranscriptome combined with phenotypic quantification reveals germplasm kinship and regulation network of bract color variation in Bougainvillea. *Frontiers in Plant Science*, *13*(November), 1–18. https://doi.org/10.3389/fpls.2022.1018846

Huang, X., Chen, S., Li, W., Tang, L., Zhang, Y., Yang, N., Zou, Y., Zhai, X., Xiao, N., Liu, W., Li, P., & Xu, C. (2021). ROS regulated reversible protein phase separation synchronizes plant flowering. *Nature Chemical Biology*, *17*(5), 549–557. https://doi.org/10.1038/s41589-021-00739-0

Huber, W., Carey, V. J., Gentleman, R., Anders, S., Carlson, M., Carvalho, B. S., Bravo, H. C., Davis, S., Gatto, L., Girke, T., Gottardo, R., Hahne, F., Hansen, K. D., Irizarry, R. A., Lawrence, M., Love, M. I., MaCdonald, J., Obenchain, V., Oleš, A. K., … Morgan, M. (2015). Orchestrating high-throughput genomic analysis with Bioconductor. *Nature Methods*, *12*(2), 115–121. https://doi.org/10.1038/nmeth.3252

Ikeda-Kawakatsu, K., Maekawa, M., Izawa, T., Itoh, J. I., & Nagato, Y. (2012). ABERRANT PANICLE ORGANIZATION 2/RFL, the rice ortholog of Arabidopsis LEAFY, suppresses the transition from

inflorescence meristem to floral meristem through interaction with APO1. *Plant Journal*, *69*(1), 168–180. https://doi.org/10.1111/j.1365-313X.2011.04781.x

Ikeda-Kawakatsu, K., Yasuno, N., Oikawa, T., Iida, S., Nagato, Y., Maekawa, M., & Kyozuka, J. (2009). Expression level of ABERRANT PANICLE ORGANIZATION1 determines rice inflorescence form through control of cell proliferation in the meristem. *Plant Physiology*, *150*(2), 736–747. https://doi.org/10.1104/pp.109.136739

Irish, V. (2017). The ABC model of floral development. *Current Biology*, *27*(17), R887–R890. https://doi.org/10.1016/j.cub.2017.03.045

Irish, V. F., & Sussex, I. M. (1990). Function of the apetala-1 Gene during Arabidopsis Floral Development. *The Plant Cell*, *2*(8), 741. https://doi.org/10.2307/3869173

Iyer, L. M., & Aravind, L. (2012). ALOG domains: Provenance of plant homeotic and developmental regulators from the DNA-binding domain of a novel class of DIRS1-type retroposons. *Biology Direct*, *7*, 1–8. https://doi.org/10.1186/1745-6150-7-39

Izhaki, A., Alvarez, J. P., Cinnamon, Y., Genin, O., Liberman-Aloni, R., & Eyal, Y. (2018). The tomato BLADE ON PETIOLE and TERMINATING FLOWER regulate leaf axil patterning along the proximal-distal axes. *Frontiers in Plant Science*, *9*(August), 1–10. https://doi.org/10.3389/fpls.2018.01126

Kanrar, S., Onguka, O., & Smith, H. M. S. (2006). Arabidopsis inflorescence architecture requires the activities of KNOX-BELL homeodomain heterodimers. *Planta*, *224*(5), 1163–1173. https://doi.org/10.1007/s00425-006-0298-9

Karim, M. R., Hirota, A., Kwiatkowska, D., Tasaka, M., & Aida, M. (2009). A role for arabidopsis PUCHI in floral meristem identity and bract suppression. *Plant Cell*, *21*(5), 1360–1372. https://doi.org/10.1105/tpc.109.067025

Kaufmann, K., Wellmer, F., Muiñ, J. M., Ferner, T., Wuest, S. E., Kumar, V., Serrano-Mislata, A., Madueño, F., Kraiewski, P., Meyerowitz, E. M., Angenent, G. C., & Riechmann, J. L. (2010). Orchestration of floral initiation by APETALA1. *Science*, *328*(5974), 85–89. https://doi.org/10.1126/scince.1185244

Khan, M., Ragni, L., Tabb, P., Salasini, B. C., Chatfield, S., Datla, R., Lock, J., Kuai, X., Després, C., Proveniers, M., Yongguo, C., Xiang, D., Morin, H., Rullière, J. P., Citerne, S., Hepworth, S. R., & Pautot, V. (2015). Repression of lateral organ boundary genes by pennywise and pound-foolish is essential for meristem maintenance and flowering in Arabidopsis. *Plant Physiology*, *169*(3), 2166–2186. https://doi.org/10.1104/pp.15.00915

Kobayashi, K., Yasuno, N., Sato, Y., Yoda, M., Yamazaki, R., Kimizu, M., Yoshida, H., Nagamura, Y., & Kyozukaa, J. (2012). Inflorescence meristem identity in rice is specified by overlapping functions of three AP1/FUL-Like MADS box genes and PAP2, a SEPALLATA MADS Box gene. *Plant Cell*, *24*(5), 1848–1859. https://doi.org/10.1105/tpc.112.097105

Komatsu, K., Maekawa, M., Ujiie, S., Satake, Y., Furutani, I., Okamoto, H., Shimamoto, K., & Kyozuka, J. (2003). LAX and SPA: Major regulators of shoot branching in rice. *Proceedings of the National Academy of Sciences of the United States of America*, *100*(20), 11765–11770. https://doi.org/10.1073/pnas.1932414100

Komatsu, M., Chujo, A., Nagato, Y., Shimamoto, K., & Kyozuka, J. (2003). Frizzy panicle is required to prevent the formation of axillary meristems and to establish floral meristem identity in rice spikelets. *Development*, *130*(16), 3841–3850. https://doi.org/10.1242/dev.00564

Komatsu, M., Maekawa, M., Shimamoto, K., & Kyozuka, J. (2001). The LAX1 and FRIZZY PANICLE 2 genes determine the inflorescence architecture of rice by controlling rachis-branch and spikelet development. *Developmental Biology*, *231*(2), 364–373. https://doi.org/10.1006/dbio.2000.9988

Lal, S., Pacis, L. B., & Smith, H. M. S. (2011). Regulation of the SQUAMOSA PROMOTER-BINDING PROTEIN-LIKE genes/microRNA156 Module by the homeodomain proteins PENNYWISE and POUND-FOOLISH in arabidopsis. *Molecular Plant*, *4*(6), 1123–1132. https://doi.org/10.1093/mp/ssr041

Landrein, B., Kiss, A., Sassi, M., Chauvet, A., Das, P., Cortizo, M., Laufs, P., Takeda, S., Aida, M., Traas, J., Vernoux, T., Boudaoud, A., & Hamant, O. (2015). Mechanical stress contributes to the expression of the STM homeobox gene in Arabidopsis shoot meristems. *ELife*, *4*, 1–27. https://doi.org/10.7554/elife.07811

Langmead, B., & Salzberg, S. L. (2012). Fast gapped-read alignment with Bowtie 2. *Nature Methods*, *9*(4), 357–359. https://doi.org/10.1038/nmeth.1923

Lee, M., Dong, X., Song, H., Yang, J. Y., Kim, S., & Hur, Y. (2020). Molecular characterization of Arabidopsis thaliana LSH1 and LSH2 genes. *Genes and Genomics*, *42*(10), 1151–1162. https://doi.org/10.1007/s13258-020-00985-x

Lei, Y., Su, S., He, L., Hu, X., & Luo, D. (2019). A member of the ALOG gene family has a novel role in regulating nodulation in Lotus japonicus. *Journal of Integrative Plant Biology*, *61*(4), 463–477. https://doi.org/10.1111/jipb.12711

Li, N., Wang, Y., Lu, J., & Liu, C. (2019). Genome-wide identification and characterization of the ALOG domain genes in rice. *International Journal of Genomics*, *2019*. https://doi.org/10.1155/2019/2146391

Li, X., Fu, Z., Wang, Y., Xiong, G., Wang, X., Liu, X., Li, J., Qian, Q., Zeng, D., Teng, S., Hiroshi, F., Yuan, M., Luo, D., & Han, B. (2003). Control of tillering in rice. *Nature*, *422*(6932), 618–621.

Liang, W. hong, Shang, F., Lin, Q. ting, Lou, C., & Zhang, J. (2014). Tillering and panicle branching genes in rice. *Gene*, *537*(1), 1–5. https://doi.org/10.1016/j.gene.2013.11.058

Liu, C., Teo, Z. W. N., Bi, Y., Song, S., Xi, W., Yang, X., Yin, Z., & Yu, H. (2013). A Conserved Genetic Pathway Determines Inflorescence Architecture in Arabidopsis and Rice. *Developmental Cell*, *24*(6), 612–622. https://doi.org/10.1016/j.devcel.2013.02.013

Liu, J., Zhang, C., Han, J., Fang, X., Xu, H., Liang, C., Li, D., Yang, Y., Cui, Z., Wang, R., & Song, J. (2022). Genome-Wide Analysis of KNOX Transcription Factors and Expression Pattern of Dwarf-Related KNOX Genes in Pear. *Frontiers in Plant Science*, *13*(January). https://doi.org/10.3389/fpls.2022.806765

Long, J., & Barton, M. K. (2000). Initiation of axillary and floral meristems in Arabidopsis. *Developmental Biology*, *218*(2), 341–353. https://doi.org/10.1006/dbio.1999.9572

Love, M. I., Huber, W., & Anders, S. (2014). Moderated estimation of fold change and dispersion for RNA-seq data with DESeq2. *Genome Biology*, *15*(12), 1–21. https://doi.org/10.1186/s13059-014-0550-8

MacAlister, C. A., Park, S. J., Jiang, K., Marcel, F., Bendahmane, A., Izkovich, Y., Eshed, Y., & Lippman, Z. B. (2012). Synchronization of the flowering transition by the tomato terminating flower gene. *Nature Genetics*, *44*(12), 1393–1398. https://doi.org/10.1038/ng.2465

Mantegazza, O., Gregis, V., Chiara, M., Selva, C., Leo, G., Horner, D. S., & Kater, M. M. (2014). Gene coexpression patterns during early development of the native Arabidopsis reproductive meristem: Novel candidate developmental regulators and patterns of functional redundancy. *Plant Journal*, *79*(5), 861–877. https://doi.org/10.1111/tpj.12585

Mantegazza, O., Gregis, V., Mendes, M. A., Morandini, P., Alves-Ferreira, M., Patreze, C. M., Nardeli, S. M., Kater, M. M., & Colombo, L. (2014). Analysis of the arabidopsis REM gene family predicts functions during flower development. *Annals of Botany*, *114*(7), 1507–1515. https://doi.org/10.1093/aob/mcu124

McKim, S. M., Stenvik, G. E., Butenko, M. A., Kristiansen, W., Cho, S. K., Hepworth, S. R., Aalen, R. B., & Haughn, G. W. (2008). The BLADE-ON-PETIOLE genes are essential for abscission zone formation in Arabidopsis. *Development*, *135*(8), 1537–1546. https://doi.org/10.1242/dev.012807

McSteen, P. (2009). Hormonal regulation of branching in grasses. *Plant Physiology*, *149*(1), 46–55. https://doi.org/10.1104/pp.108.129056

Musialak-Lange, M., Fiddeke, K., Franke, A., Kragler, F., Abel, C., & Wahl, V. (2021). Sugar Signaling Induces Dynamic Changes during Meristem Development in Arabidopsis. *BioRxiv*, 439483. https://doi.org/10.1101/2021.04.12.439483

Nakagawa, M., Shimamoto, K., & Kyozuka, J. (2002). Overexpression of RCN1 and RCN2, rice Terminal Flower 1/Centroradialis homologs, confers delay of phase transition and altered panicle morphology in rice. *Plant Journal*, *29*(6), 743–750. https://doi.org/10.1046/j.1365-313X.2002.01255.x

Norberg, M., Holmlund, M., & Nilsson, O. (2005). The BLADE ON PETIOLE genes act redundantly to control the growth and development of lateral organs. *Development*, *132*(9), 2203–2213. https://doi.org/10.1242/dev.01815

Ohno, C. K., Reddy, G. V., Heisler, M. G. B., & Meyerowitz, E. M. (2004). The Arabidopsis JAGGED gene encodes a zinc finger protein that promotes leaf tissue development. *Development*, *131*(5), 1111–1122. https://doi.org/10.1242/dev.00991

O'Malley, R. C., Huang, S. shan C., Song, L., Lewsey, M. G., Bartlett, A., Nery, J. R., Galli, M., Gallavotti, A., & Ecker, J. R. (2016). Erratum: Cistrome and Epicistrome Features Shape the Regulatory DNA Landscape (Cell (2016) 165(5) (1280–1292)). *Cell*, *166*(6), 1598. https://doi.org/10.1016/j.cell.2016.08.063

Parrish, N., Hormozdiari, F., & Eskin, E. (2014). Assembly of non-unique insertion content using next-generation sequencing. *Bioinformatics: The Impact of Accurate Quantification on Proteomic and Genetic Analysis and Research*, 21–40. https://doi.org/10.1201/b16589

Peng, P., Liu, L., Fang, J., Zhao, J., Yuan, S., & Li, X. (2017). The rice TRIANGULAR HULL1 protein acts as a transcriptional repressor in regulating lateral development of spikelet. *Scientific Reports*, *7*(1), 1–15. https://doi.org/10.1038/s41598-017-14146-w

Porri, A., Torti, S., Mateos, J., Romera-Branchat, M., García-Martínez, J. L., Fornara, F., Gregis, V., Kater, M. M., & Coupland, G. (2014). SHORT VEGETATIVE PHASE reduces gibberellin biosynthesis at the

Arabidopsis shoot apex to regulate the floral transition Fernando Andrés1. *Proceedings of the National Academy of Sciences of the United States of America*, *111*(26). https://doi.org/10.1073/pnas.1409567111

Pouteau, S., Albertini, C., Ezhova, T. A., Penin, A. A., Budaev, R. A., Ezhova, T. A., Sawa, S., Ito, T., Shimura, Y., Okada, K., Kronenberg, H. M., Drive, L., Chandler, J. W., Suh, S. S., Choi, K. R., Lee, I., Penin, A. A., Cho, E., Zambryski, P. C., … Aida, M. (2004). The BLADE ON PETIOLE genes act redundantly to control the growth and development of lateral organs. *Plant Cell*, *131*(5), 3807–3818. https://doi.org/10.1134/S1022795407030106

Prusinkiewicz, P., Erasmus, Y., Lane, B., Harder, L. D., & Coen, E. (2007). Evolution and development of inflorescence architectures. *Science*, *316*(5830), 1452–1456. https://doi.org/10.1126/science.1140429

Roth, O., Alvarez, J. P., Levy, M., Bowman, J. L., Ori, N., & Shani, E. (2018). The KNOXI transcription factor SHOOT meristemless regulates floral fate in arabidopsis[OPEN]. *Plant Cell*, *30*(6), 1309–1321. https://doi.org/10.1105/tpc.18.00222

Sato, D. S., Ohmori, Y., Nagashima, H., Toriba, T., & Hirano, H. Y. (2014). A role for TRIANGULAR HULL1 in fine-tuning spikelet morphogenesis in rice. *Genes and Genetic Systems*, *89*(2), 61–69. https://doi.org/10.1266/ggs.89.61

Schultz, E. A., & Haughn, G. W. (1991). LEAFY, a homeotic gene that regulates inflorescence development in arabidopsis. *Plant Cell*, *3*(8), 771–781. https://doi.org/10.1105/tpc.3.8.771

Smyth, D. R., Bowman, J. L., & Meyerowitz, E. M. (1990). Flowerdev-Smythplcell1990. *The Plant Cell*, *2*(August), 755–767. papers3://publication/uuid/0BFEAF50-2E5A-458F-B90B-DFF364DFB25D

Soneson, C., Love, M. I., & Robinson, M. D. (2015). Differential analyses for RNA-seq: transcript-level estimates improve gene-level inferences. *F1000Research*, *4*(2), 1521. https://doi.org/10.12688/f1000research.7563.1

Song, B., Zhang, Z. Q., Stöcklin, J., Yang, Y., Niu, Y., Chen, J. G., & Sun, H. (2013). Multifunctional bracts enhance plant fitness during flowering and seed development in Rheum nobile (Polygonaceae), a giant herb endemic to the high Himalayas. *Oecologia*, *172*(2), 359–370. https://doi.org/10.1007/s00442-012-2518-2

Spinelli, S. V., Martin, A. P., Viola, I. L., Gonzalez, D. H., & Palatnik, J. F. (2011). A mechanistic link between STM and CUC1 during Arabidopsis development. *Plant Physiology*, *156*(4), 1894–1904. https://doi.org/10.1104/pp.111.177709

Takada, S., Hibara, K., Ishida, T., & Tasaka, M. (2001). *Takada 2001 - CUC1 STM SAM - The CUP-SHAPED COTYLEDON1 gene of Arabidopsis regulates shoot apical meristem formation*. *1135*, 1127–1135.

Takeda, S., Hanano, K., Kariya, A., Shimizu, S., Zhao, L., Matsui, M., Tasaka, M., & Aida, M. (2011). CUP-SHAPED COTYLEDON1 transcription factor activates the expression of LSH4 and LSH3, two members of the ALOG gene family, in shoot organ boundary cells. *Plant Journal*, *66*(6), 1066–1077. https://doi.org/10.1111/j.1365-313X.2011.04571.x

Takeda, T., Suwa, Y., Suzuki, M., Kitano, H., Ueguchi-Tanaka, M., Ashikari, M., Matsuoka, M., & Ueguchi, C. (2003). The OsTB1 gene negatively regulates lateral branching in rice. *Plant Journal*, *33*(3), 513–520. https://doi.org/10.1046/j.1365-313X.2003.01648.x

Tanaka, W., Pautler, M., Jackson, D., & Hirano, H.-Y. (n.d.). *Grass Meristems II: Inflorescence Architecture, Flower Development and Meristem Fate*. https://doi.org/10.1093/pcp/pct016

Torti, S., Fornara, F., Vincent, C., Andrés, F., Nordström, K., Göbel, U., Knoll, D., Schoof, H., & Coupland, G. (2012). Analysis of the Arabidopsis shoot meristem transcriptome during floral transition identifies distinct regulatory patterns and a leucine-rich repeat protein that promotes flowering. *Plant Cell*, *24*(2), 444–462. https://doi.org/10.1105/tpc.111.092791

Tsuda, K., Ito, Y., Sato, Y., & Kurata, N. (2011). Positive autoregulation of a KNOX gene is essential for shoot apical meristem maintenance in rice. *Plant Cell*, *23*(12), 4368–4381. https://doi.org/10.1105/tpc.111.090050

Wang, J., Zhang, Q., Wang, Y., Huang, J., Luo, N., Wei, S., & Jin, J. (2019). Analysing the rice young panicle transcriptome reveals the gene regulatory network controlled by TRIANGULAR HULL1. *Rice*, *12*(1), 1–10. https://doi.org/10.1186/s12284-019-0265-2

Weigel, D., Alvarez, J., Smyth, D. R., Yanofsky, M. F., & Meyerowitz, E. M. (1992a). LEAFY controls floral meristem identity in Arabidopsis. *Cell*, *69*(5), 843–859. https://doi.org/10.1016/0092-8674(92)90295-N

Weigel, D., Alvarez, J., Smyth, D. R., Yanofsky, M. F., & Meyerowitz, E. M. (1992b). LEAFY controls floral meristem identity in Arabidopsis. *Cell*, *69*(5), 843–859. https://doi.org/10.1016/0092-8674(92)90295-N

Wils, C. R., & Kaufmann, K. (2017). Gene-regulatory networks controlling inflorescence and flower development in Arabidopsis thaliana. *Biochimica et Biophysica Acta - Gene Regulatory Mechanisms*, *1860*(1), 95–105. https://doi.org/10.1016/j.bbagrm.2016.07.014

Worthen, J. M., Yamburenko, M. V., Lim, J., Nimchuk, Z. L., Kieber, J. J., & Schaller, G. E. (2019). Type-B response regulators of rice play key roles in growth, development and cytokinin signaling. *Development (Cambridge)*, *146*(13), 1–11. https://doi.org/10.1242/dev.174870

Xu, C., Park, S. J., Van Eck, J., & Lippman, Z. B. (2016). Control of inflorescence architecture in tomato by BTB/POZ transcriptional regulators. *Genes and Development*, *30*(18), 2048–2061. https://doi.org/10.1101/gad.288415.116

Xu, M., Hu, T., McKim, S. M., Murmu, J., Haughn, G. W., & Hepworth, S. R. (2010). Arabidopsis BLADE-ON-PETIOLE1 and 2 promote floral meristem fate and determinacy in a previously undefined pathway targeting APETALA1 and AGAMOUS-LIKE24. *Plant Journal*, *63*(6), 974–989. https://doi.org/10.1111/j.1365-313X.2010.04299.x

Yamaguchi, N. (2021). *LEAFY , a Pioneer Transcription Factor in Plants : A Mini-Review*. *12*(July), 1–9. https://doi.org/10.3389/fpls.2021.701406

Yoshida, A., Ohmori, Y., Kitano, H., Taguchi-Shiobara, F., & Hirano, H. Y. (2012). ABERRANT SPIKELET and PANICLE1, encoding a TOPLESS-related transcriptional co-repressor, is involved in the regulation of meristem fate in rice. *Plant Journal*, *70*(2), 327–339. https://doi.org/10.1111/j.1365-313X.2011.04872.x

Yoshida, A., Sasao, M., Yasuno, N., Takagi, K., Daimon, Y., Chen, R., Yamazaki, R., Tokunaga, H., Kitaguchi, Y., Sato, Y., Nagamura, Y., Ushijima, T., Kumamaru, T., Iida, S., Maekawa, M., & Kyozuka, J. (2013). TAWAWA1, a regulator of rice inflorescence architecture, functions through the

suppression of meristem phase transition. *Proceedings of the National Academy of Sciences of the United States of America*, *110*(2), 767–772. https://doi.org/10.1073/pnas.1216151110

Yoshida, A., Suzaki, T., Tanaka, W., & Hirano, H. Y. (2009). The homeotic gene long sterile lemma (G1) specifies sterile lemma identity in the rice spikelet. *Proceedings of the National Academy of Sciences of the United States of America*, *106*(47), 20103–20108. https://doi.org/10.1073/pnas.0907896106

Yuan, H., Xu, Z., Tan, X., Gao, P., Jin, M., Song, W., Wang, S., Kang, Y., Liu, P., Tu, B., Wang, Y., Qin, P., Li, S., Ma, B., & Chen, W. (2021). A natural allele of TAW1 contributes to high grain number and grain yield in rice. *Crop Journal*, *9*(5), 1060–1069. https://doi.org/10.1016/j.cj.2020.11.004

Žádníková, P., & Simon, R. (2014). How boundaries control plant development. *Current Opinion in Plant Biology*, *17*(1), 116–125. https://doi.org/10.1016/j.pbi.2013.11.013

Zhao, L., Nakazawa, M., Takase, T., Manabe, K., Kobayashi, M., Seki, M., Shinozaki, K., & Matsui, M. (2004). Overexpression of LSH1, a member of an uncharacterised gene family, causes enhanced light regulation of seedling development. *Plant Journal*, *37*(5), 694–706. https://doi.org/10.1111/j.1365-313X.2003.01993.x

Zhu, W., Yang, L., Wu, D., Meng, Q., Deng, X., Huang, G., Zhang, J., Chen, X., Ferrándiz, C., Liang, W., Dreni, L., & Zhang, D. (2022). Rice SEPALLATA genes OsMADS5 and OsMADS34 cooperate to limit inflorescence branching by repressing the TERMINAL FLOWER1-like gene RCN4. *New Phytologist*, *233*(4), 1682–1700. https://doi.org/10.1111/nph.17855

APPENDIX

Supplemental images of "The *ALOG* family members *OsG1L1* and *OsG1L2* regulate inflorescence branching in rice"

A

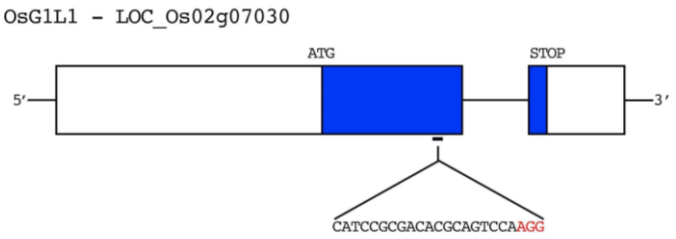

B

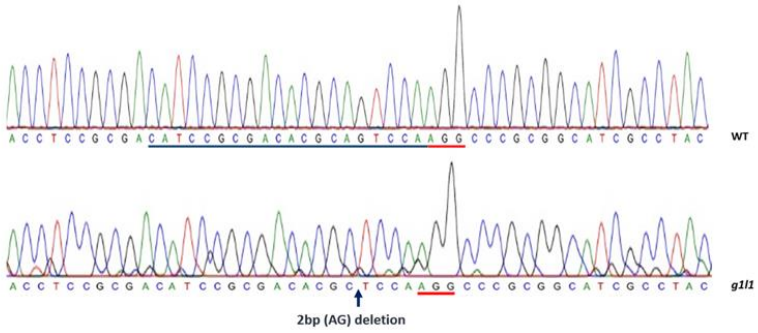

C

```
OsG1L1              MDMIGMASPAESPGGGGTARPSRYESQKRRDWQTFGQYLRNHRPPLELSRCSGAHVLEFL      60
AG deletion         MDMIGMASPAESPGGGGTARPSRYESQKRRDWQTFGQYLRNHRPPLELSRCSGAHVLEFL      60
AGT deletion        MDMIGMASPAESPGGGGTARPSRYESQKRRDWQTFGQYLRNHRPPLELSRCSGAHVLEFL      60
GCATGC deletion     MDMIGMASPAESPGGGGTARPSRYESQKRRDWQTFGQYLRNHRPPLELSRCSGAHVLEFL      60
                    ************************************************************
OsG1L1              RYLDQFGKTKVHAHGCPFFGHPSPPAPCPCPLRQAWGSLDALVGRLRAAFEEHGGRPESN      120
AG deletion         RYLDQFGKTKVHAHGCPFFGHPSPPAPCPCPLRQAWGSLDALVGRLRAAFEEHGGRPESN      120
AGT deletion        RYLDQFGKTKVHAHGCPFFGHPSPPAPCPCPLRQAWGSLDALVGRLRAAFEEHGGRPESN      120
GCATGC deletion     RYLDQFGKTKVHAHGCPFFGHPSPPAPCPCPLRQAWGSLDALVGRLRAAFEEHGGRPESN      120
                    ************************************************************
                                Point of mutation
                                ▼
OsG1L1              PFGARAVRLYLRDIRDTQSKARGIAYEKKRRKRAAASHTKQKQQQQQLVEQAVAPPAAAA      180
AG deletion         PFGARAVRLYLRDIRDTLQGPRHRLREEAPQARRRLP-----------HQAEAAAAAAG      168
AGT deletion        PFGARAVRLYLRDIRDT-PKARGIAYEKKRRKRAAASHTKQKQQQQQLVEQAVAPPAAAA      179
GCATGC deletion     PFGARAVRLYLRDIRDT--KARGIAYEKKRRKRAAASHTKQKQQQQQLVEQAVAPPAAAA      178
                    ****************    *   *:  : *                .** *  ***.
OsG1L1              ----------------AAAALPDMETTTTTTTVPHFLFPAHFLHGHYFLAPAGEQPGG--      222
AG deletion         GTGGGAARRRRRRRGAAGHGDDDDDHGAALLVPGALPPRPLLPGTGRRAARRRRRRGVD      228
AGT deletion        ----------------AAAALPDMETTTTTTTVPHFLFPAHFLHGHYFLAPAGEQPGG--      221
GCATGC deletion     ----------------AAAALPDMETTTTTTTVPHFLFPAHFLHGHYFLAPAGEQPGG--      220
                                    *. .  * :   ::  **  * *  :* *    *   .:  *
OsG1L1              -GDVAAS---TGGAAGAPSG--GGGEDLV-LAMAAAAAAAEAHAAGCMMPLSVFM*      270
AG deletion         GRRCRCSQRRRRGGPGAGHGGGGGGRRGARRRLHDA-------TVGVQL-------      270
AGT deletion        -GDVAAS---TGGAAGAPSG--GGGEDLV-LAMAAAAAAAEAHAAGCMMPLSVFM*      269
GCATGC deletion     -GDVAAS---TGGAAGAPSG--GGGEDLV-LAMAAAAAAAEAHAAGCMMPLSVFM*      268
                       .*     *. **  *  ***.  .   :  *       :.*  :
```

D

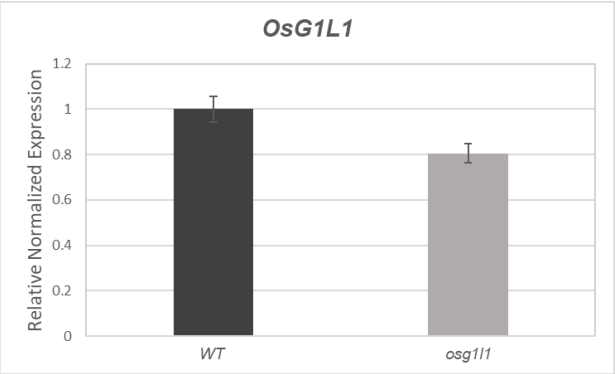

Supplemental Figure S1. A, *OsG1L1* gene structure. The blue rectangle represents the exons, the black line represents the introns and the white rectangles represent respectively the 5' UTR and 3' UTR. The position and the target sequence of the sgRNA, which targets the first exon, 397 bp downstream the ATG site are indicated. The PAM sequence is indicated in red. B, chromatograms showing the *OsG1L1* genomic sequence and *osg1l1* with 2bp AG deletion 4bp upstream of the PAM site. The black arrow indicates the point of the mutation. C, Amino acid sequence alignments of *OsG1L1* and *osg1l1* mutants. On the left are indicated the different alleles observed (deletions of different numbers of nucleotides). The ALOG domain is underlined in yellow, the green rectangle indicates a putative NLS and stop codons (*) are circled in blue. The point where the mutation occurred is marked with an arrow. Only the deletion of 2 bp (AG) causes a disruption of the sequence, the NLS included. The alleles with the deletion of 3 nucleotides (AGT) and 6 nucleotides (GCATGC) only showed the absence of one and two amino acids respectively. D, Expression analysis of *OsG1L1* in wild type (WT) and *osg1l1* mutant that presents an AG deletion. Expression of *OsG1L1* was normalized to that of *Elongation Factor 1* and the expression level of the wild type was set to 1. The expression of *OsG1L1* didn't significatively change in the mutant with respect to the wild type.

A

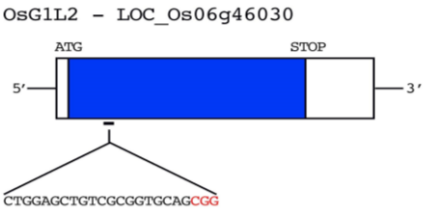

B

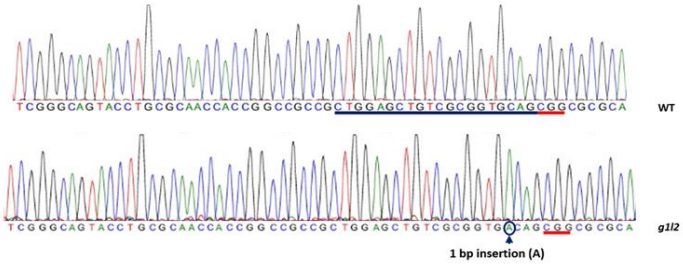

C

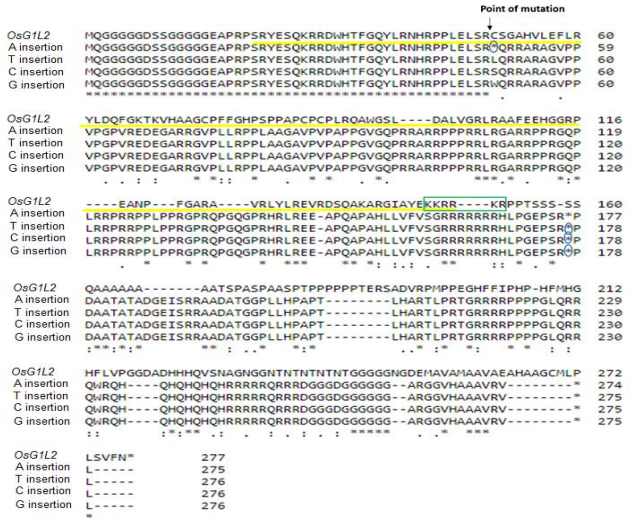

D

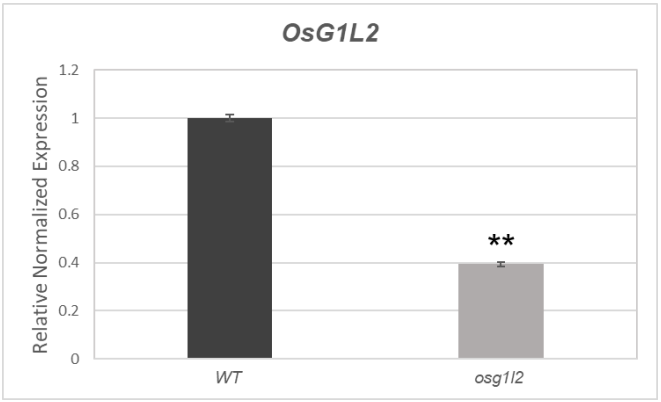

Supplemental Figure S2. A, *OsG1L2* gene structure. The blue rectangle represents the exons, the black line represents the introns, and the white rectangle represents the 5’ and 3’ UTRs respectively. The position and the target sequence of the sgRNA, which targets the first exon, 131 bp downstream the ATG site are indicated. The PAM sequence is indicated in red. B, chromatograms showing WT *OsG1L2* genomic sequence and *osg1l2* mutant with 1bp A insertion, 3bp upstream of PAM site. The black arrow indicates the position of the mutation.

C, Amino acid sequence alignments of *OsG1L2* and the *osg1l2* mutants. On the left are indicated the different base pairs insertions obtained in mutant plants. The ALOG domain is underlined in yellow, the green rectangle indicates the putative NLS and premature stop codons (*) are circled in blue. The A insertion caused a frameshift and the formation of a premature stop codon. In all cases, the ALOG domain and the NLS result to be disrupted. D, Expression analysis of *OsG1L2* in wild type (WT) and *osg1l2* mutant that presents an A insertion. Expression of *OsG1L2* was normalized to that of *Elongation Factor 1* and the expression level of the wild type was set to 1. The expression of *OsG1L2* significatively changed in the mutant with respect to the wild type. The asterisks indicate: *** p< 0,001; **p<0,01; * p<0,05, student's t-test.

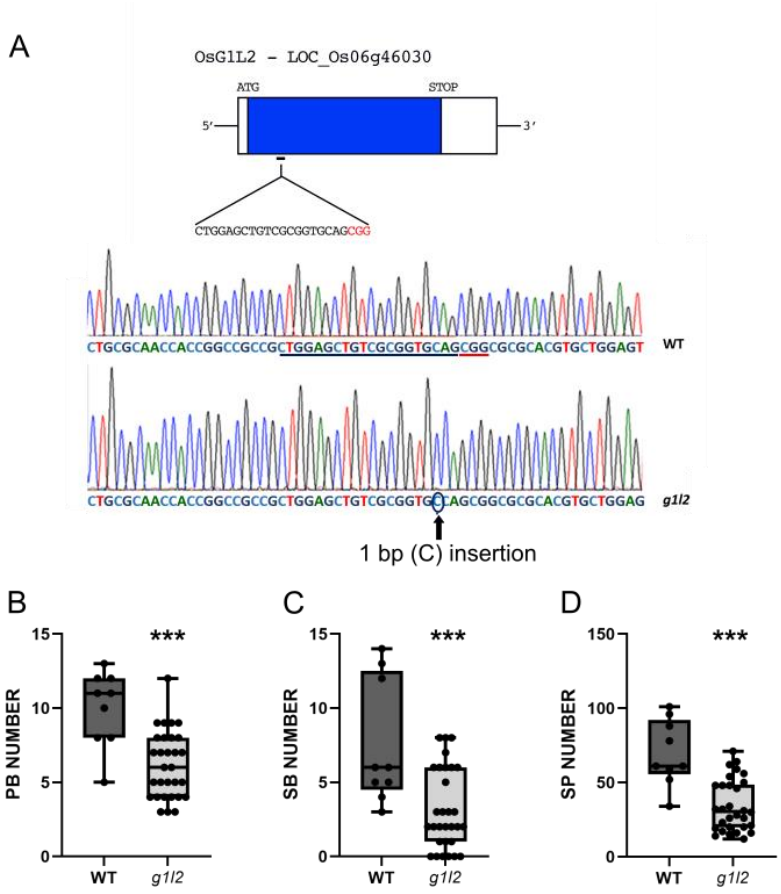

Supplemental Figure S3. A, Gene structure and chromatograms showing *OsG1L2* genomic sequence and *osg1l2* mutant allele with 1 bp C insertion 3bp upstream of PAM sequence. The black arrow indicates the point of the mutation. B-D, Phenotypical analysis on WT vs. *osg1l2* mutant (C insertion). The analysis has been done on 9 WT and 30 mutant panicles of the T2 generation. Mutant plants produced panicles bearing on average 4 PBs, 4 SBs and 35 SPs less than the WT. PBs, primary branches; SBs, Secondary branches; SPs, spikelet. Student's T-test highlighted the statistical difference between wild-type and osg1l2 mutant (*** p< 0,001; **p<0,01; * p<0,05). Charts were realized using GraphPad Prism 8.

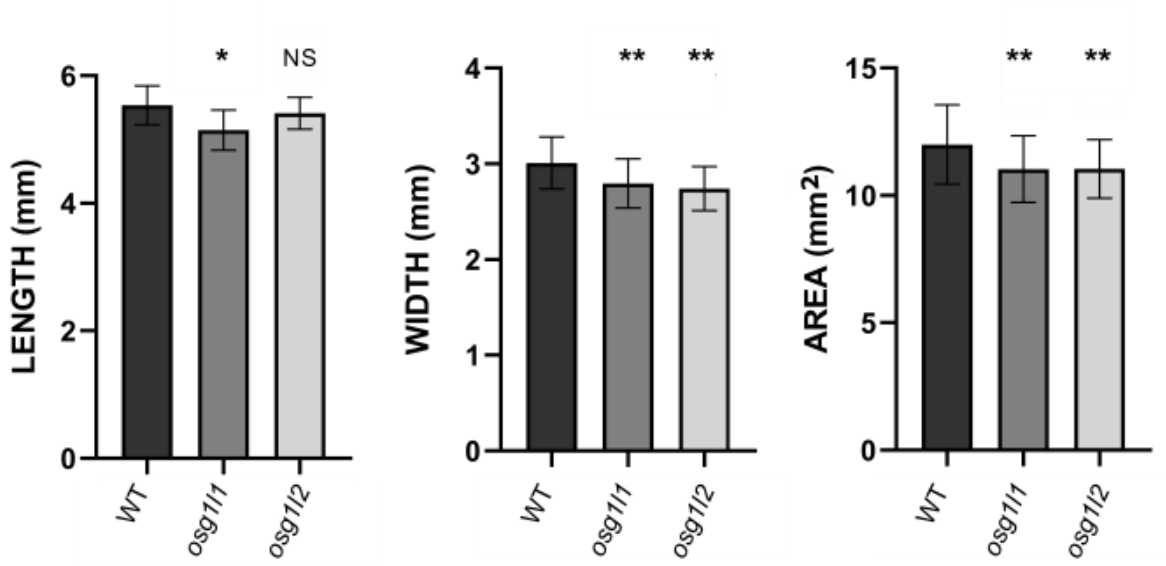

Supplemental Figure S4. Size measurements of wild type, *osg1l1* and *osg1l2* grains. Graphs resulting from the analysis of length, width and area of wild type (WT), *osg1l1* and *osg1l2* grains using the Smart Grain software (Tanabata et al., 2012). 100 grains for each genotype were analyzed. Statistical One-Way ANOVA with Tukey test: **p<0,01; * p<0,05. NS = not significant.

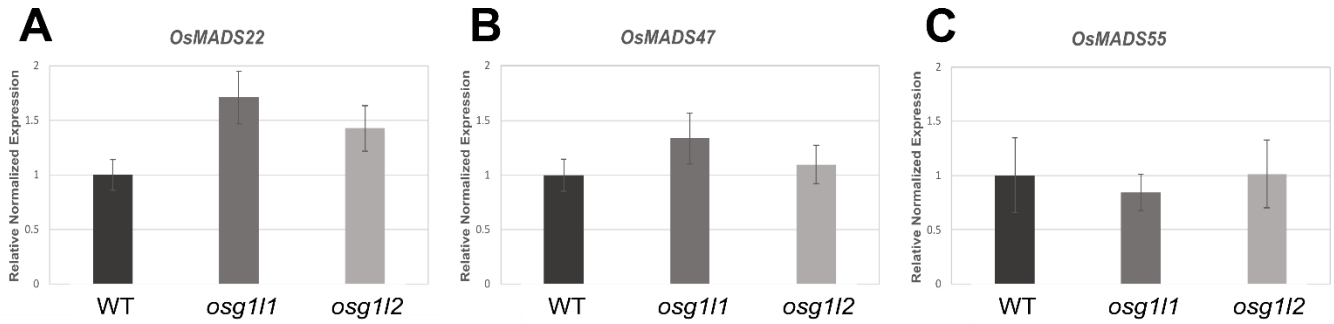

Supplemental Figure S5. Expression analysis of *OsMADS22* (A), ***OsMADS47*** (B) **and *OsMADS55*** (C) in wild type (WT), *osg1l1* and *osg1l2* background. Expression of *OsMADS22*, *OsMADS47* and *OsMADS55* was normalized to that of *Elongation Factor 1* and the expression level of the wild type was set to 1.

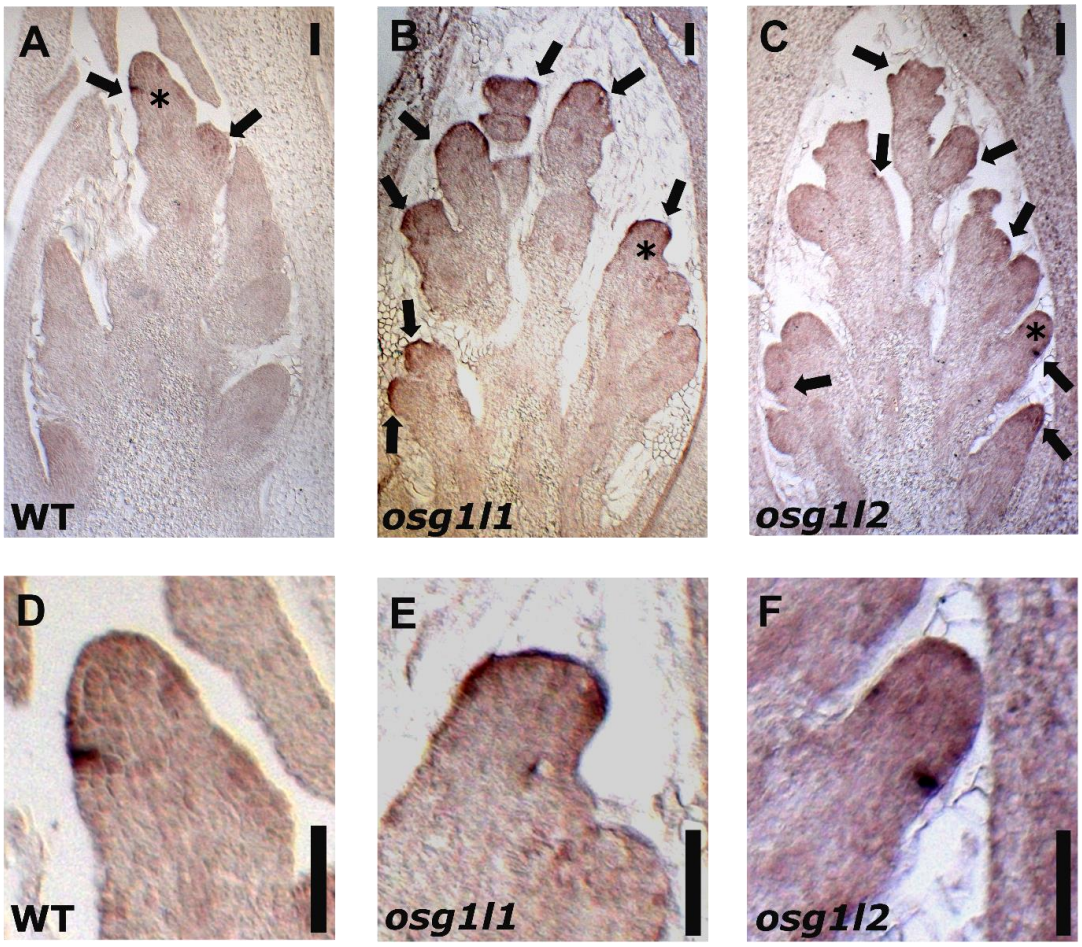

Supplemental Figure S6. Expression pattern of *FZP* analyzed by *in situ* hybridization at the ePBM/AM stage in wild type (WT, A) *osg1l1* (B) and *osg1l2* (C) background. In D, E and F are shown enlargements of regions of the developing panicles where *FZP* signal is present [Scale bars represent 50 μm; black arrows indicate *FZP* signal, black asterisks indicate the region of the developing panicle enlarged in D-F].

A

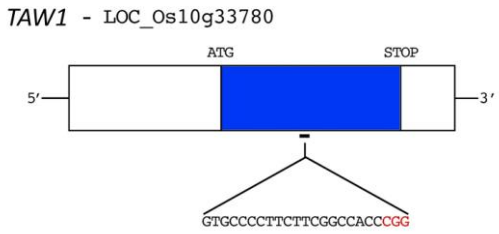

B

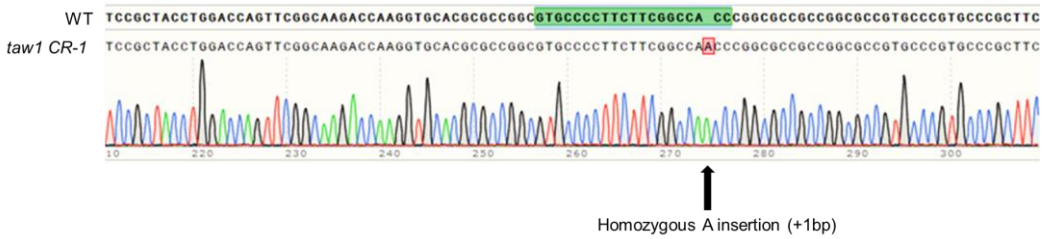

C

D

```
                1
TAW1            MEFVAHAAAP DSPHSDSGGG GGGMATGATS ASAAGASPSR YESQKRRDWN TFGQYLRNHR PPLSLARCSG
A insertion     MEFVAHAAAP DSPHSDSGGG GGGMATGATS ASAAGASPSR YESQKRRDWN TFGQYLRNHR PPLSLARCSG
                                          Point of mutation
               71                         |
TAW1            AHVLEFLRYL DQFGKTKVHA PACPFFGHPA PPAPCPCPLR QAWG------ --SLDALVGR LRAAYEENGG
A insertion     AHVLEFLRYL DQFGKTKVHA PACPFFGQPG AAGAVPVPAS PGVGQPRRPR RPPPRRLRGE RRPPREQPLR

              141
TAW1            RPENNPFGAR AVRL----YL REVREHQA-- ------RARG VSYEKKKRKK PPHPSSAAAA H---------
A insertion     RPRRPPLPPR GPRAPGARTR RQLREEEAQE ATPPLLRRRR ARRRRQRRPP PPPPHAAASS RRRRLSRAEL

              211
TAW1            ------DDAA NGALHHHHHM PPPPPGAAA*
A insertion     APRSPENELL ASYACTSYST PLHSTMIPS*
```

Supplemental Figure S7. A, *TAW1* gene structure. The blue rectangle represents the exons, the black line represents the introns and the white rectangle represents the 5’ and 3’ UTRs respectively. The position and the

target sequence of the sgRNA, which targets the exon, 275 bp downstream the ATG site are indicated. The PAM sequence is indicated in red. B, chromatograms showing WT *TAW1* genomic sequence and *taw1 CR-1* mutant with 1bp A insertion, 2bp upstream of PAM site. The black arrow indicates the position of the mutation. C, Main panicles of WT and *taw1 CR-1* (2 cm scale bars). D, Amino acid sequence alignments of *TAW1* and the *taw1 CR-1* mutants. On the left is indicated the base insertion obtained in mutant plants. The black arrow indicates the point where the mutation occurred. The ALOG domain is underlined in yellow, the green rectangle indicates the putative NLS and the stop codons (*) are circled in blue. The A insertion caused a frameshift and the disruption of the ALOG domain and the NLS.

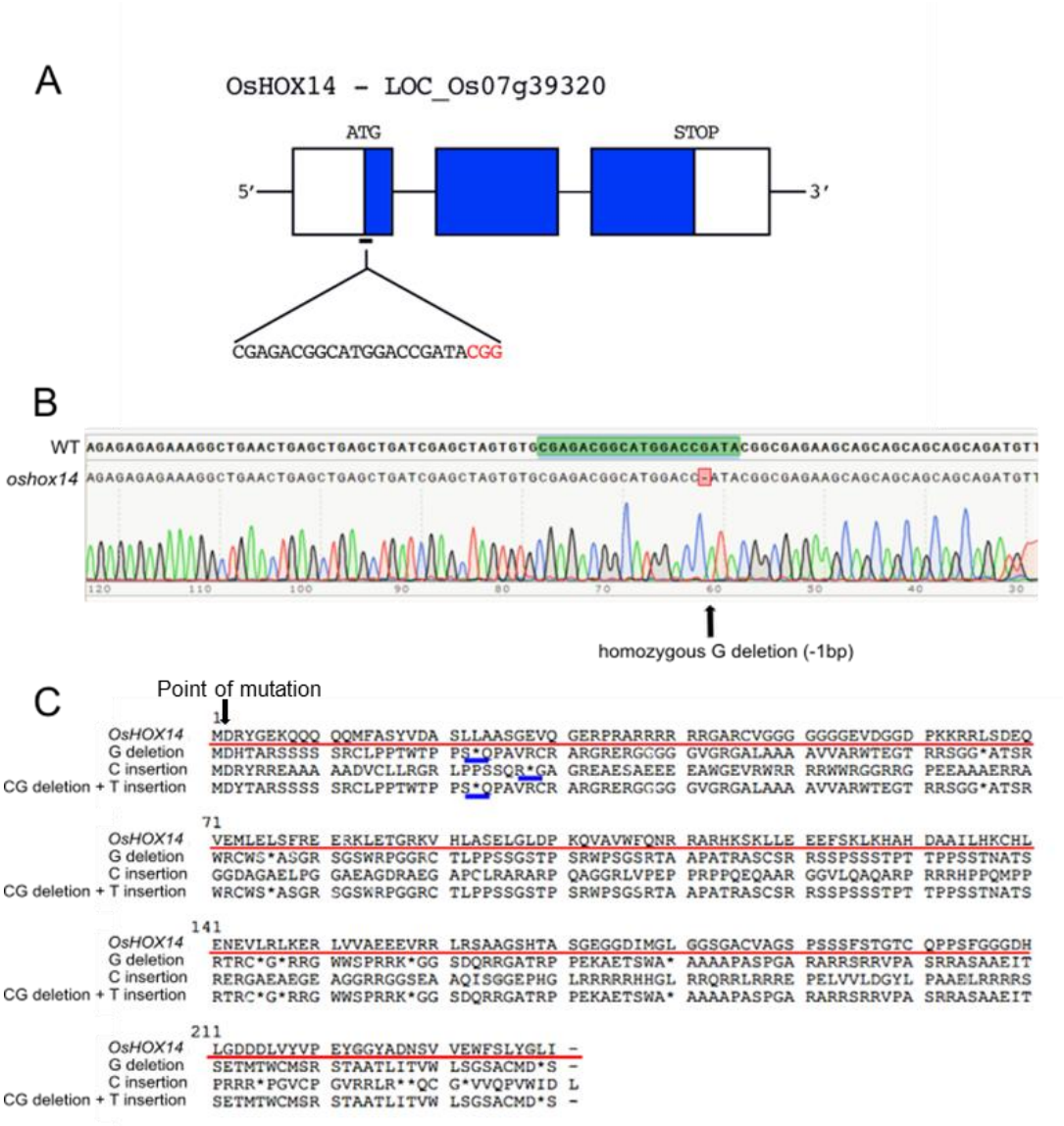

Supplemental Figure S8. A, *OsHOX14* gene structure, showing the composition in intron (black lines) and exons (blue rectangles). The white rectangle represents respectively the 5' and 3' UTRs. The nucleotide sequence of the gRNA, which starts 9 bp upstream the ATG, is indicated with black letters and the PAM sequence with red ones. B, chromatogram showing the comparison between wild-type and the *oshox14* mutant carrying the G deletion. The sgRNA sequence is highlighted in green. The black arrow indicates the position of the mutation. C, Amino acid sequence alignment of wild-type *OsHOX14* and *oshox14* mutants. On the left

are indicated the different mutant alleles obtained. The wild type *OsHOX14* protein sequence is underlined in red. The black arrow indicates the point of the mutation. The premature stop codons formed because of the frameshift in the sequence are underlined in blue. The three different insertions and deletions are listed on the left.

A

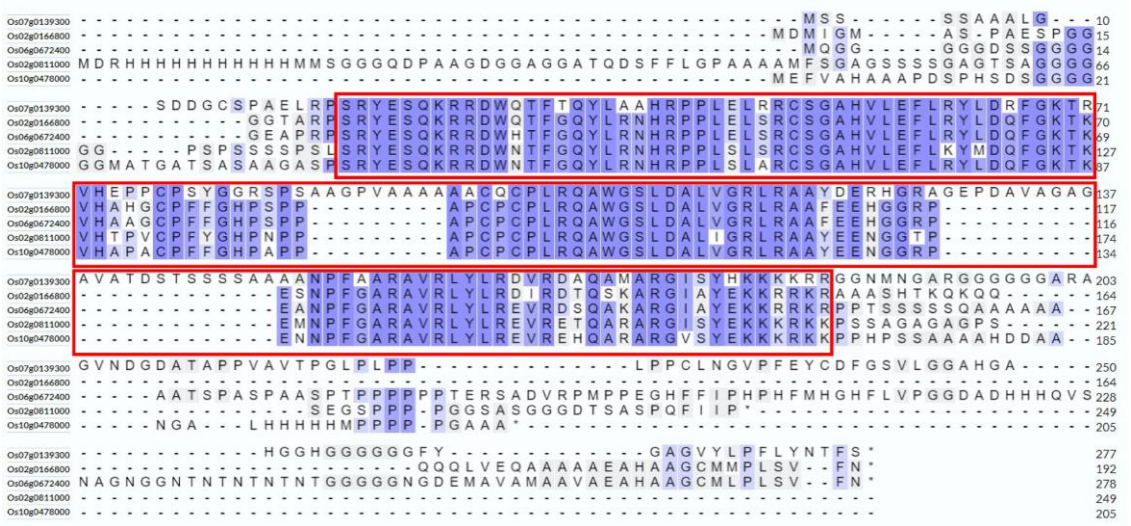

B

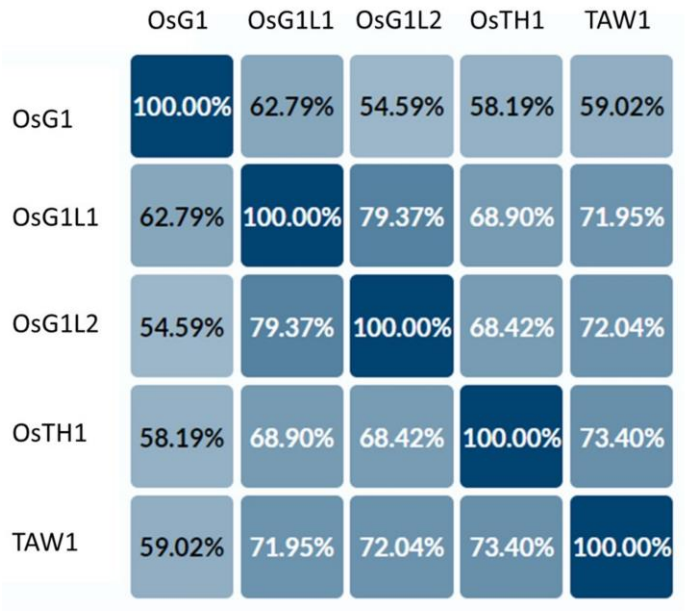

Supplemental Figure S9. A, Protein alignment among OsG1 (Os07g0139300), OsG1L1 (Os02g0166800), OsG1L2 (Os06g0672400) OsTH1 (Os02g0811000) and TAW1 (Os10g0478000). The ALOG domain is highlighted in red **B,** percent identity matrix among OsG1 (Os07g0139300), OsG1L1 (Os02g0166800), OsG1L2 (Os06g0672400), TAW1 (Os10g0478000) and OsTH1 (Os02g0811000) proteins.

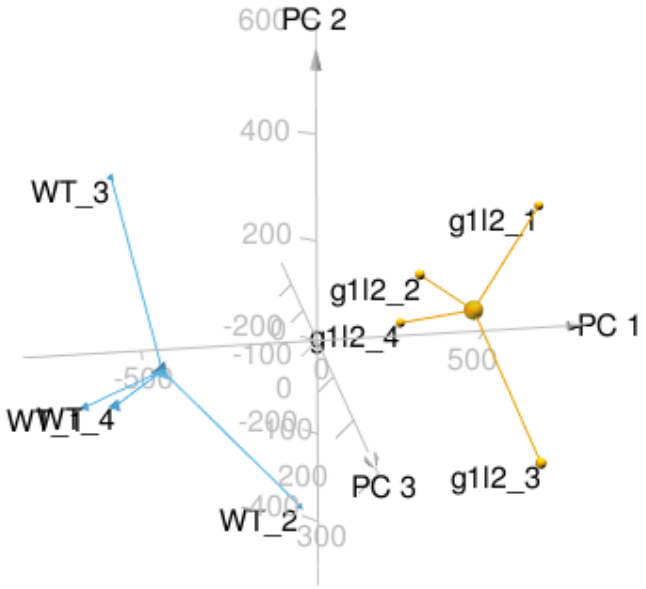

Supplemental Figure S10. PCA output of transcriptome dataset across three Principal Components: PC1, PC2 and PC3.